Radiofrequency Lesion Assessment by Cardiac Magnetic Resonance Imaging following Atrial Fibrillation Catheter Ablation

Arujuna, Aruna

Awarding institution:
King's College London

Title: Radiofrequency Lesion Assessment by Cardiac Magnetic Resonance Imaging following Atrial Fibrillation Catheter Ablation

Author: Aruna Arujuna

Radiofrequency Lesion Assessment by Cardiac Magnetic Resonance Imaging following Atrial Fibrillation Catheter Ablation

by

Dr Aruna Vishnu Arujuna

MBChB MRCP (UK)

Division of Imaging Sciences and Biomedical Engineering

School of Medicine, King's College London

A dissertation submitted to graduate school of King's College London in partial fulfilment of the requirements for the degree

of

Doctorate of Medicine

For their selflessness, warmth and affection that saw through the coldest days, their support and constant care that negotiated the many bends and most importantly their love, bright as the stars, and planets beaming with light , this work is dedicated to amma and pappa.

Table of content

List of Abbreviations

AAD	Anti-arrhythmic drugs
AF	Atrial fibrillation
ANOVA	Analysis of variance
AT	Atrial tacchycardia
AV	Atrionentricular
CA	Catheter ablation
CFAE	Complex fractionated atrial electrograms
CMR	Cardiac Magnetic Resonance
CNR	Contrast to noise ratio
CPVA	Circumferential pulmonary-vein ablation
CS	Coronary sinus
DE	Delayed enhancement
DIR	Dual inversion recovery
EF	Ejection Fraction
EP	Electrophysiological
FA	Flip angle
FWHM	Full width half maximum
HARP	Harmonic phase
IR	Inversion recovery
LA	Left atrium
LPVs	Left pulmonary veins
MIP	Maximum intensity projection
MRA	Magnetic resonance angiography
MRI	Magnetic resonance imaging
PAF	Paroysmal atrial fibrillation
PV	Pulmonary vein
PVI	Pulmonary vein isolation
RCM	Robotic catheter manipulation
RF	Radio-frquency
ROI	Region of interest
RPVs	Right pulmonary veins
RRNS	Remote robotic navigation system
SENSE	Sensitivity encoding
SNR	Signal to noise ratio
SPAMM	Spatial modulation of magnetization
SPIR	Spectral presaturation inversion recovery
SR	Sinus rhythm
SSFP	Steady state free precession
T2	T2-weighted signal
TE	Echo time
TFE	Turbo field echo
TR	Repetition time
TOE	Transoesophageal echocardiography
TSE	Turbo spin echo
TTE	Transthoracic echocardiography
WACA	Wide area circumferential ablation

Abstract

Single ablative therapy for PAF has moderate success and many patients present with recurrent arrhythmia. We propose that the structure of the RF lesion applied during ablation is important in determining recurrences. The nature of the RF lesion was studied using MRI with gadolinium delayed enhanced (DE) imaging and high signal T2 weighted imaging. Levels of DE and T2 were low in pre-procedural scans but rose dramatically immediately following the procedure. Acute DE was greater in patients without recurrences compared to those with recurrences. Conversely T2 levels were lower in patients without recurrences and higher in those with recurrences. On the late scans, T2 reduced to baseline. DE however remained and was greater in patients without recurrences. We therefore propose that acute RF ablation injury is composed of two types of tissue damage. DE infers largely necrotic tissue injury which lasts longer and causes persistent conduction block. T2 is a transitory phenomenon co-existing with DE, causing acute conduction block. We propose that resolution of oedema is associated with recurrences of PV connection and therefore arrhythmia recurrences. Modifications in our ablative techniques to achieve more DE at the acute ablation would potentially be important in conferring better ablation outcomes.

The role of DE imaging was utilised to compare left atrial catheter ablation with robotic assisted navigation and standard navigation. A greater circumferential lesion extent by DE was observed in the robotic group . This suggests that catheter stability improves tissue contact permitting the creation of more contiguous durable scar around the PV antrum. We also sought to improve DE imaging sequences to optimise scar visualisation and tested the feasibility of an automatic scar quantification tool to improve reproducibility whilst maintainin accuracy

1 Summary

1.1 Summary of thesis

1.1.1 Introduction

Catheter ablation (CA) of paroxysmal atrial fibrillation (AF) is an established treatment modality for symptomatic patients with drug refractory paroxysmal AF.

The principal objective of atrial fibrillation ablation is the electrical disconnection of the pulmonary-vein triggers from the atrial substrate pulmonary vein isolation (PVI).

Whilst acute electrical isolation is almost homogenously achieved, the long term results appear heterogenous with between 2-3 repeat ablation procedures being needed to ensure freedom from arrhythmia .

This has subsequently led to a need for an effective tool in assessing catheter ablation lesions in patients. Understanding the nature of these radiofrequency lesions (full thickness versus partial thickness) assessing their distribution in relation to anatomic landmarks and following-up these lesions over time may help improve our knowledge in understanding the variation in catheter ablation outcome results and possible underlying mechanisms responsible for AF initiation and maintenance.

The recent advancement in novel cardiac magnetic resonance imaging sequences has allowed for the visualisation, quantification and characterisation of post-procedural radiofrequency lesions in vivo. Delayed enhancement (DE) imaging performed has been accepted to signify areas of scar tissue whilst T2 imaging signifies oedema.

1.1.2 Aims

-Within the framework of this project, we sought to assess the relationship between DE, T2 and a combination of DE&T2 to clinical outcome by performing acute and late CMR scans. --Next, we examined the importance of catheter stability and contact force in lesion delivery. A cardiac MR comparison of radiofrequency ablation lesions created by using robotic navigated systems and catheters with contact force measurement against lesions created in the conventional way using standard catheter was performed.

-In order to refine delayed enhancement image acquisition, a novel double inversion recovery sequence was examined.

-The application of an automatic lesion segmentation tool that was being developed to segment out areas of delayed enhancement on CMR was assessed.

-Finally, the proof of concept and feasibility of a prototype echo-fluoroscopy view-synchronized platform was clinically evaluated

1.1.3 Methodology

Left atrial lesions created following catheter ablation was assessed on CMR by using delayed enhancement and T2 signal. Pre-procedural and both acute (between 18 and 24hours following CA) and late post-procedural images (3 months and beyond post CA) were acquired. We performed five studies which are summarised as follows:

(a) Characterisation of post ablation lesions into reversible and irreversible atrial tissue injury following catheter ablation
(b) An assessment of the temporal relationship between DE and T2 signal over time following catheter ablation and its clinical relevance
(c) A CMR comparison of lesions created using robotic navigated systems and catheters with contact force measurement against lesions created in the conventional way

(d) A comparison of the non-specific dual inversion recovery technique to standard inversion recovery by performing both sequenecs in the same patients at pre-determined time points following contrast administration

(e) An evaluation of a novel automatic delayed enhancement lesion segmentation tool by comparing areas of DE recognized and automatically segmented by the tool to manually segmented DE areas by experienced operators

1.1.4 Results

We found that acute pulmonary vein isolation was achieved by a combination of reversible and irreversible circumferential tissue injury at the PV-LA junction. The greater the ablation extent accounted for by reversible injury, the higher is the incidence of AF recurrence. Areas of DE over time became more distinct and smaller, whilst T2 signal regressing to almost baseline levels. The cardiac MR examination findings in the robotic versus standard ablation study suggest that remote robotic assisted navigation systems permit the creation of more contiguous, durable scar around the PV antrum. Higher amount of DE quantified on the late scans corresponding to a better clinical outcome was noted in this group. Non-specific dual inversion recovery achieved better atrial blood pool suppression conferring improved delayed enhancement visualisation alongside facilitating a reduction in scanning time. The automatic lesion segmentation tool recognised areas of delayed enhancement and performed appropriate segmentation which corresponded to the manual operator segmented areas of DE.

1.1.5 Conclusion

Clinical outcome correlates with cardiac MR findings strongly suggest that the creation of scar which is contiguous and circumferential results in a better long term outcome. Post catheter ablation cardiac MR atrial lesion assessment is a unique invaluable tool that permits visualisation, characterisation and quantification of atrial tissue injury. The examination of tissue injured areas and a temporal assessment allows for an understanding of the possible

mechanisms promoting mid-long term procedural success. The presence of greater amount of delayed enhancement on the late scans suggest a more favourable clinical outcome. The overall better results observed in the robotic group is likely a resultant of increased catheter stability improving tissue contact and greater catheter control allowing for more accurate lesion delivery. Dual inversion recovery technique allows for better signal to noise ratio (SNR) and contrast to noise ratio (CNR) allowing better visualisation of areas of delayed enhancement. The appropriate and successful automatic DE segmentation by the novel software allows for greater reproducibility in the absence of inter-observer variability. The practicability of real-time hybrid X-ray fluoroscopy was demonstrated in both a phantom model and a porcine experimental study, followed by a clinical series demonstrating work-flow feasibility.

Atrial Fibrillation; Catheter Ablation; Cardiac Magnetic Resonance; Pulmonary Vein Isolation; Wide Area Circumferential Ablation, Delayed Enhancement, T2 Signal; Remote Robotic Navigation System; Dual Inversion Recovery; Automatic Segmentation; Real-Time Hybrid X-Ray Fluoroscopy

1.2 Keywords

Atrial Fibrillation; Catheter Ablation; Cardiac Magnetic Resonance; Pulmonary Vein Isolation; Wide Area Circumferential Ablation, Delayed Enhancement, T2 Signal; Remote Robotic Navigation System; Dual Inversion Recovery; Automatic Segmentation; Real-Time Hybrid X-Ray Fluoroscopy

1.3 Overview of Thesis

1.3.1 Description of chapters

Chapter 2 gives an overview of atrial fibrillation including mechanisms for AF, rationale for catheter ablation, potential targets for ablation and present technical improvements. This is

followed by an introduction into magnetic resonance imaging with an overview of the basic principles and techniques for CMR. Key concepts for this thesis is introduced, including left atrial imaging, delayed enhancement and T2 assessment, robotic navigation system and inversion recovery.

Chapter 3 describes the general methods used for the experimental work in this thesis.

Chapter 4 reports the acute and late left atrial CMR findings by DE and T2 assessment following catheter ablation, the clinical significance of these findings are crystallised by correlating the signal evaluation to clinical outcome.

Chapter 5 reports the CMR study findings comparing lesions created using robotic navigated systems and catheters with contact force measurement against lesions created in the conventional way.

Chapter 6 describes the study comparing the non-specific dual inversion recovery technique to standard inversion recovery following contrast administration.

Chapter 7 describes a novel automatic segmentation tool utilized to facilitate lesion assessment

Chapter 8 discusses the relevant findings and explores the clinical utility of fusion imaging

Chapter 9 describes conclusions from the studies which comprise this thesis

1.3.2 Contribution of candidate and colleagues

I designed the clinical studies described within this thesis. I identified and recruited patients for the studies. I performed CMR imaging, along with a clinical radiographer, for the patients involved in these studies. I assisted in the clinical procedures of AF catheter ablation in both standard and robotic assisted navigation systems, with Dr Jaswinder Gill and Dr Mark

O'Neill as first operators for these cases. Cases were also contributed by Drs Michael Cooklin and Dr Aldo Rinaldi. I was responsible for data acquisition and data analysis for these studies. Drs Bernet Kato and Niloufar Zarinabad provided statistical advice and help in some of the data analysis. For the Dual-Inversion Recovery study, Professor Rene Botnar alongside Sarah Peel assisted in developing the sequence and quantifying the SNR and CNR. The work on developing an automatic lesion segmentation tool was performed by Dr Rashed Karim with lesion quantification being performed by Richard Gere, Dr Rashed Karim and myself. The data analysis in this section was performed by both Richard Gere and Dr Rashed Karim. The development, phantom and porcine experiments performed in the real-time hybrid echo-fluoro study were carried out in conjunction with a team in Phillips comprising a team of mathematical and computer experts, and locally by Dr Gang Gao, James Housden and Dr Ying Liang Ma. TOE image acquisition was performed by Dr Ronak Rajani and Dr Stam Kapetanakis.

2 Background

The electrophysiological basis of atrial fibrillation requires both a trigger that initiates the dysrhythmia and a substrate that can sustain it. [1, 2] The most common triggers of atrial fibrillation are ectopic atrial beats that arise from the muscle sleeves of the pulmonary veins. [3, 4] These triggers may be provoked by the intrinsic activity of cardiac ganglionic plexi, which are clustered in the vicinity of the pulmonary vein–left atrial junction.[5, 6] The pulmonary vein–left atrial junction and an enlarged atrium harboring fibrosis and inflammation serve as the substrate for sustaining wavelets of atrial fibrillation. Episodes of atrial fibrillation lead to electrophysiological changes in the atria — namely, shortening of the refractory period of the atrial muscle — occurs and predisposes to the development of other triggers and wavelets (electrical remodelling). This process results in perpetuation of atrial fibrillation and in a greater predisposition to atrial fibrillation. Maintenance of sinus rhythm can reverse these changes and mechanisms. Hence, atrial fibrillation begets atrial fibrillation, and sinus rhythm begets sinus rhythm. [7-9] More persistent atrial fibrillation results in anatomical changes including fibrosis and hypertrophy which are more difficult to reverse (anatomical remodelling).

Atrial fibrillation ablation is a therapeutic technique that uses radiofrequency energy or freezing to destroy atrial tissue that is involved in the propagation of the dysrhythmia. Radiofrequency ablation generates an alternating electrical current that passes through myocardial tissue, creating heat energy that conducts to deeper tissue layers. At temperatures of 50°C or higher, most tissues undergo irreversible coagulation necrosis resulting in non-conducting myocardial scar tissue.[10, 11] Cryoablation destroys tissue by freezing and recently laserablation by coagulation necrosis.

The principal objective of atrial fibrillation ablation is the electrical disconnection of the pulmonary-vein triggers from the atrial substrate (often called “pulmonary-vein isolation”).[12,

[13] To achieve this goal, ablation is performed around the pulmonary-vein to obtain electrical disconnection between the vein and the atrium. Ablation of sites beyond the pulmonary vein–left atrial junction in the atrial substrate itself, targeting so-called complex fractionated electrograms, is not necessary in paroxysmal atrial fibrillation but may be very important in patients with persistent atrial fibrillation.[13] Although acute electrical isolation of the pulmonary veins is achieved in the electrophysiology laboratory, the long term results at present time are not as favourable. Pulmonary vein reconnection is common and between 2-3 repeat ablation procedures may be needed to ensure pulmonary vein isolation and freedom from arrhythmia .[13]

This has subsequently led to a need for an effective tool in assessing catheter ablation lesions in patients. Understanding the nature of these radiofrequency lesions (full thickness versus partial thickness) assessing their distribution in relation to anatomic landmarks and following-up these lesions over time may help improve our knowledge in understanding the variation in catheter ablation outcome results and possible underlying mechanisms responsible for AF initiation and maintenance. Previously parameters affecting lesion creation have been assessed in animal models looking at temperatures achieved, power delivered, tissue contact force, catheter orientation, duration of energy delivery and blood flow within the cardiac chambers. However, there are technical limitations in extrapolating this data directly into patients as catheter orientation, catheter stability, blood flow and exact tissue contact force achieved has been difficult to assess.

The recent advancement [7,8,9,10]in novel cardiac magnetic resonance imaging sequences has allowed for the visualisation, quantification, qualitation and characterisation of post-procedural radiofrequency lesions in vivo. This new tool is rapidly proving to be an invaluable commodity for researchers, electrophysiologists and patients offering numerous benefits in improving the quality and standards of care given to AF patients. Cardiac

magnetic resonance (CMR) imaging is an imaging technique with excellent soft tissue contrast and provides high resolution two-dimensional (2D) and three-dimensional (3D) images.

The following paragraphs presents the historical perspective of atrial fibrillation, possible mechanisms for atrial fibrillation, rationale for catheter ablation and a summary of the present cardiac magnetic resonance studies evaluating the left atrium following catheter ablation.

2.1 Historical Perspective

Table 2-1 Chronological overview of events pertaining to the history of Atrial Fibrillation

Huang Ti Nei, Ching Su Wen 3000BC	Description of what may have been AF in the Yellow Emperor's Classic of Internal Medicine	Velupian 1874	Animal studies confirming fibrillation of the atrium in response to ' faradic current '
William Harvey 1628	Movement of the right atrium was described as 'obscure' and 'undulating'	Arthur Cushny 1899	First published case report of AF occurring following ovarian surgery
William Withering late 1700s	Foxglove leaves *(Digitalispurpurea)* use in restoring regular pulse	Fredericq 1904	Severance at the level of the Bundle of His left the atrium fibrillating but the ventricles contracting regularly, confirming the atrium as the origin for irregular beats
Robert Adams 1827	Irregular pulses in association with mitral stenosis as first described following the invention of the stethoscope	William Einthoven 1900	String galvanometer was invented
Nothnagal 1887	Used recently developed graphical techniques for analyzing arterial pulses	Thomas Lewis 1909	First documentation of atrial fibrillation electrocardiographically with fibrillation waves (f waves) associated with irregular ventricular activation (QRScomplexes)

Atrial Fibrillation' was defined in 1909 by Sir Thomas Lewis[14] as:

'when the auricles pass into fibrillation they cease to beat, their walls standing in position of diastole, exhibit small flickering tremulous movements which are the

expression of in-coordinate activity'

Almost a century later the American College of Cardiology jointly with the European Society of Cardiology in 2006 defined atrial fibrillation as[15]:

'*..a supraventricular tachyarrhythmia characterized by uncoordinated atrial activation with consequent deterioration of atrial mechanical function. On the electrocardiogram, AF is described by the replacement of consistent P waves by rapid oscillations or fibrillatory waves that vary in size, shape, and timing, associated with an irregular, frequently rapid ventricular response when atrioventricular conduction is intact'* (Figure 2.1)

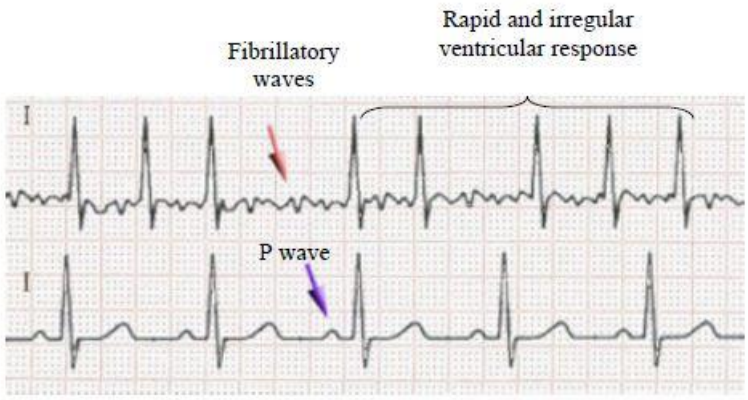

Figure 2-1: Electrocardiogram showing atrial fibrillation (top tracing) with fibrillatory waves and sinus rhythm (bottom tracing) with consistent p waves.

Of note, the Chinese chronicles approximately 4000 years ago in the Yellow Emperor's Classic of Internal Medicine (Huang Ti NeiChing Su Wen) [16] was the earliest description of what may have been atrial fibrillation:

'When the pulse is irregular and tremulous and the beats occur at intervals, then the impulse of life fades…'

Whilst the chaotic irregularity of the pulse was clearly acknowledged by most of the ancient

physicians, the first description of 'fibrillation of the auricles' was made by William Harvey in 1628, who described the movement of the right atrium as 'obscure' and 'undulating'. In the late 1700s, William Withering described a patient with a 'weak and irregular pulse' that later became 'full and more regular' after treatment with extracts from the foxglove (*Digitalis purpurea*) [17]. With the aid of Laennec's recently invented stethoscope, Robert Adams reported in 1827 the association of irregular pulses with mitral stenosis, with Etienne Marey later publishing a pulse tracing from such patient.[16] Numerous terms were coined for this abnormal heart rhythm with Bouilland in1835 describing 'ataxia of the pulse', referring to a pulse with varying inter-beat intervals and in 1887 Nothnagal using recently developed graphical techniques for analyzing arterial pulses, publishing three pulse recordings that he termed 'delirium cordis':

'*heartbeats follow each other in complete irregularity…, the height and tension*

of the individual pulse waves are continuously changing'

At around the same time, animal studies were being developed in order to evaluate the reported clinical observations. In 1874 Velupian described a fibrillating atrium in response to application of a strong, continuous (faradic) current who applied the term 'frémissementfibrillaire'. Later in 1899 Arthur Cushny, professor of pharmacology at University College London published the first case report of atrial fibrillation. His patient was 3 days following surgery on an ovarian fibroid when she developed a 'very irregular' pulse at a rate of 120-160 beats per minute. Her pulse was recorded by a 'Jacques sphygmochronograph', which showed the radial pulse pressure against time. He linked the findings of irregularity of the arterial pulse curves, to experimental dogs with induced atrial fibrillation. However, doubts existed as to the mechanism of ventricular irregularity associated with a fibrillating atrium.

Fredericq in 1904 found that whilst the atria continued to fibrillate after cutting the bundle of His, the ventricles however began to beat regularly. This confirmed the atria as the source for the arrhythmia with irregular impulse propagation to the ventricles through the Bundle of His. The main clinical diagnostic breakthrough was the invention of the string galvanometer by William Einthoven in 1900. Subsequently, in 1909, a close friend of Einthoven, Sir Thomas Lewis at the University College Hospital London, taking advantage of the newly developed galvanometer, was the first to document atrial fibrillation electrocardiographically with fibrillation waves (f waves) associated with irregular ventricular activation (QRScomplexes) (Figure 2.2)[14]:

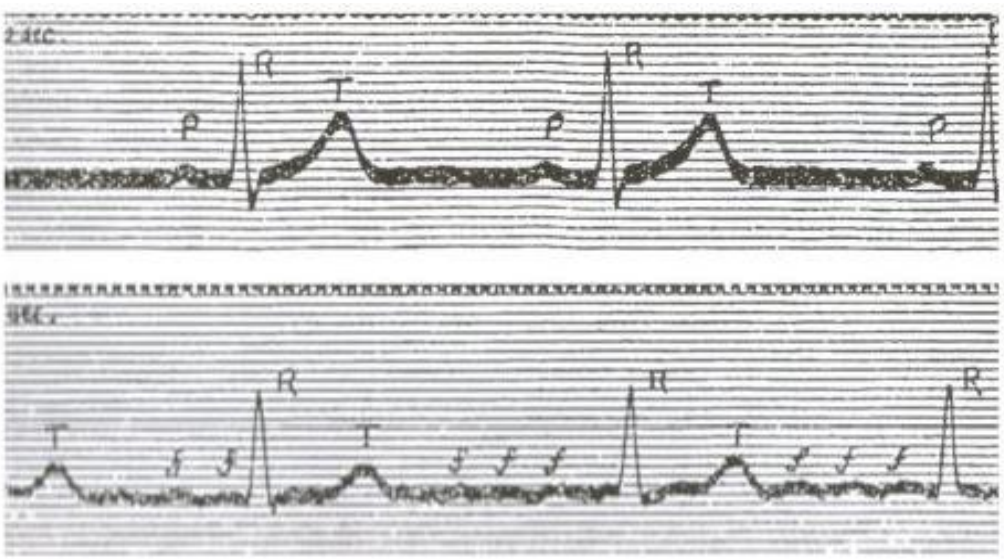

Figure 2-2: Electrocardiogram recorded by Thomas Lewis showing sinus rhythm in one patient (upper panel) and atrial fibrillation in another patient (lower panel). Fibrillating (f) waves are demonstrated

Subsequently Lewis was able to link this type of electrical activity with fibrillation of the atria, which he visually observed in open-chested dogs.

2.2 Mechanisms of Atrial Fibrillation

Following these initial observations, there has been a lot of speculation on the precise mechanisms giving rise to atrial fibrillation. With improvements in technology and the

development of several animal models of AF and data from patient studies, we have come to appreciate that AF probably has several mechanisms.

In the 1900s, three theories of AF had evolved (Figure 2.3):

i) "hyperectopia theory" in which single or multiple rapidly-firing atrial ectopic foci lead to fibrillation (Engelmann, Winterberg, Haissaguerre).

ii) rapid single circuit re-entry ("mother wave") with fibrillatory conduction (Lewis).

iii) multiple simultaneous functional re-entry circuits (Mines, Garrey,Allessie).

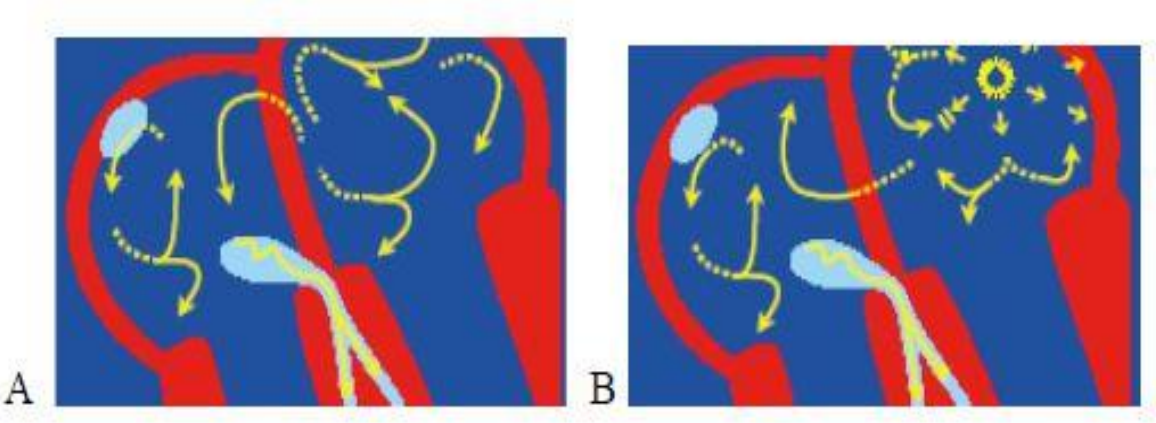

Figure 2-3: Proposed mechanisms of atrial fibrillation, A. Multiple wavelet theory, B.Ectopic focus.(Adapted from Garrey, Miles, AllessieEnglemann, Rothberger, Haissaguerre)

2.2.1 Multiple Re-entry circuits

Re-entry is a disorder of impulse propagation and occurs when an impulse travels around an abnormal circuit repetitively based on a central non-conducting area. Re-entry requires an appropriately timed stimulus (trigger) that is able enter the circuit, but encounters an area of refractory tissue on one side (unidirectional block) and excitable tissue on the other where it is able to propagate. When the wavefront reaches the distal end of the circuit there is recovery of excitability of the previously refractory tissue, thus allowing the wavefront to pass back up this pathway initiating reentry.

In 1906, Mayer had noted that a single stimulus applied to the ring of jellyfish tissue can propagate in one direction only and on returning to its origin find that the tissue again is excitable and then traverse the circuit over and over again.

This was the first experiment to demonstrate reentry. Later Mines used strips of tortoise atria and ventricle to form a ring of sufficient size that wavefronts might recirculate.[18]

In 1914, Garrey et al published a seminal paper establishing the fundamental concept that a critical mass of tissue was necessary to maintain atrial fibrillation. He induced atrial fibrillation by introducing faradic current to the tip of one of the atrial appendages.

When he separated the tip of the atrial appendage using a soft clamp from the rest of the atrium the tip of the appendage failed to fibrillate whereas the rest of the atrium did. From such observations he concluded that:

'*any small auricular piece will cease fibrillating even though the excised pieces retained their normal properties*'.

This suggested that not all parts of the atria fibrillate as a result of rapidly discharging foci but were dependent on stimulation from surrounding areas. Using all the information he acquired he proposed that fibrillation was the result of circulating impulses which were either halted by areas of conduction block or diverted around these areas to take random paths around refractory tissue, termed 'circus movement'.

Influenced by the work of Mines and Mayer, Garrey later proposed that AF was due to:

'*a series of ring-like circuits of shifting location and multiple complexity*'.

Subsequently Lewis in 1920 [18,19] influenced by the previous work by Mines, Mayer and Garrey proposed the following:

'*In fibrillation a single movement does exist, but the path changes…grossly; but in general the same broad path is used over and over again. It is possible to conceive circuit movements*

of many types. We might even assume several circuits, completely or transiently independent of each other.'

Since the 1960's, the most popular theory has held that AF consists of multiple wavelets of functional re-entry. In 1959, largely based on studies of a vagally mediated model of AF in the canine heart, Moe and Abildskov[1, 19-21] proposed the multiple wavelet theory for AF. They suggested that during AF, multiple wavelets wander through the atrial myocardium without re-entry to the site of origin. The pathways of these wavelets were not anatomically determined but rather were determined by local atrial refractoriness and excitability, in other words areas of functional conduction block. Because of this, the wavelets could collide and annihilate, divide, or fluctuate in size and velocity. Using a computer model they noted the importance of sufficient atrial mass and a short and heterogeneous refractory period to sustain these multiple wavelets[20]

Just over 25 years ago in 1985, Allessie and coworkers[22] tested the multiple wavelet hypothesis by mapping the spread of excitation of induced AF in isolated blood-perfused canine atria. Here, they confirmed the presence of multiple wandering wavelets, which exhibited various properties such as fluctuations in size and changes in direction and propagation (see Figure 2.4):

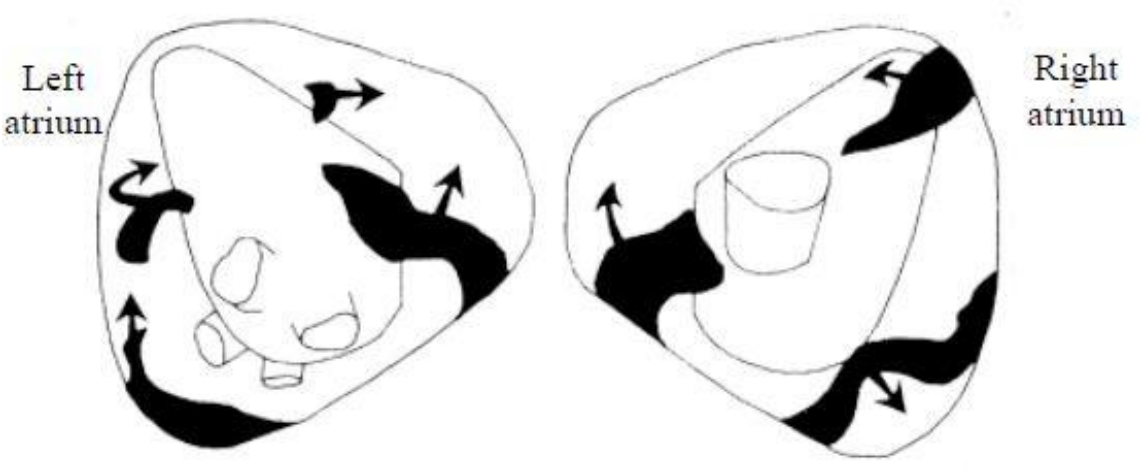

Figure 2-4: Multiple re-entry wavelets during sustained atrial fibrillation in Lagendorffperfusedcanine hearts. This figure demonstrates the presence of four waves of re-entry in the left atrium and three in the right atrium[23]

2.2.2 Multiple ectopic foci

Despite the above theories, some groups suggested that AF was due to rapidly firing atrial foci. Engelmann[24] first reported that individual heart fibres can generate significant spontaneous rhythmicity. In 1907, Winterberg[25] further developed the theory that multiple ectopic foci produce the uncoordinated atrial activity associated with AF. In 1915 Rothberger and Winterberg suggested that a single rapidly firing focus at 3000 beats per minute underlies AF [26]. Support for this concept came from work of Scherf *et* al in the 1950's [27-29]. They placed aconitine, a plant alkaloid, on the atria and demonstrated that a rapid and irregular atrial rhythm could be generated. When the site of the aconitine application was excluded by cooling, the tachycardia terminated.

Subsequent studies in the 1970's by Goto*etal*[30]and Azuma *et al* [31] found that aconitine placed on rabbit atria indeed caused abnormal automaticity with induction of AF. These studies were not widely accepted, however recently it is now appreciated that an atrial "focus" firing rapidly not only initiates but also is capable of sustaining AF and may be the mechanism in some patients with paroxysmal AF. Haissaguerre[12]*et al* reported this observation in a series of 45 patients with 69 foci of atrial fibrillation. The majority of these

foci appeared around the pulmonary veins (n=65), in particular the main trunk of the left upper pulmonary vein (n=31) (Figure 2.5).

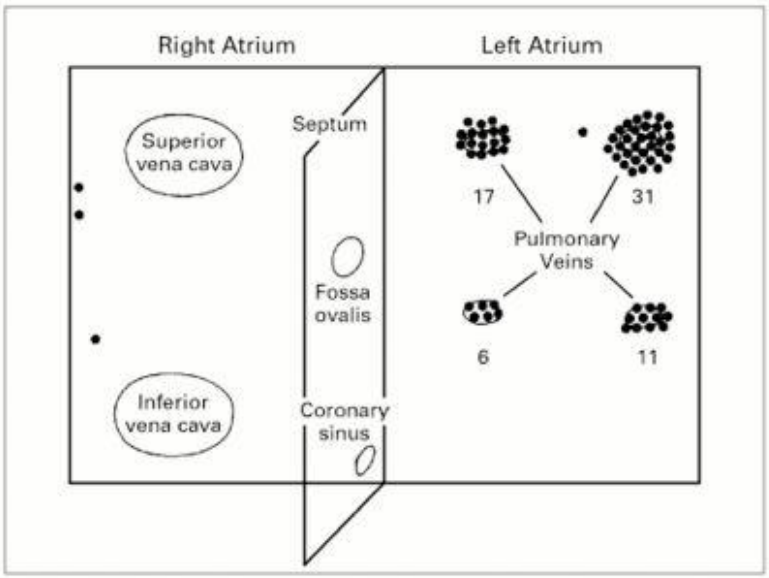

Figure 2-5: Sites of atrial foci thought to be responsible for triggering atrial fibrillation in patients with paroxysmal AF(Adapted from Haissaguerre et.al [12])

Haissaguerre postulated that AF occurred as a result of a single focal discharge or a short burst of two or more repetitive focal discharges. He also demonstrated that application of radiofrequency energy in 38 patients successfully abolished these foci and their paroxysms of AF supporting the theory that these foci were triggering AF. It was later determined that in patients with frequent paroxysms of AF, the muscular sleeve of the pulmonary veins displays electrophysiological properties distinct from those of both the adjacent left atrial muscle and the muscular sleeve of the pulmonary veins in control subjects without AF[32]. Although atrial tissue and the muscular sleeves of other cardiac veins, including the coronary sinus [33], the vein of Marshall [34] and the superior vena cava [35, 36], have been implicated as triggers for AF, none do so with nearly the frequency of the pulmonary veins.

These foci have gained a lot of attention as potential 'curative' targets for patients with paroxysmal AF and forms the basis of the present clinical ablative strategy widely employed.

It is important to note that the demonstration of focal tachyarrhythmias in patients with paroxysmal AF has challenged the multiple wavelet hypothesis. The relative contribution of these 2 competing mechanisms in explaining AF in patients with and without structural heart disease remains largely unknown. These theories are not mutually exclusive and a possible scenario is that ectopic foci can provide the trigger for initiating re-entry within the atria, or if it is rapid and sustained, may maintain AF for short periods. The trigger by a single focal source can be explained by the concept of 'fibrillatory conduction' whereby a single impulse might divide and reenter either functionally or around anatomical boundaries [37]. However after a critical period, physiological and anatomical changes develop in the atria such that AF persists despite the disappearance of the precipitating driver or drivers [38], in which case AF becomes persistent and self-perpetuates.

2.3 Self Perpetuation of Atrial Fibrillation

2.3.1 2.3.1 Background

In 1987, Kopecky[39]showed that between 18%-24% of patients having paroxysmal AF went on to develop persistent AF in the absence of progressive underlying heart disease. This suggested that the arrhythmia itself causes changes that result in its own self-perpetuation. An animal study published as an abstract in 1985 indicated that when AF was maintained by electrical stimulation for several weeks in dogs, it often sustained itself when electrical stimulation was discontinued [40]. Further work was carried out in 1994 by Wijfells et al . Here a goat model of AF was created with the implantation of epicardial electrodes which stimulated the atria with 50Hz of atrial burst pacing into atrial fibrillation whenever sinus

rhythm was detected; and conversely burst pacing was inhibited when atrial fibrillation was detected (see Figure 2.6)[9].

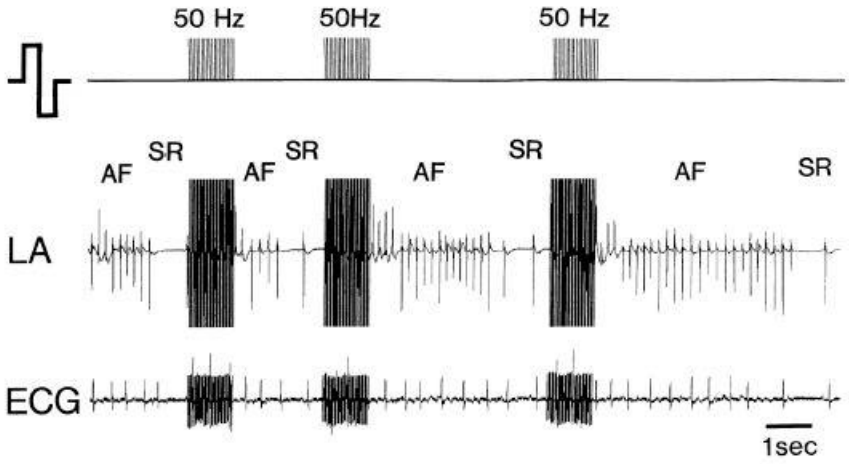

Figure 2-6:The functioning of the automatic fibrillation pacemaker (Adapted from Wijffels et.al.[9]).

At the start of the protocol the induced AF episodes were short (lasting a few seconds) after which a new episode was induced automatically. With an increased duration of the stimulation protocol, the induced AF episodes prolonged until AF did not convert spontaneously, in other words becoming persistent AF (see Figure 2.7). This landmark paper titled '*Atrial Fibrillation begets atrial fibrillation*' was the first published study to characterise the self-perpetuating nature of atrial fibrillation [9].

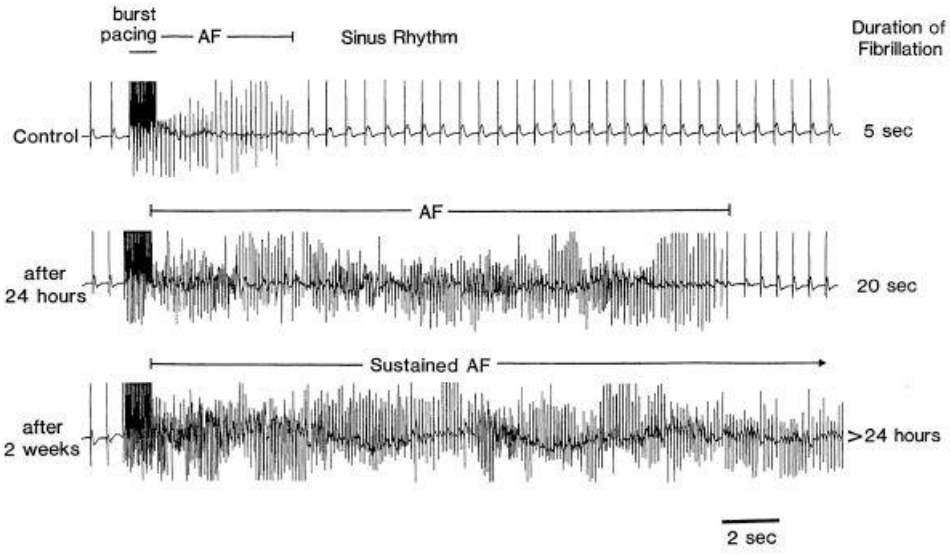

Figure 2-7: Prolongation of the duration of episodes of electrically induced atrial fibrillation after maintaining AF for 24 hours and 2 weeks (Adapted from Wijffels et.al [9])

In the same year Morillo *et al* [7]showed that 6 weeks of rapid atrial pacing (400bpm) in dogs strongly promoted the ability to maintain AF, with changes similar to those observed by Wijfells *et al* [9].

2.3.2 Underlying mechanism for the self-perpetuation of AF

As described earlier, in the 1960s Moe and coworkers introduced the multiple wavelet hypothesis of functional re-entry and postulated that the self-perpetuation of AF could be explained by this theory based on the average number of wavelets present in the atria[20, 21]. If the number of wavelets is high then the probability that all the wavelets will extinguish simultaneously is low, therefore AF would self-perpetuate. The critical number of wavelets needed to stabilize AF was estimated to be between four and six[22]. Figure 2.8 shows an example of high density maps from the right atrial free wall during a short episode of AF and persistent AF in the goat.

During acute AF the right atrium was activated by a single wave (type I AF) and therefore terminated quickly, whereas after more prolonged AF the atrium was activated by numerous wavelets which are much more disorganized (type III AF), resulting in more stable AF[41].

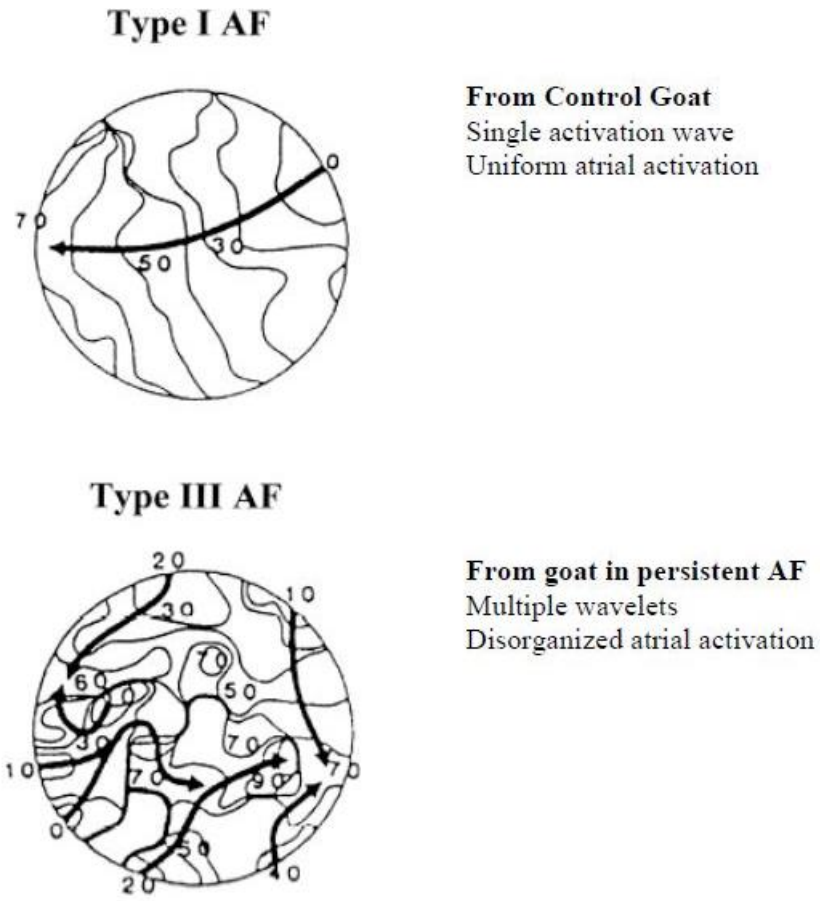

Figure 2-8: High density mapping of the right atrial free wall in a goat during acutely induced (top) and persistent AF (bottom). The direction of the propagation is indicated by the arrows(Adapted from Konings et.al.[41]).

It was recognized that the number of wavelets that can coexist in the atria is dependant on the wavelength of the atrial impulse (distance traveled by the electrical impulse) and the total surface area of the atria[42-44]. The importance of the wavelength for re-entry was first discussed by Lewis in 1925 [14] and later defined by Wiener and Rosenbleuth[45] in 1946 as the product of conduction velocity and the effective refractory period. Rensma *et al* [43]conducted

experiments in dogs to determine the effect of wavelength on inducibility of arrhythmias. They verified that premature impulses associated with small wavelengths were more likely to induce AF whereas longer wavelengths induced repetitive responses only. In addition interventions which decrease the wavelength (such as vagal stimulation) reduces the circuit size and permits more reentry circuits to coexist, making simultaneous spontaneous termination of all circuits unlikely and promoting AF, whereas interventions that increase wavelength reduce the number of circuits and suppress AF[44, 46]. This has important clinical relevance as drugs that increase the wavelength are more likely to terminate AF.

This is indeed considered to be the mechanism of action for many anti-arrhythmic drugs such as propafenone, sotalol[47] and flecainide[48]. Support for this came from pharmacological experiments by Wang *et al* in which termination of AF by class IC antiarrhythmic drugs was preceded by a decrease in the mean number of wavelets[44, 47].

2.4 Rationale for Catheter Ablation in Atrial Fibrillation

Although the mechanistic understanding of fibrillatory process remains to be confirmed, the development of recent controlled studies indicate a greater effect of catheter ablation on episodes of atrial fibrillation in comparison to AAD's for paroxysmal atrial fibrillation (A4 study and Thermocool). The lack of anti-arrhythmic drug (AAD) efficacy and the development of catheter-based technologies over the last decade have fuelled catheter AF ablation from an investigational technique to an effective alternative to AAD. The impressive improvement in the results of catheter ablation in all forms of AF compared with AAD over the last decade indicates that this approach can be considered early in the management of patients with AF, regardless of their baseline left ventricular function.

How are the above AF mechanisms addressed by catheter ablation ?

2.4.1 Multiple Wavelet Hypothesis

The multiple wavelet hypothesis as discussed above by Moe,[19] with supportive/contributory experimental work by Allessie,[22] was the predominant hypothesis prior to the late 1990s, and formed the basis on which Cox's Maze procedure was developed. The developments of surgical ablation of AF culminated in the Maze III[49], which incorporates four lesion sets: (i) encirclement of the pulmonary veins; (ii) a lesion joining the circumferential PV lesion to the mitral annulus with amputation of the left atrial appendage; (iii) a circumferential lesion in the coronary sinus; (iv) ablation of the right atrium. Although catheter ablation approaches based on the early surgical approaches were tried by a number of groups, the success rate was disappointing, with an unacceptable high complication rate.[50]

2.4.2 Focal Source Hypothesis

The observation that AF could be triggered from ectopics originating from the pulmonary veins,[12] with ablation at the source of the ectopy eliminating AF, changed the emphasis of catheter ablation away from linear lesions compartmentalizing the atria to treating focal sources. Although focal sources, incorporating automaticity and/or local re-entry, have been implicated in both atria,[51-53] the majority reside within the left atrium, which is consistent with a dominant role for the left atrium in human AF.

2.4.3 Catheter Ablation

Catheter ablation of AF is now a realistic therapeutic option across a broad spectrum of patients -from patients with paroxysmal AF to those with long-lasting persistent AF[54], including patients with moderate-to-severe left ventricular impairment.[13, 55] There is evidence to suggest that restoration and maintenance of sinus rhythm by catheter ablation may lead to improved outcomes in these patients.[55, 56]

Most centres, accept patients for catheter ablation if they have symptomatic paroxysmal AF and have failed at least one antiarrhythmic drug. Patients with long-lasting persistent atrial

fibrillation are considered for ablation if they are symptomatic and have failed treatment with more than one conventional antiarrhythmic drug, electrical cardioversion, or both. In nearly half of patients with long-lasting persistent AF, a second procedure is necessary to maintain sinus rhythm, and there are no absolute exclusion criteria nor is there a predetermined limit to the number of procedures performed per patient. With the growing body of evidence to support a safe and effective role for catheter ablation in patients with both atrial fibrillation and heart failure,[55, 56]ablation is offered to patients with atrial fibrillation, echocardiographic evidence of left ventricular dysfunction, New York Heart Association heart failure symptoms of grade II or more, and the absence of an alternative explanation for their cardiac dysfunction.

2.4.3.1 Paroxysmal Atrial Fibrillation

Pulmonary vein isolation, whether ostial or antral, is the cornerstone in treatment for paroxysmal AF. Electrical isolation of all pulmonary veins is the endpoint of ablation, and this objective measure of pulmonary vein disconnection is easy to confirm and results in maintenance of sinus rhythm in between 60% and 85% of patients.[57, 58] The difficulty is how to improve on this. Although most of the clinical recurrences associated with this procedure are due to lesion recovery, this does not account for all recurrences.[59-61]

The role of additional substrate modification in paroxysmal AF is controversial. Strategies based on targeting of complex fractionated atrial electrograms (CFAE) result in maintenance of sinus rhythm in a mixed population of patients with both paroxysmal and long-lasting persistent AF in 76% of patients with a single procedure, without necessarily achieving pulmonary vein isolation. A majority of lesions in patients with paroxysmal AF, however, were located around the pulmonary veins. The addition of linear lesions (a roof line connecting the left and right superior pulmonary veins, and/or a mitral line connecting the

mitral annulus to the inferior pulmonary vein) to pulmonary vein isolation improves success rates from 69% to 91% at 18-month follow-up.[62, 63]

The question that is not yet fully answered is how to determine which patients require substrate modification in addition to pulmonary vein isolation during the index procedure. Non-inducibility of AF can be used as an endpoint in paroxysmal AF and the subsequent need for substrate modification, yet this may lead to an overtreatment, that is, excessive ablation, in some patients[64-66]. An alternative option is to perform substrate modification during a second procedure in patients with recurrent AF despite proven pulmonary vein isolation.

2.4.3.2 Long-Lasting Persistent Atrial Fibrillation

The mechanisms underlying long-lasting persistent AF are more complex and multifactorial. Numerous early studies of pulmonary vein isolation (PVI) included patients with both paroxysmal and long-lasting persistent AF, universally demonstrating a much lower freedom of recurrent AF in patients with long-lasting persistent AF. With circumferential pulmonary vein ablation using an electroanatomic mapping technique, freedom from AF was reported in 85% of patients with paroxysmal AF and 68% of those with chronic AF.[67] A further study, also using a circumferential mapping catheter-guided approach, reported an even lower freedom from recurrent AF in persistent (22%) versus paroxysmal (70%) AF, despite achieving electrical isolation in 94% of targeted veins.[68] Using a basket catheter to achieve a 100% rate of PV isolation, freedom from AF was demonstrated in 70% of patients with paroxysmal but in only 44% of patients with persistent AF,[69] further confirming that extension of the technique of PVI alone from patients with paroxysmal to long-lasting persistent AF was inadequate.

The addition of left atrial substrate modification using electrogram-based or linear ablation considerably improves the outcomes in patients with long-lasting persistent AF.[70] In one

randomized study, the addition of left atrial linear lesions (left atrial roof line and a mitral isthmus line) improved the outcome in patients at 16-month follow-up from 20% with PVI alone to 69% with PVI and substrate modification. This was despite evidence of bidirectional block in only 44% of patients with a roof line and 72% with a mitral isthmus line.[70] The incremental benefit of substrate modification (PVI and left atrial linear lesions with bidirectional block) was also seen in a population of patients with heart failure, with 69% of patients being in sinus rhythm, off all antiarrhythmic medication at 1 year.[55]

In the above approaches, the endpoint is a technical endpoint, that is, completion of PVI or linear block; but the procedure is terminated by DC or pharmacological cardioversion in 55% to 90% of cases. In contrast to paroxysmal AF, where noninducibility of AF can be achieved in most patients,[63, 71]the same is not true in long-lasting persistent AF as AF/AT is consistently inducible in the large majority of patients at the end of the index procedure.

2.5 Targets of Catheter Ablation

The therapeutic mechanisms of action and target substrates of catheter ablation for atrial fibrillation are now thought to be more complex than previously recognized. Whilst catheter ablation for atrial fibrillation was initially focused on pulmonary vein isolation, more recently the net has widened substantially to include further supplementary approaches. Four different approaches to catheter ablation of atrial fibrillation are described below:

- 1 Isolation of the triggers and perpetuating reentrant circuits residing in the pulmonary veins (pioneered by Jais and Haissaguerre).
- 2 Disruption of the substrate for perpetuating rotors in the antra of the pulmonary veins and the posterior left atrium (pioneered by Pappone).
- 3 Targeted ablation of ganglionated autonomic plexi in the epicardial fat pads (pioneered by Platt, Jackman, and Scherlag).

- 4 Disruption of putative dominant rotors in the left and right atria proper as recognized by high-frequency complex fractionated electrograms during mapping of atrial fibrillation (pioneered by Nadamanee).
- 5 Mapping of rotors using multipolar catheters (pioneered by Narayan)

Procedural targets of catheter ablation for AF include PV electrical disconnection and additional lesion lines (mitral and roof lines, the endocardial/pericardial coronary sinus [CS] disconnection). The sequence of multiple targets essentially depends on the clinical form of AF (paroxysmal, persistent or permanent AF) and the patient's clinical characteristics.

2.5.1 Pulmonary Vein Disconnection

PV isolation is the primary step in all AF patients undergoing catheter ablation, and is performed by eliminating PV potentials as guided by the Lasso catheter or by encircling atrium he point by point (wide area circumferential ablation). PV disconnection is obtained by optimal catheter stability and tissue contact, which results in attenuation of atrial electrograms during each radiofrequency (RF) energy application. Partially ablated signals require further RF applications before moving on to the next ablation site.

2.5.2 Autonomic Targets with Vagal Denervation

Where possible, elimination of vagal reflexes at innervation sites during the procedure represents one of the most important targets, since vagal denervation is a strong predictor for long-term[77]. Haissaguerre's group were the first to demonstrate that CPVA induces a long-term but transient vagal denervation that enhances the efficacy of the procedure in terms of longterm outcome.[72] These results have been confirmed by many other authors using various AF ablation approaches, and vagal denervation now constitutes a fascinating new AF ablation strategy. Haissaguerre's results on the modification of heart-rate variability (HRV) parameters after ablation provide new insights into the mechanisms of AF and its treatment.

While performing the standard CPVA lesion set, RF applications evoke vagal reflexes in up to 30% of patients. Vagal reflexes are considered to include sinus bradycardia (<40 beats per minute), asystole, AV block and hypotension that occurs within a few seconds after the onset of RF application. If a reflex is elicited, RF energy is delivered until such reflexes are abolished, or for up to 30 seconds. The end-point of ablation at these sites is termination of the reflex, followed by sinus tachycardia or AF. Failure to reproduce the reflexes with repeated RF applications is considered as confirmation of denervation. Complete local vagal denervation is defined by the abolition of all vagal reflexes. Haissaguerre's group reported a detailed 'autonomic map' of the left atrium as a target for ablation, showing that, like the left superior PV, the septal region is richly innervated.[72]

2.5.3 Linear Lesions

Additional ablation lines alter the AF substrate by eliminating large macro-re-entrant circuits able to sustain AF and/or AT.[10–16] Standard CPVA linear lesions include the mitral isthmus line, the roof line and the posterior wall line.[11–16] Multiple additional linear lesions in the left atrium or right atrium (bi-atrial lesions) are required in patients with permanent AF to obtain stable sinus rhythm or AF/AT non-inducibility at the end of the index procedure (CPVA stepwise approach). Each ablation target is performed sequentially based on the cumulative increase of AF cycle length until conversion to sinus rhythm or an AT, which is then mapped conventionally and ablated.[73] In our experience, completeness of lesion lines is important, but in many cases achievement of complete block is unnecessary – particularly in the mitral isthmus line, where a delay of about 100ms is sufficient to prevent post-ablation macro-re-entrant left AT.[74] If necessary, adjunctive linear ablation (usually the septum or the base of the left anterior ascending [LAA]) is performed before CS isolation, which is the last target.

2.5.4 Coronary Sinus Disconnection

If AF/AT inducibility persists even after cardioversion, we accurately revisit lesion lines and encircled areas to check for residual potentials, and apply RF where needed. Conduction block is assessed by the presence of a corridor of double potentials and demonstration of activation moving towards the line of block on both sides. Rapid atrial activity from the musculature of the CS may be a driver for long-lasting or permanent AF. Electrical disconnection of the coronary sinus from the atrium is performed by endocardial or epicardial ablation, or both. Total elimination of CS activity is the ideal end-point, but organisation of CS activity and/or slowing of local rate with dissociation between CS and left atrium potential activity is also considered proof of CS isolation. Endocardial and/or epicardial CS sites are frequent ablation targets in patients with permanent AF and enlarged atria.

2.5.5 Post-ablation Artrial Fibrillation

If targets are successfully achieved in the index procedure, post-ablation ATs may occur in patients, and usually are macro- or microre- entrant gap-related rather than focal tachycardias.[75] Here,PVreconduction is the main cause of AT.[76] In addressing this with a further procedure, PV isolation should be systematically checked as the first step in the AT mapping process. The next step is to exclude macroreentry around the mitral annulus or utilizing the roof by sequential mapping around the mitral annulus for the former and the anterior and posterior walls for the latter, with confirmation with entrainment maneuvers. If macroreentry as a mechanism is eliminated, the next step is to map the atria to find a region with centrifugal activation. Whilst these tachycardias have been previously thought to be "focal," Haissaguirre's group have found that a majority of so-called focal ATs are actually due to small localized re-entry (Figure 2.9 and 2.10).

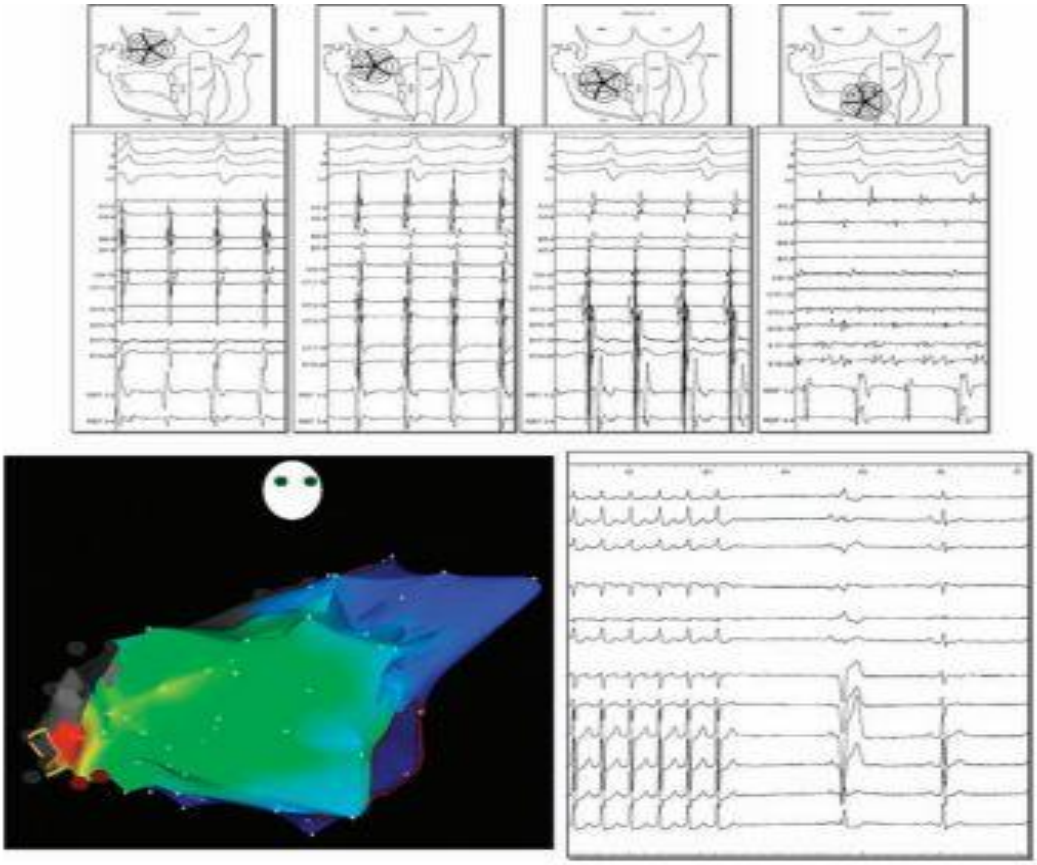

Figure 2-9: Mapping focal sources during atrial tachycardia-differing perspectives dependent upon the mapping system.Upper panel. Using the multipolepentaray catheter, discrete electrograms with a consistent activation sequence are seen. When the catheter is placed near the left superior pulmonary vein, activation in all spines appears on time, with the reference catheter in the coronary sinus, on the bottom of the trace. As the catheter is moved progressively toward the source, activation becomes progressively earlier in spine D, indicating the direction of activation. In the septum there is a dramatic change of mapping through the pentaray catheter, switching from relatively synchronous activation to complex activation, spanning all the cycle length when the catheter is placed directly above the small localized source. This source is likely due to small localized reentry, as confirmed by entrainment mapping. In the lower panel, the electroanatomical map from this patient gives a different perspective. The earliest activation can be seen to come from the inferior septum; but, in fact, considerable postprocessing was necessary to achieve a map, such as the one demonstrated, as it is difficult to assign temporal information to the signals seen in the upper panel, when the mapping catheter is directly above the source. The multiple electrograms at the source have been assigned a single, earliest, timepoint. Ablation at the source location restored sinus rhythm within 10 seconds (righthand panel). This example demonstrates that without a global perspective, given by the multipole catheter, point by point activation mapping would be extremely difficult (Adapted from, Wright et.al. [77]).

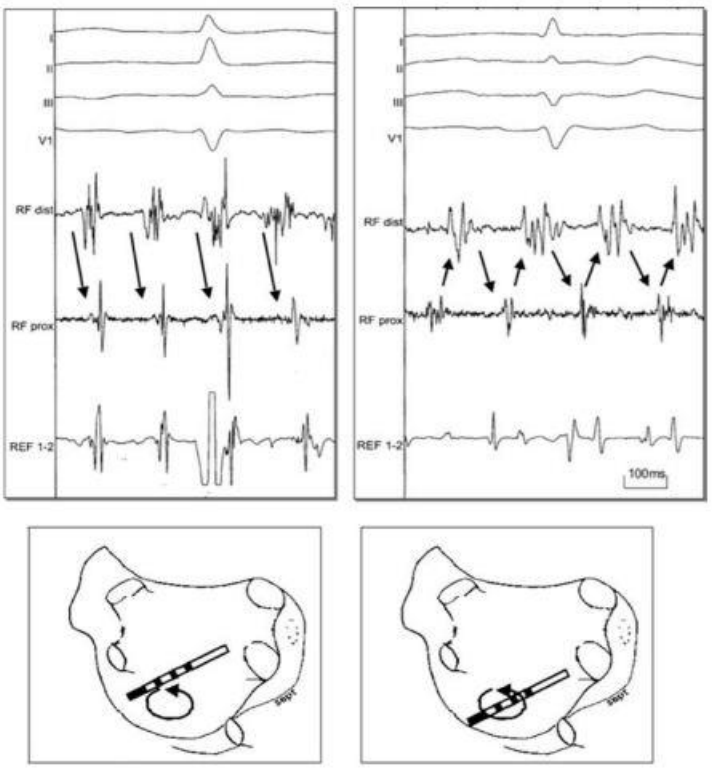

Figure 2-10: Localized temporal gradient. In this example, a source is located in the inferior left atrium. As the mapping catheter is brought to the periphery there is an activation gradient between the two bipoles; as the mapping catheter is placed across the source, the gradient becomes more pronounced, suggesting that the catheter is across two parts of a small localized circuit, or rotor, that may be capable of sustaining AF.((Adapted from, Wright et.al [77]).

2.6 Technical Improvement

2.6.1 Remote Robotic Navigation Systems

Currently, most catheter ablation procedures in patients with AF are performed with manual catheters, which requires advanced operator skills and experience with catheter manipulation and ablation. The feasibility of the remote system, which is not operator-dependent, may represent an attractive alternative approach in many laboratories worldwide to reproduce the success rates of the pioneering groups while minimising risks. Currently, two main systems for magnetic and robotic navigation are available for clinical use (Stereotaxis and Hansen systems, respectively). The safety profile for both systems have been examined and FDA approval for clinical use in America has been obtained with the use in UK and Europe now

entering the third year. Clinical efficacy results to-date have been largely based on single centre studies and further larger multi-centre studies are needed to establish this tools clinical utility and justify the additional costs incurred in purchasing the systems.

2.6.2 Balloon Technology

Balloon technology for PV isolation is not frequently used, as in most patients with AF catheter ablation is not limited to PV disconnection alone, and the achievement of additional multiple targets requires a combination of standard catheter ablation alongside this technology. One advantage of the balloon shaped catheter is the shorter time needed in energy delivery to the PV-LA junction. Neverthless, PVs have largely variable anatomies from patient to patient, with a wide range of diameters, and the frequent presence of common ostia in up to 30% of patients makes the use of balloon-based catheters challenging.

2.6.3 Newer Energy Sources

The safety and efficacy of cryo energy and more recently laser energy appear promising and require large multi-centre studies to ascertain both safety and long term efficacy.

2.6.4 Force Sensing Catheter

Adequate tissue contact is integral in creating durable ablation lesions. Catheters with force sensing features allows the operator to ascertain catheter-tissue contact and titrate the delivery of force applied accordingly in order to create full thickness transmural lesions. Preliminary results on the safety of this catheter has appeared to be promising in the Toccata study and further multi-centre studies are on the way to assess mid-long term efficacy.

2.7 Variations in reported post-ablation clinical outcome

Differences in success rates for similar procedural techniques for catheter ablation of atrial fibrillation reported by different centers arise from a number of factors including:

- 1 Duration and location of clinical and electrocardiographic follow-up (on-site vs remote third party).
- 2 Inclusion of long periods of cardiac monitoring to detect asymptomatic recurrences of paroxysmal atrial fibrillation (pioneered by Kottkamp and Hindricks). The prevalence of asymptomatic recurrences of atrial fibrillation postablation may have been previously underestimated. Reduction of symptomatic episodes post-ablation may arise from a placebo effect or autonomic denervation, and exclusive reliance on patient reporting of symptomatic recurrences as the sole endpoint for determination of efficacy may contribute significantly to the variation in clinical outcome reported by different centres.
- 3 Inclusion or exclusion of early recurrences of atrial fibrillation as procedural failures (blanking period). It is recognized that a transient increase in atrial arrhythmias may be seen in the early post-procedural period (presumably due to subclinical pericarditis after catheter ablation), and over time, a significant proportion of such patients subsequently become free of atrial fibrillation.
- 4 Use of Kaplan-Meier curves of freedom from atrial fibrillation recurrence as opposed to incidence of occurrence during predetermined serial time windows on follow-up (e.g., 3, 6, and 12 months postprocedure—use of a Kaplan-Meier curve and time to first recurrence results in a lower success rate being reported). Time to first recurrence has the advantage of being relatively simple to apply and easy to compare with outcome of antiarrhythmic drug therapy but is clinically less meaningful.

Consideration may need to be given to the adoption of a subclassification of atrial fibrillation based on clinical criteria if the magnitude of therapeutic impact of catheter ablation on patients' quality of life is to be meaningfully assessed. For a patient who is transformed from a predominant pattern of highly symptomatic persistent atrial fibrillation with occasional

spontaneous terminations preablation to a pattern of asymptomatic or symptomatic short-lived episodes of transient atrial fibrillation (lasting 30 seconds or 1 minute) postablation, the procedure could be deemed clinically successful. In contrast, a binary outcome analysis limited to whether a patient has any recurrence of atrial fibrillation at any time or is free of atrial fibrillation recurrence would classify the ablation as a failed procedure and any clinical benefit to the patient would not be recognized. These endpoints extend to pharmacologic therapy.

Beyond differences in follow-up and outcome analysis, variations in procedural techniques undoubtedly contribute to the wide range of outcomes reported from different centers. The vast majority of investigators continue to employ radiofrequency energy as the primary ablation modality. However, there are substantial differences in procedural technique including the variation in electrodes size (4 mm, 8 mm, and irrigated), duration of radiofrequency applications (5–60 seconds), power settings (30–70 W), temperature limits (40°C–43°C for irrigated and 50°C–70°C for nonirrigated) currently used at different laboratories. In some centers, different settings are now used in different atrial locations with lower settings used for the posterior left atrial wall because of the risk of esophageal fistula formation. In vitro and in vivo studies have shown that differences of >40°C can develop between electrode tip temperatures at the endocardial interface and intramyocardial temperatures and, thus, steam pops can occur without prior achievement of a high electrode temperatures (Bunch and Packer). This temperature difference is greater for 8 mm electrodes than for 4 mm electrodes. More thrombus formation is seen with 8 mm electrodes compared to irrigated electrodes (Nakagawa and Jackman).

2.8 Magnetic resonance imaging

2.8.1 Brief Historical Perspective of MR Imaging

The phenomenon of nuclear magnetic resonance was described in the 1940's independently by both Felix Bloch and Edward Purcell. This was used widely over the subsequent two decades for analysing chemical compounds. It was only in the 1970's following MR tissue characterisation by Damadian when MRI application entered the clinical arena. It's imaging application began with Lauterbur having the idea of applying magnetic field gradients in three dimensions to derive spatial orientation using MRI. Subsequent introduction of phase and frequency encoding introduced by Ernst alongside the Fourier transformation forms the basis of modern MRI techniques. This was taken a step further with Mansfield developing echo-planar imaging, with improvements in the use of gradients and signal analysis.

2.8.2 Basic Principles of CMR

The hydrogen atom consists of a positively charged proton and is abundant in the human body. This forms the basis for the use of MRI in medical imaging. The proton has an inherent spin, which creates a tiny magnetic field. In the tissues of the body, the magnetic fields resulting from each proton are randomly distributed. When the body is placed in a large and powerful magnet, these tiny magnetic fields align with the large external magnetic field and reach equilibrium. This equilibrium can be disturbed by applying energy to the to the body's tissues ("excitation"). The latter is achieved by using a radiofrequency (RF) pulse, provided the pulse is of the same resonance frequency as that of the protons. The result of the excitation with the RF pulse is a rotational movement of the total magnetization, called precession. (The frequency of precessioin for protons is proportional to the magnetic field strength and the strength of the magnetization is dependent on the proton density in the tissue.) The angle of magnetization is moved to an angle away from the main magnetic field depending on the amplitudeand duration of the RF pulse. The magnetization rotates around

the main axis of the magnetic field, resulting in high frequency alternating magnetic field. This gives rise to a signal, which is a voltage that can be measured in a receiver coil.

However the signal is only transient, as the nuclei gives off the acquired energy back to the surrounding tissues and the magnetization realigns in the longitudinal plane with the main magnetic field, at an exponential rate. This is termed longitudinal relaxation. The rate at which this happens depends on the characteristics of the tissue – if the equilibrium is restored more quickly, the tissue has a short T1 (longitudinal) relaxation time. The second aspect of restoring equilibrium is loss of the transverse component of magnetisizationie that which is in the plane perpendicular to the axis of the magnetic field. This happens because of the interaction between different protons causing inhomogeneities in the magnetic field. The rotating vector of magnetisization are fanned out in ("dephased") such that they are all not pointing in the same direction. Although they remain within the plane perpendicular to the magnetic field. As a result, the sum of these rotating vectors is reduced and so is the signal. This is known as a transverse relaxation. Again, the speed at which this occurs is dependent on tissue properties which govern the T2 (transverse) relaxation time.

Special orientation is necessary in order to create an image. This is made possible using gradient fields. In contrast to the static field of the magnet, gradient fields can be altered over time in all 3 dimensions. In this way, a 2D slice can be selected by applying a gradient in the direction perpendicular to it, whilst the excitation RF pulse is transmitted. The pulse will only have an effect on the slice of tissue in which the protons have the same resonance frequency as the pulse itself. The signal in-doctored in the detector coil is described by sine function. The frequency of this function are used to define spatial orientation. Phase differences result from the use of a gradient field in one direction ("phase encoding") and frequency differences in the signal result from a gradient field applied in the other direction of the field of view ("frequency encoding"). This sampling process is repeated

multiple times (this is the number of phase encoding steps) in order to acquire all of the spatial frequency components needed to make the image. The time between consecutive measurements is called the repetition time ("TR"). The image can then be calculated using these individual spatial frequency components using Fourier transformation. This gives a representation of the signals in the frequency domain. The digitized representations of these signals are converted into a data matrix called k-space which is derived on one axis from frequency encoding information and on the other from phase encoding information. Data in the centre of k-space encodes contrast information – as it has low spatial frequency but high amplitude – whereas data in the periphery of k-space provides image sharpness, as it has high spatial frequency but low amplitude.

2.8.3 Techniques for CMR

2.8.3.1 Spin Echo

This sequence uses a 180 degree pulse at a given time after the excitation RF pulse, in order to reverse the dephasing of the transverse magnetisization. This magnetisization vectors come back into phase and produce a spin-echo. The echo time ("TE") is the time between the initial RF pulse (a 90 degree pulse) and the maximum spin echo signal, so the 180 degree pulse is applied half way through this period.

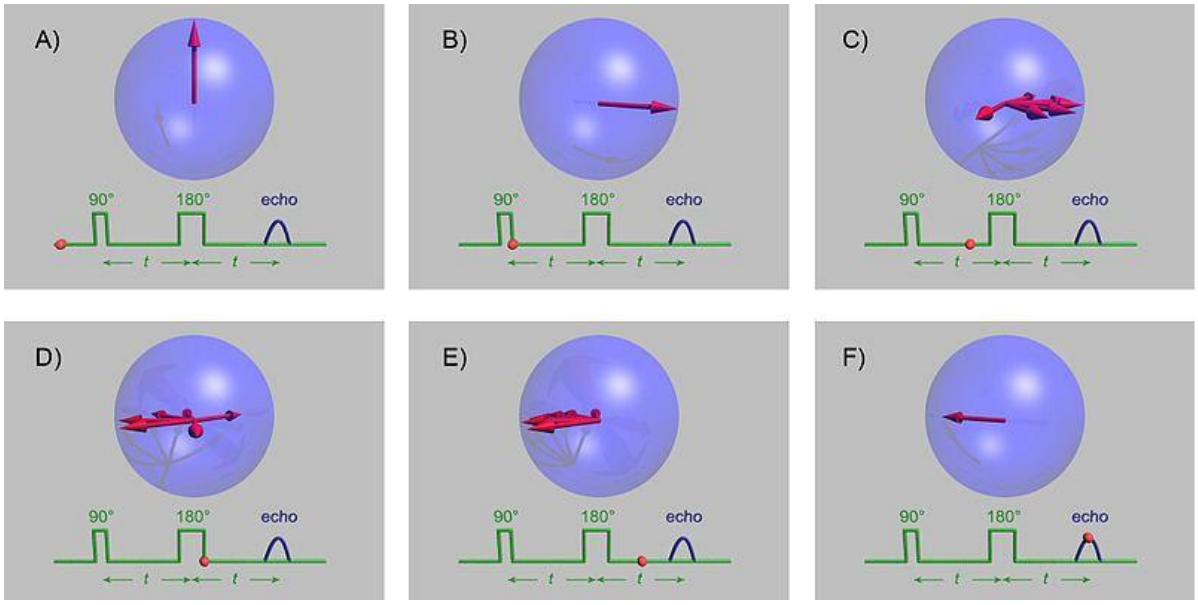

Figure 2-11: The spin echo sequence. A) - The vertical red arrow is the average magnetic moment of a group of spins, such as protons. All are vertical in the vertical magnetic field and spinning on their long axis, but this illustration is in a rotating reference frame where the spins are stationary on average. B) A 90 degree pulse has been applied that flips the arrow into the horizontal (x-y) plane. C) Due to local magnetic field in-homogeneities (variations in the magnetic field at different parts of the sample that are constant in time), as the net moment processes, some spins slow down due to lower local field strength (and so begin to progressively trail behind) while some speed up due to higher field strength and start getting ahead of the others. This makes the signal decay. D) A 180 degree pulse is now applied so that the slower spins lead ahead of the main moment and the fast ones trail behind. E) Progressively, the fast moments catch up with the main moment and the slow moments drift back toward the main moment. F) Complete refocusing has occurred and at this time, an accurate T2 echo can be measured with all T2 * effects removed. Quite separately, return of the red arrow towards the vertical (not shown) would reflect the T1 relaxation.

Spin echo sequences are primarily used to define anatomy in a two dimensional image. This is very little signal from the blood pool, so these are often called black-blood images. This sequences are often used to visualize cardiovascular in detail. ECG and respiratory gating are needed to avoid motion artefact. Image acquisition in the past was relatively slow but has been improved with fast spin echo sequences to allow acquisition within a single breath-hold. A great strength of spin echo imaging is in the tissue characterisation. Depending on the weighting to T1 or T2 different tissue properties can be exploited. For example, myocardium oedema is best seen on T2 weighted imaging.

2.8.3.2 Gradient Echo

Gradient echo sequences allow much shorter acquisition times than spin echo sequences. This is because of the angle of the excitation pulse is smaller (less than 90 degrees) so the time needed for longitudinal relaxation is shorter. Therefore repetition times can be used. This permits imaging of multiple phases throughout the cardiac cycle, and is used to provide cine images using ECG gating. The typical gradient echo sequence is a steady-state free precision (SSFP), which is well suited to assess cardiac function as there is a good contrast between blood and myocardium. A steady state free precision imaging allows visualization of cardiac function in conventional views, as would be used in 2-D echocardiography. The advantages of this approach over echocardiography include special resolution, lack of dependence of acoustic windows and freedom from operator variability.

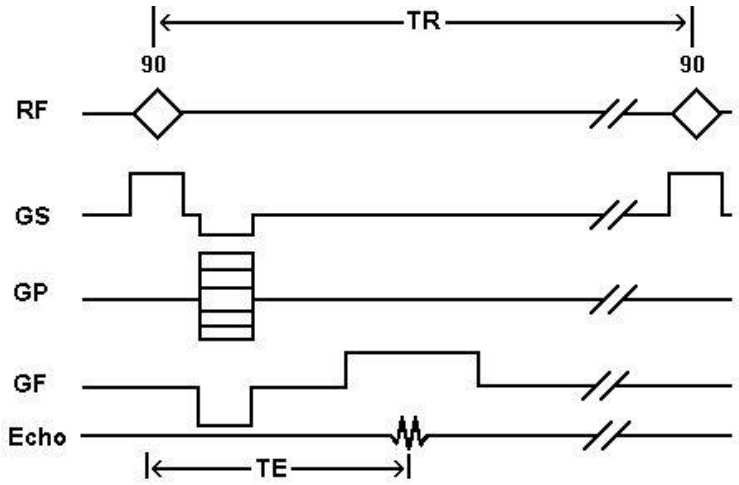

Figure 2-12: The gradient echo sequences show a wide range of variations compared to the spin echo and inversion recovery sequences. Not only is the basic sequence varied by adding dephasing or rephasing gradients at the end of the sequence, but there is a significant extra variable to specify in addition to things like the TR and TE. This variable is the flip or tip angle of the spins. The flip angle is usually at or close to 90 degrees for a spin echo sequence but commonly varies over a range of about 10 to 80 degrees with gradient echo sequences.

Global right and left ventricular function can be quantified using a series of parallel breath-hold images (a stack) either in short axis or axial plane. Regional LV function is conventionally assessed in the 2,3 or 4 chamber long axis views, or in the short axis views.

SSFP images provide a high signal to noise ratio and may also be used for the 3 dimensional imaging of the heart to give angiographic images without the need for a contrast agent.

2.8.3.3 Parallel Imaging

In order to eliminate the effect of respiratory motion, breath-hold images are often used in CMR. Parallel imaging is one technique to reduce the acquisition time so that the duration of the breath-hold can be minimised. An approach that is commonly used is sensitivity encoding (SENSE). There are several RF surface coils (or phase array coils), which receive the signal, and are at different positions. The sensitivity of each coil reduces with the distance of the coil from alternating magnetic field which is generating the signal. Therefore the coils have different sensitivity maps. The sensitivity maps of different coils can be used to reconstruct the image from a smaller field of view by separating out signal from within this area, from signal which is folded-over from outside this area. This allows the time taken to perform the scan to be reduced. Alternatively, using SENSE with the same acquisition time permits greater temporal or spatial resolution to be achieved.

2.8.3.4 Delayed Enhancement Imaging

This technique is used to visualise myocardium damage, such as scar or fibrosis. An intravenous contrast agent is administered most frequently as a chelate of gadolinium. This agent is extracellular. Therefore it is distributed into the intravascular and interstitial space, but does not penetrate healthy myocardial cells. Areas of acute or chronic infarction show higher signal than normal tissue. The inversion recovery technique is used to null the healthy myocardium – by suppressing the magnetisation, the tissue appears dark. The contrast agent accumulates in areas of damaged myocardium, an appears bright due to faster T1 relaxation. The distribution and percentage thickness of delayed enhancement can be used to assess tissue injury and myocardial viability.

2.8.3.5 Whole Heart 3-D Imaging

This gives detailed anatomic information with whole heart coverage. The patient can breathe normally throughout the scan (free breathing). Scans are ECG gated to commence at mid-late diastole when the heart is relatively static. The timing of this acquisition is based on a 3 or 4 chamber SSFP cine image. Artefact due to respiratory motion is avoided using a respiratory navigator, which is a visual marker positioned over the dome of the diaphragm. Data for image reconstruction are then only accepted during a limited window in the cardiac and respiratory cycles. This approach provides good signal to noise ratio and gives higher resolution images than breath-hold techniques. Nevertheless, due to relatively small window of acquisition, these sequences take several minutes to acquire.

2.9 Left Atrial CMR Imaging

Cardiac magnetic resonance (CMR) imaging is an imaging technique with excellent soft tissue contrast and provides high resolution two-dimensional (2D) and three-dimensional (3D) images. The use of paramagnetic contrast agents have previously established areas of cardiac pathology - tissue necrosis and inflammation within the left ventricle. [78-81] This is made possible through the poor washout kinetics of the contrast agent[78]. Areas of irreversible injury become visible under MRI following the administration of the contrast agent which are retained in these areas but are washed out faster in healthy areas, leading to a phenomenon known as delayed enhancement (DE) or late enhancement (LE). MRI is also sensitive to variations in water content, and thus is effective at the detection of oedema in the left ventricle. Numerous studies have demonstrated a linear relationship between T2 relaxation time and myocardial water content[82-86]. Recent progress in motion correction leading to better spatial resolution has allowed DE and oedema imaging of the left atrium.

2.9.1 The role of pre-ablation CMR imaging

Atrial fibrillation promotes atrial structural and electrical remodelling. Animal work has correlated areas of discrete low voltage with abnormal atrial tissue, including atrial scar. There are multiple mechanisms at work promoting the formation of scar in the fibrillation atrium and this is of clinical relevance as there is a well recognised correlation between the presence of pre-existing left atrial scar and procedural outcome following catheter ablation. However, this information is rarely available prior to an ablation procedure as the left atrial voltage distribution can only be accurately assessed by direct measurement made from within the chamber at invasive EP study.

DE-CMR imaging of the left atrium allows for the quantification of pre-existing scar non-invasively. Previous DE-MRI work has been performed extensively in the left ventricle to characterise tissue heterogeneity that can potentially increase arrhythmia initiation and ischaemic ventricles to differentiate hibernating myocardium from non-viable tissue. Recent advances in improved MR sequences and reconstruction software has allowed for the visualisation and analysis of LA tissue.

There are some clear areas in which the clinical relevance of pre-ablation LA delayed enhancement imaging may be useful: (i) Global chamber quantification of scar and its regional distribution may inform the decision to ablate and the likelihood of success, (ii) knowledge of scar burden with co-existing different disease processes, (ischaemic heart disease, thyroid disease, hypertension, diabetes) may predict clinical outcome, (iii) the pattern of scar following previous left atrial intervention may predict sites critical to arrhythmia recurrence eg visible discontinuities in circumferential or linear ablation lesions and therefore inform ablation strategy (iv) scar information may inform choice to drug therapy, favouring “anti-remodelling” medication over anti-antiarrhythmic drugs as has been the case for ventricular dysfunction (v) knowledge of scar distribution and its correlation with regional

atrial electrophysiology will improve our understanding of the role and mechanism of atrial fibrosis in AF.

(i) Scar burden and AF disease progression

Fibrillation and fibrosis is likely to be a bi-directional process. In animal models, increased AF occurrence is seen following experimentally induced atrial fibrosis.[87] Similiarly, an increase in collagen -1 and fibronectin-1 in atrial tissue is seen following rapid pacing of cardiac myocytes.[88] In human LA tissue obtained during cardiac by-pass surgery, increased tissue fibrosis has been documented in patients with AF.[89] Quantifying this pre-existent fibrosis in-vivo non-invasively to assess the extent of AF disease progression is important. To-date, published work[90] showing a lesser degree of delayed enhancement in patients with AF of shorter duration than in patients with long lasting persistent AF. This observation helps corroborate the link between the degree of fibrosis and disease severity.

Whilst the association between atrial fibrosis and atrial fibrillation remains a combination of mechanisms, it is well accepted that more fibrosis means more severe disease. This has led to the Utah staging system based on the increasing extent of pre-existing DE-LA MRI.[90] There are four stages in this system, Utah 1: no or minimal fibrosis; Utah 2: 5-20% fibrosis, Utah 3: 20-35% fibrosis and Utah 4 more than 35% fibrosis in the atria. This classification system may have a potential role in tailoring treatment modality.

(ii) Pre-existing scar and clinical response to ablation

The greater the burden of scar and atrial fibrosis, the less the likelihood of functioning atrial myocardium. Oakes et al[90] have demonstrated an association between increased areas of LA enhancement and AF recurrence following catheter ablation. Patients with a greater degree of delayed enhancement in the LA wall incur a higher recurrence rate. Not only was the amount of DE important, but also the anatomical distribution. Patients with DE confined only to the

LA posterior wall and septum had a better clinical outcome following catheter ablation compared to patients with enhancement in all portions of the LA. Larger similar multi-centre studies confirming the significance of pre-exisiting enhancement and procedural outcome data may allow this to be an independent prognostic marker for AF ablation . The earlier described Utah staging system of left atrial DE can be a useful utility once validated in patient selection, especially in the persistent AF cohort. Candidates with a high pre-existing atrial scar maybe best served by medical optimisation. On the whole, better patient selection does translate into more optimum resource utilisation; leading to greater cost efficiency and reduced unnecessary patient procedural exposures. Patients can also be better advised on outcome possibilities, those with greater quantified areas of enhancement can have a reduced long term success expectation should they agree to proceed.

(iii) Scar distribution following prior LA intervention

Whilst some patients undergo ablation procedures with left atria that is naïve to previous radiofrequency energy delivery, a good number of patients have previously had an ablation either in the same centre or another one. In this case, establishing the lesion set achieved during the previous procedure may enable planning a better ablation strategy. DE MRI of the left atrium allows for this in-vivo visualisation of scar in relation to the anatomic structures. This gives the electrophysiologist an idea of how much of the previous ablation procedure was successful in creating areas of intended scar and thus how much further ablation work that is necessary. The role of DE MRI in re-do procedures shall be discussed further in the subsequent section.

(iv) Scar distribution and atrial electrophysiological characterisation

Having established the role of delayed enhancement in assessing scar burden, and potentially playing a future role in patient selection, it would be appropriate to try and correlate various delayed enhancement regions within the left atrium to the intracardiacelectrograms. This will

entail the quantification of scar within various regions of the atrium and assessing the electrical potentiality in these regions in the cardiac catheter laboratory prior to catheter ablation. Establishing a correlation between various MR signal intensity range to electrical activity may allow for an indirect way of electrophysiologically characterising areas of delayed enhancement into zones of electrical activity versus electrical inertia.

Aside tissue characterization and delayed enhancement (fibrosis) quantification, basic anatomical data, volumes and function can be obtained. Whilst LA anatomy is more often homogenous, PV anatomy heterogeneity is common. This non-pathologic variation does occur with a 30-40% incidence [91]; the most common being a single left common pulmonary vein or an additional right pulmonary vein.[92]

2.9.2 The role of post-ablation CMR imaging

Pulmonary vein antrum ablation is the cornerstone technique for catheter ablation in treating patients with PAF. This method involves delivery of radiofrequency energy in a wide encirclement pattern around ipsilateral pairs of pulmonary veins with subsequent completion of electrical isolation guided by a circumferential mapping cathether. Energy delivery this way creates scar barriers between the PV and the left atrium. Areas of tissue injury following catheter ablation can be visualised using delayed enhancement CMR. A correlation between the presence of greater DE post ablation and a better clinical outcome has been established.[93]

2.9.3 Re-do catheter ablation procedures

Electrical reconnection of the PVs to the LA is common following AF ablation and can occur in up to 80% of cases. [94, 95] This is thought to account for the majority of cases of AF recurrence. [96] Recurrences also may arise due to gaps within the pulmonary vein antrum lesion set due to incomplete encirclement. Pulmonary vein antrum isolation is a technically challenging procedure requiring contiguous lesions within the complex and heterogeneous

Left Atrium (LA)-Pulmonary Vein(PV) structure. Conventional fluoroscopy uniformly used for real time visualization of catheter position only provides a two-dimensional representation, resulting in the possibility of some anatomic variations being inadequately visualized. Despite the use of electroanatomic mapping systems, precise catheter location can be affected by both the beating heart and respiratory motion, impacting on accuracy and spatial referencing within the three-dimensional mapping systems .[97]

Post ablation DE MR scans suggests that a continuous complete circumferential encirclement around the pulmonary vein is infrequently achieved.[98] These CMR scans have the potential to providing a road map to areas of successful scar formation following energy delivery and lesion creation. This in return allows for the identification of gaps in lesion sets which can be useful in planning further subsequent ablation procedures. Anatomical targets observed on these CMR scans may assist in developing a catheter ablation strategy in cases with recurrences. Importantly, the completion of conduction gaps during repeat procedures have proven to eliminate further arrhythmias recurrence.[98, 99] This information can be used together with electrophysiological findings during catheter ablation to understand the relationship between ablation lesion sets and post-ablation arrhythmias. Further imaging can be performed to confirm the completion of these gaps following the repeat procedure.

2.9.4 Correlating points on mapping systems to MR ablation lesions

Electro-anatomic mapping systems have emerged to help locate the substrate for cardiac arrhythmias and to guide ablation. These consist of data acquisition and display systems that analyse acquired electrical signals, determine the location of the catheter tip and use the gathered anatomical and elecrophysiological data to generate 3D electroanatomical maps.[100] These maps, however cannot anticipate variations in anatomy and may be incomplete or

inaccurate. Typically, the points at which ablation energy is delivered are marked on the map when there is a reduction in the local electrogram voltage, but this does not necessarily establish the creation of a permanent ablation lesion or continuous ablation line.[101] The degree of contact between the ablation catheter tip and atrial wall as well as wall thickness are likely to be important factors in forming adequate ablation lesions but are poorly assessed by fluoroscopy or electro-anatomical mapping systems.[102] Integration of images obtained from CT can improve soft tissue delineation but have been shown to be inaccurate when a system-independent assay of accuracy is performed.[103]

Recent developments in computer software and programming have allowed for overlaying CMR or computed tomographic anatomical data with electrophysiological anatomical data. This has been driven by the prospects of improved anatomy depiction which in turn may translate in increasing more effective ablation delivery whilst reducing procedure time and radiation dose. Whilst ablation points are recorded on the EAM system, however the efficacy of each ablation point is difficult to determine during the procedure.

Utilising LA MR imaging and using custom designed registration computer software, intended points of ablation on the EAM system can now be evaluated against the actual late enhancement (scar) areas on the MR scan. Recent work comparing ablation points on CartoBiosense Webster and the LE images has demonstrated both a good registration between the Carto surface points and the MRA surface.[104] Whilst an average distance of 3.6±1.3mm between Carto ablation points and LGE scar was recorded, 20% of sectors with sites of Carto ablation showed no evidence of LGE.

The use of this utility now allows the possibility of assessing current mapping tools and further improving present technology.

2.9.5 Potential future roles

The role of inflammation is now increasingly being implicated in the initiation and perpetuation of AF. [105]This has been corroborated by various inflammatory markers including CRP [106], IL-1, IL-6 and TNF-alpha. [107] This inflammation may lead to atrial remodelling and long term fibrosis. Whilst the exact mechanism of inflammation initiating and perpetuating AF can only be speculated, medications such as statins and ACE-inhibitors are being used in primary and secondary prevention of AF.

MR imaging can offer a potential role in assessing LA reverse remodelling, qualifying and quantifying reduction in DE (fibrotic areas) whilst calculating functional parameters such as atrial ejection fractions. In vivo data of the extent of disease modification can be closely studied and similarly the therapeutic effects of other pharmaceutical agents can also be followed- through.

Also, new catheter ablation tools can be studied using MR imaging. Both the quality and character of lesions delivered in-vivo can be assessed. The use of newer materials utilised in catheter design (eg. gold), catheter shapes and dimensions which may confer unique ablation lesion set patterns can be studied. In this way, devices that favourably promote more scar formation can be assessed in vivo in humans for the first time. Simultaneously, alternative energy sources may also be assessed.

3 General Methodology

Patients

The St Thomas' Hospital local ethics committee approved the studies (Appendix 1). All patients provided written informed consent. Studies were performed in compliance with the Declaration of Helsinki.

3.1 Patient selection

3.1.1 Inclusion Criteria

a) Patient has documented symptomatic paroxysmal AF whilst taking one or more anti-arrhythmic medication.

b) Paroxysmal AF of at least 3 months duration.

c) Between 18 and 75 years of age

e) Patients of childbearing potential must have a negative pregnancy test (within 7 days of the procedure)

f) Patient must provide written informed consent.

g) Patient is willing and able to comply with the follow-up protocol

3.2.2 Exclusion Criteria

a) AF associated with a recent unstable cardiovascular status (i.e. ischaemic chest pain or haemodynamic instability).

b) Medical condition unknown to worsen or precipitate AF (eg hyperthyroidism) that is not under current stable medical treatment.

c) Previous Pulmonary Vein Isolation.

d) Contraindications for an MR scan (eg implanted metallic prosthesis, pacemakers)

e) Significant renal impairment (eGFR<30ml/min/1.73m^2)

f) Cardiac surgery during the previous 3 months, myocardial infarction within 6 weeks or having unstable angina.

g) History of pulmonary stenosis (with or without symptoms).

h) Known or suspected coagulopathy or bleeding diasthesis.

i) Contrast allergy.

j) Presence of an intra-cardiac thrombus on a pre-procedure TOE.

k) Contraindication or an inability to comply with long-term anticoagulation therapy.

l) History of stroke or TIA in the last 3 months

m) Left atrial dimension of >5.5cm

n) History of inability to obtain vascular access and/or transseptal puncture is contraindicated.

o) Evidence of sepsis or acute metabolic illness

3.2 Qualifying Baseline Assessments

The following baseline assessments were performed to determine the presence of atrial fibrillation and eligibility to enter the study:

- Medical history, including documentation of AF, previous anti-arrhythmic intervention/therapies and anti-arrhythmic medication history.

- Routine Haematology, Biochemistry and Clotting Profile
- Standard 12 Lead ECG
- Cardiac MR scans
- Perform or retain documented Trans-oesophageal echocardiogram (TOE) to exclude the presence of LAA thrombus in patients who at risk of it based on the CHADS2 score system. A score 2 and greater will qualify a patient for a TOE.
- Perform or retain documented Transthoracic Echocardiogram (TTE) [completed within 3 months prior to procedure] to evaluate standard structural measures – ejection fraction, LA size and valve measurements]

Transoesophageal echocardiogram (TOE) were performed in patients who required it (i.e. CHADS2 score 2 and above) within 24 hours of scheduled procedure if the INR was measured at <2 at anytime in the preceding 4 weeks. If the TOE showed the presence of an intra-cardiac thrombus, the patient was excluded.

Urine or serum pregnancy test was performed within 24 hours prior to the scheduled procedure as appropriate. Patients confirmed pregnant were excluded from the study.

Patients were stabilised on warfarin with INR > 2.0 4 weeks prior to the procedure.

3.3 Catheter Ablation

3.3.1 Set up

All ablation procedures were performed at St Thomas' EP catheter laboratory. Patients were attached to standard haemodynamic monitoring and electrocardiographic equipment. RF generator ground pads will be securely attached to the patient's skin with a sufficient quantity of conductive gel. Conscious sedation anaesthesia was administered accordingly to standard institutional practice.

3.3.2 Access, Anti-coagulation and 3-D left atrial maps

Intravenous access was achieved via both right and left femoral veins. A 6F decapolar catheter was placed in the coronary sinus to provide a reference for electroanatomic mapping and to enable LA pacing. Double transseptal punctures from the right femoral vein was performed manually and access to the left atrium was obtained using 8.5Fr non-deflectable long sheaths, (St. Jude Medical Inc., St. Paul, MN, USA). Patients with a Patent Foramen Ovale (PFO) had the transseptal systems placed through the PFO. Following the first transseptal puncture, intravenous heparin bolus was administered to achieve an activated clotting time of between 300 and 400 seconds. Both circular mapping catheter (Inquiry™Optima™, St. Jude Medical Inc.) and NaviStar® ThermoCool® 3.5 mm irrigated tip catheter (Biosense Webster Inc., Diamond Bar, CA, USA) were employed to create a 3-dimensional geometry of the left atrium with either NavX™ (St. Jude Medical Inc., St. Paul, MN, USA) or CARTO XP (Biosense Webster Inc., Diamond Bar, CA, USA). transeptal puncture to the left atrium performed in the standard way.

All sheaths and guiding catheters were aspirated and flushed with heparinised saline to remove all air prior to any catheter insertion or removal. A continuous heparinised saline drip was used at a rate that will ensure luminal patency and prevent clot formation in all sheaths. ACTs were measured regularly, and subsequent heparin boluses were administered accordingly to achieve a target range of between 250-350 seconds.

3.3.3 Pulmonary Vein Encirclement

All pulmonary veins were isolated using the wide area pulmonary antral circumferential ablation (WACA) approach. The circular mapping catheter was placed in each pulmonary vein in turn while the corresponding LA-PV antrum was targeted with wide area circumferential ablation. Pulmonary vein isolation was confirmed by the lack of potentials in the pulmonary veins or the presence of dissociated PV potentials. Ablation lesions were

marked on the LA geometry when there had been an 80 % reduction in the local electrogram voltage or after 30 seconds of energy delivery. One tag was applied to the shell per 30s RF energy delivery and a standard tag size was used throughout the study. If LA-PV conduction persisted despite wide area circumferential ablation, additional lesions were delivered at sites of earliest activation on the circular mapping catheter until entry block in all 4 veins was confirmed by observing the elimination or dissociation of pulmonary vein potentials. Exit block was not routinely assessed. Neither adenosine nor isoprenaline was routinely administered to test the integrity of PVI or to search for non-PV triggers of AF. No linear ablation was performed in patients with paroxysmal AF.

3.3.4 Tissue Contact Assessment

The ablation catheter was observed on the fluoroscope and mapping system display to confirm correct positioning. Bipolar electrical signals was observed from the electrode catheter. For manual procedures, sharp electrograms with high frequency signal components, low electrical noise and large relative signal amplitudes, together with operator assessment, was used to indicate good contact. For robotic procedures, these indicators was used in conjunction with Intellisense readings. Intellisense will be targeted in the 20-30g range.[18, 19]

3.3.5 Tissue Ablation

In both Hansen Robotic Assisted and Standard Catheter ablation groups, energy was delivered until local electrograms were attenuated. In the Hansen group the power, duration and force settings of between 15-30W at the intellisense range of 20-30g (recommended not above 40g) were applied. In the manual group, 60 scond applications were delivered at power settings between 40-60W. Force applied was operator dependent accordingly.

3.4 Cardiac MRI

3.4.1 Acquisition

CMR scans were performed on a 1.5 Tesla Philips Achieva MR system (Philips Healthcare, Best, Netherlands), using initially a 5 channel and then moving onto the 32 channel surface coil (Invivo, Orlando, Florida, USA).

3.4.2 Interactive planning

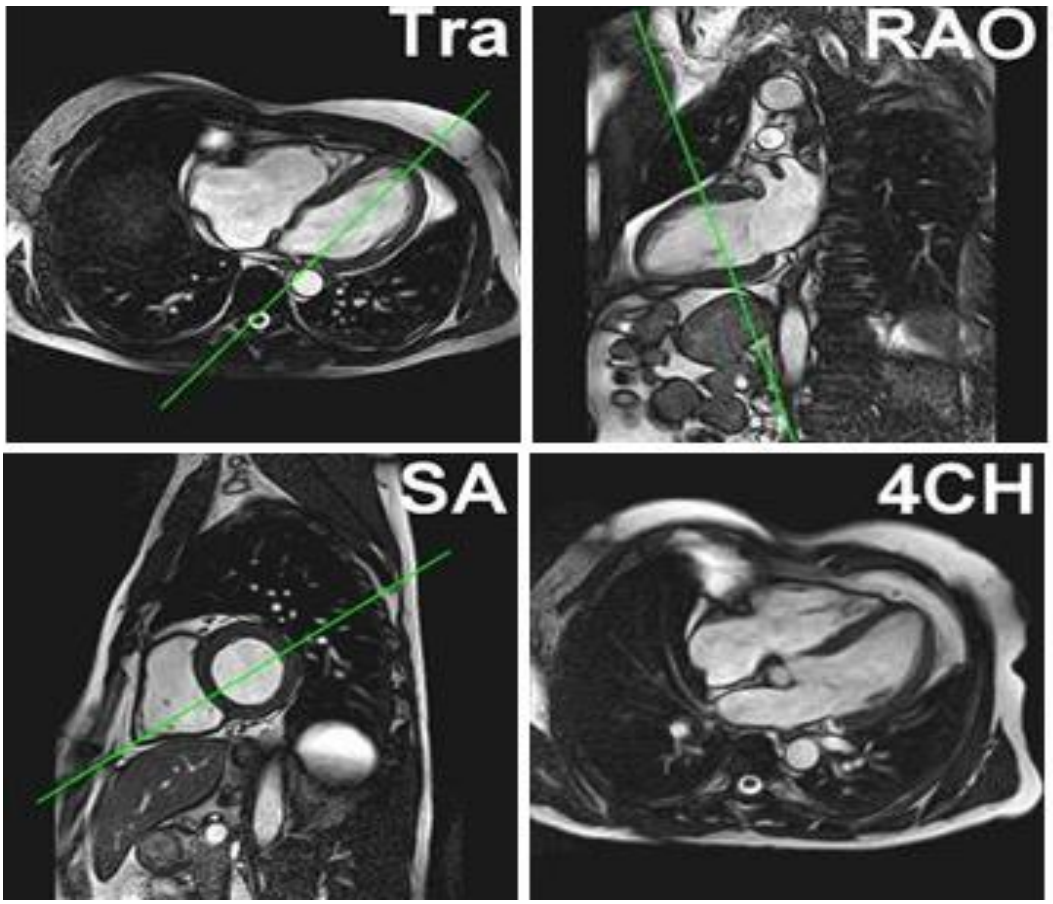

Figure 3-1: Interactive planning of cardiac MR in one of the study patients.

The cardiac MR examination began with a survey and reference scans, and an interactive scan to determine the four-chamber orientation of the heart. Interactive imaging was performed using rapid SSFP sequences to manipulate the geometry of the imaging plane.This

allowed planning of the geometry to be used in subsequent sequences. Four viewing windows were used to show theactive imaging plane as well as its relationship to three previously acquired images, with the active imaging plane depicted by a line in these images. The line in any of the three images couldbe moved in order to change the angle of the active imaging plane itself. In addition the active imaging plane could be displaced in parallel planes to that which is showing the "push/pull" function. Geometrics were stored for use later in the MR examination.

3.4.3 2D-Cine

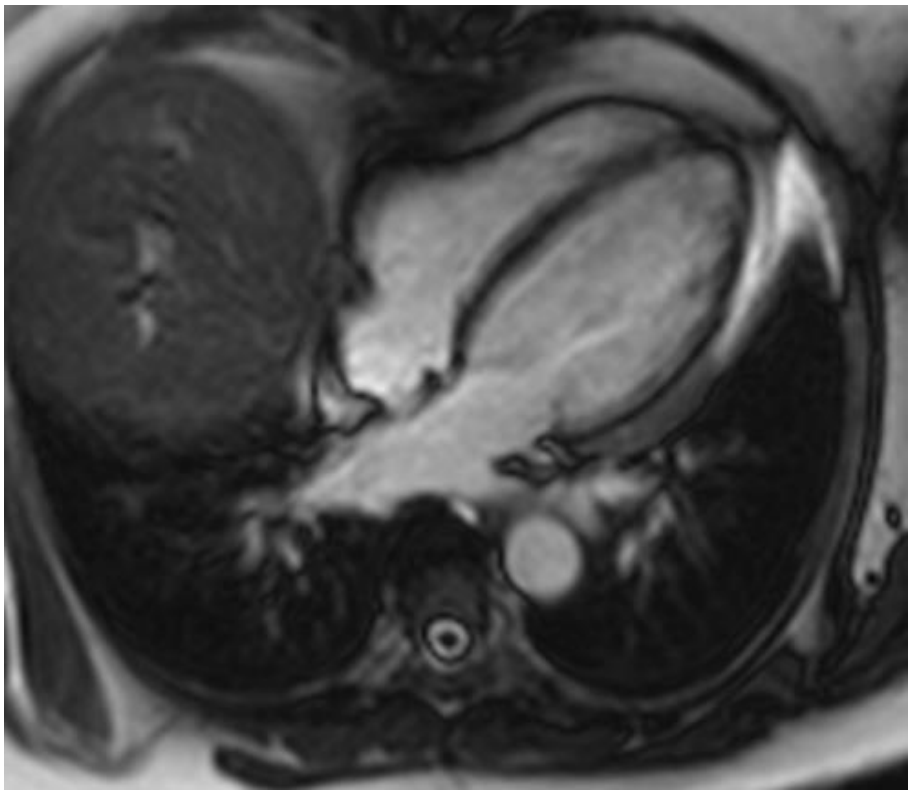

Figure 3-2: An example of a 2D cine scan acquired in the four chamber orientation that is used to determine the trigger delay time

A 2D cine scan was performed to acquire the four chamber orientation to determine the time after the R-wave at which atrial motion was at a minimum, commonly found at ventricular

end-systole. All subsequent ECG triggered scans was set to the trigger delay time determined from the cine, to reduce cardiac motion and optimise image acquisition.

3.4.4 T2-Weighted Imaging

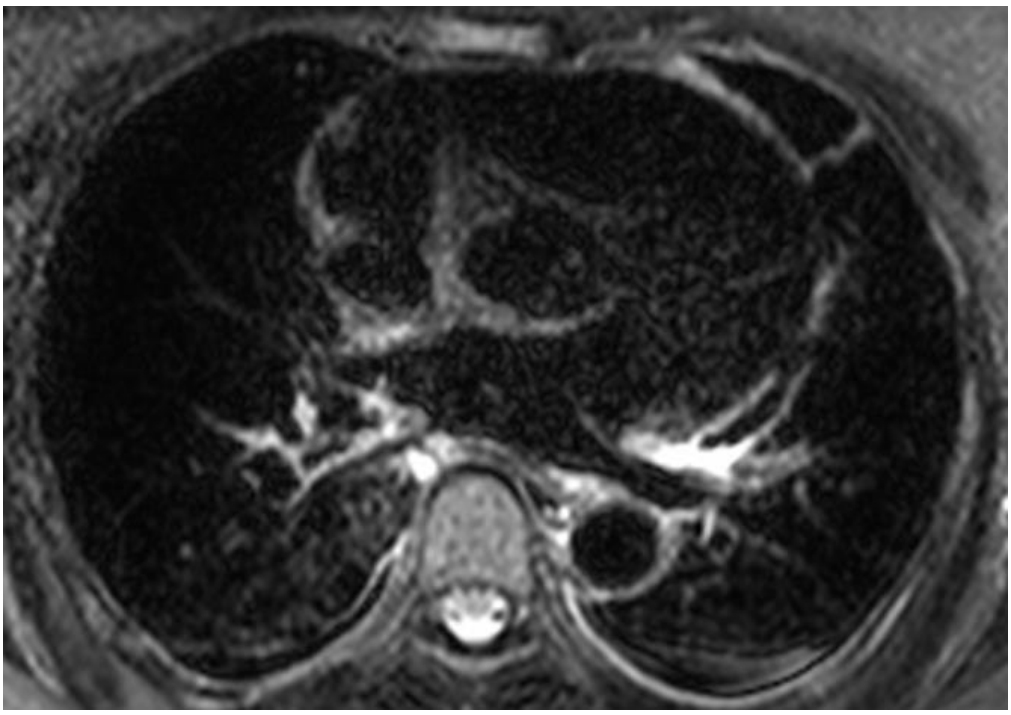

Figure 3-3: T2-Weighted imaging acquired using multi-slice Turbo Spin Echo (TSE) with double inversion recovery (DIR).

T2-Weighted images were acquired using a multi-slice Turbo Spin Echo (TSE) acquisition technique with a double inversion recovery (DIR) pre-pulse for black-blood imaging. Spatial pre-saturation with inversion recovery (SPIR) fat suppression was used. Echo time used was set at 120ms to the centre of k-space using a linear profile ordering. Image resolution was set at 1.5x1.5mm2 with a slice thickness of 5mm. The number of slices was set accordingly to provide complete coverage of the left atrium, approximately 20-25 slices. Image acquisition was programmed to occur at every second R-wave. To minimise differences in respiratory phase between slices, image acquisition was respiratory navigated.

3.4.5 Magnetic Resonance Angiography (MRA)

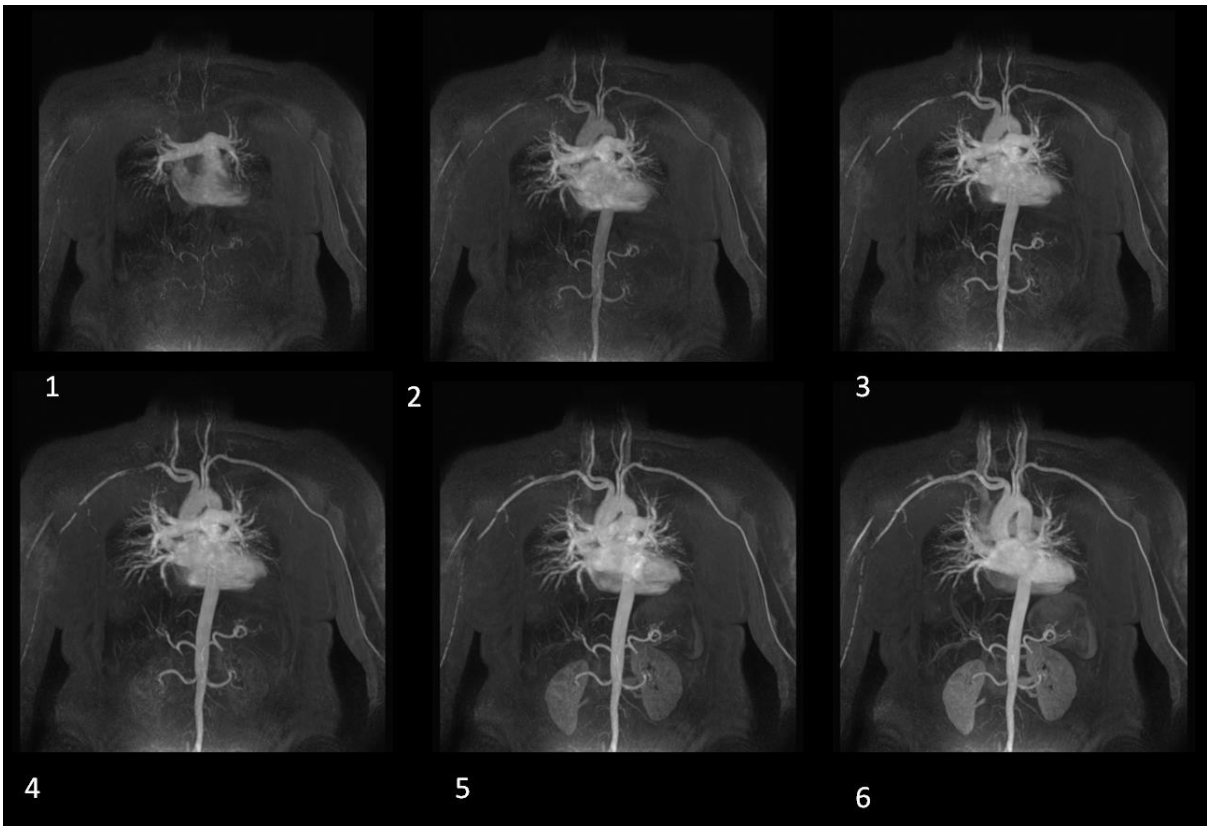

Figure 3-4: An example of 3D magnetic resonance angiography (MRA) following 0.04ml/kg Magnevist

For anatomical information a 3D magnetic resonance angiography (MRA) scan was acquired following contrast agent injection. This scan did not require ECG gating. A gadolinium-based contrast agent (gadopentetatedimeglumine–Magnevist, Bayer Health Care) was administered intravenously. A dose of 0.04ml/kg was given according to body weight. Importantly, patients with renal impairment were excluded from the study as administration of a contrast agent in a patient with renal failure is a relative contraindication as there is an increased risk of nephrogenic systemic fibrosis. A Glomerular filtration rate of <30ml/min/1.73m^2 was set as a cut off for exclusion.

3.4.6 Whole-Heart 3D Imaging

Figure 3-5: Whole heart imaging performed in sagittal orientation using a 3D balanced steady state free precession (b-SSFP)

This was followed by a 3D balanced steady state free precession (b-SSFP) acquisition in a sagittal orientation with whole-heart coverage and 2.7mm isotropic resolution and T2 preparation of 30ms and respiratory navigation.

3.4.7 Delayed Enhancement Imaging

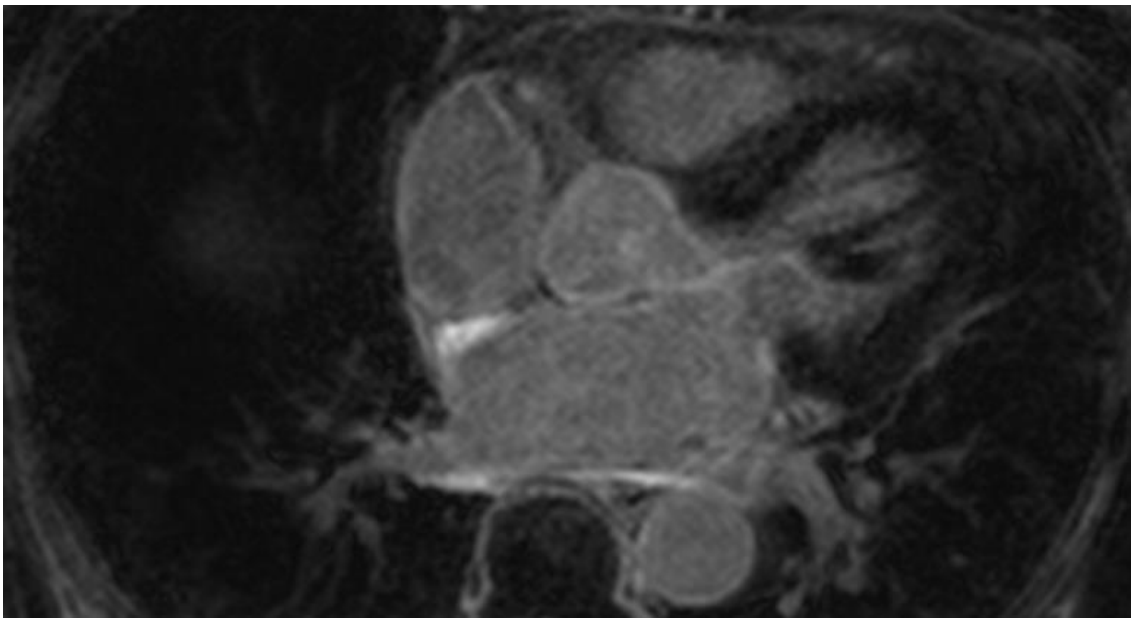

Figure 3-6: Delayed enhancement imaging were acquired using a free breathing inversion recovery (IR) turbo field echo (TFE) with both respiratory navigation and ECG triggering.

The scan for the visualization of delayed enhancement was a respiratory navigated 3D ECG-triggered, free breathing inversion recovery (IR) turbo field echo (TFE) with a pixel resolution of 1.3x1.3x4mm3, which was subsequently reconstructed to 2mm slice thickness.

Data was acquired with in a window of 150ms at every 1RR interval, with a low-high k-space ordering and SPIR fat suppression. The IR delay time was determined from the Look-Locker sequence and set at a TI intermediate between the optimal TIs to null myocardium and blood.

This nulling has been performed by our CMR group and has resulted in the most efficient visualisation of the late enhancement signal from the necrotic tissue. This scan was performed approximately 25-30 minutes following contrast agent administration. A gadolinium-based contrast agent (gadopentetatedimeglumine – Magnevist, Bayer Health Care) was administered intravenously. The number of slices was set for complete coverage of the

left/right atria (typically 30-40 slices). Slice orientation was in the four chamber view to optimise visualization of the PVs.

3.5 Image Processing

A major aim of this study was to quantify PV antrum percentage encirclement on CMR to assess tissue necrosis by delayed enhancement (DE), tissue oedema by increased T2 enhancement (T2) and combination of tissue necrosis and oedema (DE&T2).

To achieve this, a novel automated 3D method for visualizing and quantifying myocardial injury following ablation was developed [16]. First, the left atrium was semi-automatically segmented from the MRA by using the ITK Snap software [17]. This uses a combination of thresholding and region growing for segmentation. Utilising in-house software built on the Visualisation Toolkit libraries (VTK, KitwareInc), a left atrial surface was generated using marching cubes alogorithm. This was then fused with the delayed enhancement or T2-weighted images using intensity-based image registration. The vectors perpendicular to the surface at each vertex were computed and a maximum intensity projection (MIP) of the image intensity values in the DE or T2-weighted images was performed along each normal vector at a length of +/- 3 mm from the surface. The LA surface was then colour coded according to the MIP values, ranging from green (minimum) to red (maximum). Areas of DE or high T2 signal intensity were defined as being more than three standard deviations above the mean signal intensity of an area of healthy myocardium distant from the ablation target sites (usually defined in the left ventricular myocardium)

These 3D MR reconstructions were analyzed independently by two experienced readers. Both readers assessed all image data twice. The % delayed gadolinium enhancement (DE), high T2-weighted signal (T2) and combination of delayed gadolinium enhancement and T2 (DE+T2)

encircling the pulmonary veins was estimated on visual inspection. Source images were also analyzed to ensure that the degree of enhancement or high T2 signal detected by our automated method was accurate.

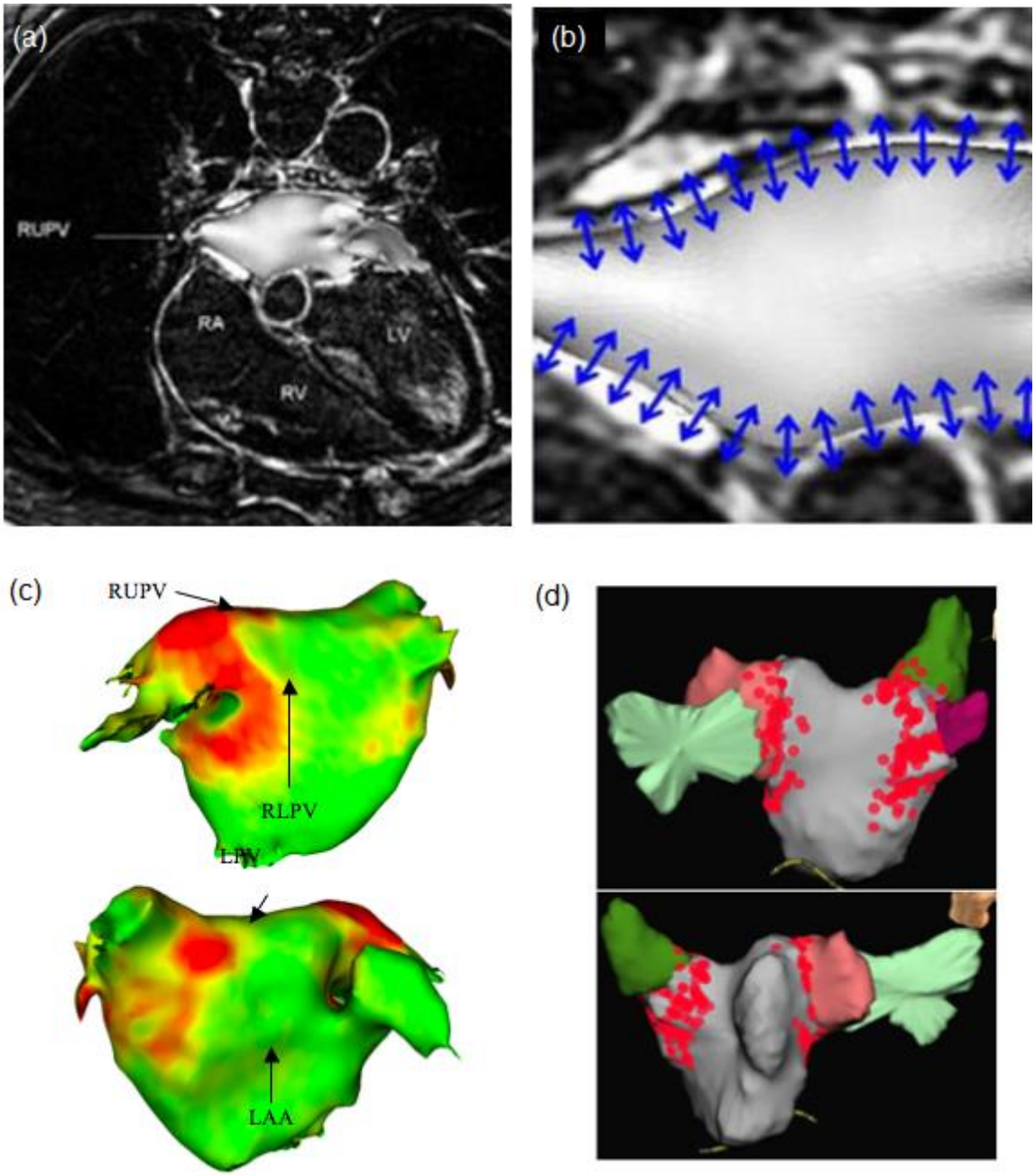

Figure 3-7: (a) Fusion of MRA-derived surface of the LA with the delayed- enhancement image acquired in the four-chamber view. (b) Close-up of the surface fused with the delayed-enhancement image and arrows indicating the direction in which the MIP is taken. (c) Projection of the MR signal intensities onto the surface shell. The higher the signal intensity, the brighter the surface shell colour. (d) NavX shell geometry with the corresponding ablation lesions placed. On visual assessment, a good correlation is observed between the NavX points around the PV and the corresponding bright red areas on the surface shell

4 Acute and Chronic Cardiac Magnetic Resonance Imaging Following Atrial Fibrillation Catheter Ablation

Introduction

Paroxysmal atrial fibrillation (AF) is often triggered by spontaneous ectopic beats of pulmonary venous origin,[12] an observation which has led to the emergence of pulmonary vein isolation (PVI) as an effective treatment for AF. Typically, ablation is performed at the left atrial-pulmonary vein (LA-PV) junction,[108, 109] with the intention of causing acute tissue necrosis to eliminate conduction between the LA and PVs. Clinical recurrences of AF following catheter ablation are common and recovery of LA-PV conduction ubiquitous in patients with and without documented AF during follow-up.[94] Single procedure success rates are modest, suggesting that the factors which contribute to acute PVI are not well understood.[110]

Delayed enhancement MRI following the administration of gadolinium has been used extensively to image ventricular scar after myocardial infarction secondary to coronary occlusion.[111] More recent work has demonstrated the potential utility of cardiac magnetic resonance imaging (CMR) for assessment of atrial fibrosis prior to ablation and of atrial injury following ablation.[98, 112] Although gadolinium diffuses into the intracellular space following the loss of cell membrane integrity associated with acute tissue destruction, it can also accumulate acutely in the increased extracellular space created by myocardial edema, which may represent a reversible form of cardiac injury and is therefore not specific to necrotic tissue.[113] An alternative method to visualize myocardial edema uses the linear relationship between T2 relaxation time and myocardial water content, and may be a more sensitive in-vivo marker of myocardial edema than DE MRI.[114]

The aim of the study was to use DE- and T2-weighted CMRI to characterize the tissue effect of left atrial ablation and to relate the pattern of acute atrial injury to clinical outcome. We hypothesize that acute PVI is caused by a combination of irreversible tissue destruction and reversible tissue injury at the LA-PV junction.

4.2 Methods

4.2.1 Patient population

Twenty-five patients (17 male, mean age 55±11 years) with symptomatic, drug refractory paroxysmal AF undergoing their first PVI completed the study. 29 patients were consented for the study but four were excluded (3 because of claustrophobia with failure to complete scan and 1 due to an ineffective respiratory navigator). All scans used for the purposes of data analysis were deemed of adequate quality for analysis by an experienced CMR operator.. Therapeutic anti-coagulation with an INR >2 for at least 4 weeks prior to the procedure was mandated. The study was approved by the Local Research Ethics Committee.

Acute procedural success was defined as PVI confirmed using a circumferential mapping catheter. Clinical outcomes are reported at 6 months follow-up. Patients were followed in clinic to assess symptoms. 24 hour-Holter monitors were performed at 6 months. Every effort was made to obtain ECG recordings of symptomatic recurrences. Recurrences were defined on the basis of 1) symptoms with ECG evidence of the presence of atrial fibrillation/flutter/tachycardia or 2) the presence of symptomatic or asymptomatic episodes of atrial arrhythmia lasting for >30 seconds on ambulatory cardiac monitoring.

4.2.2 MR Image acquisition

All participants underwent MR imaging in a 1.5 Tesla Philips Achieva MR system (Philips Healthcare, Best, Netherlands) using either a 32 channel surface coil (Invivo, Orlando, Florida, USA) or a large two-channel flex coil.

T2-weighted images were acquired using a multi-slice Turbo Spin Echo (TSE) acquisition technique with a double inversion recovery (DIR) pre-pulse for black-blood imaging. Spatial pre-saturation with inversion recovery (SPIR) fat suppression was applied. The echo time used was set at 120ms with a linear profile ordering. This enabled the image resolution to be set at 1.5x1.5mm^2 with a slice thickness of 5mm. The number of slices was set to provide complete coverage of the left atrium (20-25 slices). Diaphragmatic motion was tracked and respiratory motion correction applied to minimize motion blurring and differences in respiratory phase between slices during image acquisition.

To visualize DE, a 3D ECG-triggered, free-breathing inversion recovery (IR) turbo field echo (TFE) scan with respiratory navigator motion correction was performed with a pixel resolution of 1.3x1.3x4mm^3, which was then reconstructed to 1.3x1.3x2mm^3. Data were acquired at mid-diastole with a 150ms acquisition window and a low-high k-space ordering as well as SPIR fat suppression. The IR delay time was determined from a Look-Locker sequence and was set at a TI intermediate between the optimal TIs to null myocardium and blood. Previous work has validated this method for reproducible visualization of the late enhancement signal from necrotic tissue.[115] DE scans were performed 20 minutes following contrast agent administration. The number of slices was set for complete atrial coverage (30-40 slices). To optimize visualization of the PVs, slice orientation was performed in the four-chamber view. Images obtained with this method appear to reflect the pulmonary veins at their maximal size. Similar MR sequences were used for images acquired (i) prior to ablation, (ii) within 24 hours of ablation and (3) 3-6 months following ablation.

4.2.3 Ablation procedure

A 6F decapolar catheter was placed in the coronary sinus to provide a reference for electroanatomic mapping and to enable LA pacing. Two transseptal punctures were made and access to the left atrium was obtained using 8.5Fr non-deflectable long sheaths, (St. Jude

Medical Inc., St. Paul, MN, USA). Following the first transseptal puncture, intravenous heparin was administered to achieve an activated clotting time of between 300 and 400 seconds. A 3-dimensional geometry of the left atrium was created using either NavX™ (St. Jude Medical Inc., St. Paul, MN, USA) or CARTO XP (Biosense Webster Inc., Diamond Bar, CA, USA). A circular mapping catheter (Inquiry™Optima™, St. Jude Medical Inc.) was then placed in each pulmonary vein in turn while the corresponding LA-PV antrum was targeted with wide area circumferential ablation. Energy was delivered through a NaviStar® ThermoCool® 3.5 mm irrigated tip catheter (Biosense Webster Inc., Diamond Bar, CA, USA) with flow limited to 17 ml/min, power limited to 30 W on the anterior wall and 25 W on the posterior wall and temperature limited to 50^0C. Ablation lesions were marked on the LA geometry when there had been an 80 % reduction in the local electrogram voltage or after 30 seconds of energy delivery. One tag was applied to the shell per 30s RF energy delivery and a standard tag size was used throughout the study. If LA-PV conduction persisted despite wide area circumferential ablation, additional lesions were delivered at sites of earliest activation on the circular mapping catheter until entry block in all 4 veins was confirmed by observing the elimination or dissociation of pulmonary vein potentials. Exit block was not routinely assessed. Neither adenosine nor isoprenaline was routinely administered to test the integrity of PVI or to search for non-PV triggers of AF.

4.2.4 Image processing, analysis and its validation

Using CMR, this study sought to quantify the extent of PV antral encirclement as demonstrated by DE- and T2-weighted CMRI, individually and combined. To achieve this, an automated 3D method for visualizing and quantifying myocardial injury following ablation (Figure 4.1) was used which has previously been described in detail.[115]

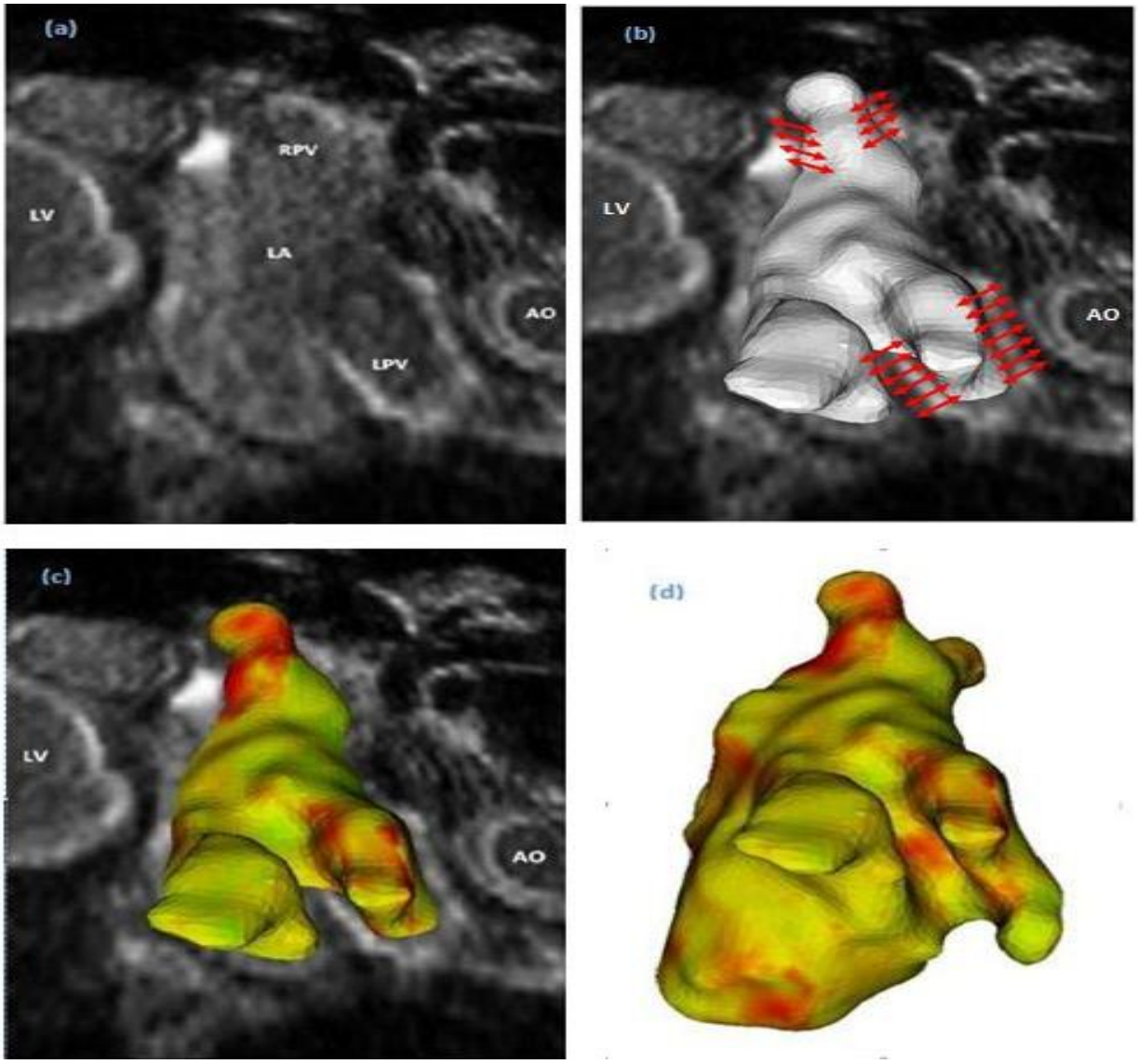

Figure 4-1:.(a) Raw MR scan image of the LA and PVs showing areas of delayed enhancement. (b) Fusion of the MR derived 3-D LA shell into the delayed-enhancement image. The red arrows indicate the direction in which the maximum intensity projection (MIP) is taken. (c) Projection of the MR signal intensities onto the surface shell. The surface shell colour is set within a range going from green to yellow to red corresponding with low to high signal intensity. (d) 3-D colour LA shell harvested from the delayed-enhancement MR image.

3D-MR reconstructions were analyzed independently twice by two experienced readers, blinded to clinical outcome and to the timing of the scan following catheter ablation. T2 and DE signal circumferential quantification was performed by reconstructing all CMR scans into individual left atrial shells . PVs were analyzed as ipsilateral pairs for each of the 25 patients at three time points, permitting analysis of 150 PV pairs. For each PV pair, T2 and DE was

quantified as occupying a percentage of the antral circumference. Percentage delayed gadolinium enhancement (DE), high T2-weighted signal (T2) and combination of delayed gadolinium enhancement and T2 (DE+T2) encircling the pulmonary veins was determined independently by both readers and consensus reached. A high degree of interobserver agreement was seen on a Bland Altman test with a maximum observed difference of 10% seen. The mean±SD inter-observer error for DE, T2 and DE&T2 was 1.5±2.5%, 1.5±3.5% and 0.8±2.2% which was acceptable for the purposes of data analysis.

4.2.5 Statistical analysis

Summaries for continuous variables are expressed as mean ± confidence interval. Follow-up times are reported as the median and interquartile range (IQR).Categorical variables were compared among recurrences and non-recurrences groups using a chi-square test. The % circumferential encirclement by DE, T2 and DE&T2 groups were compared to test for differences between group means. Statistical analyses were performed using Stata (StataCorp 2009). A linear regression model with predictor (code 1 for no recurrence and 0 for recurrence) and outcome T2, DE, T2&DE, DE/(T2&DE) respectively was applied and run in Stata. We used the vce (cluster subject) option in Stata[116] to allow for inter-subject dependence (left and right pulmonary vein measurements from the same patient). Analyses for acute and chronic pulmonary vein findings on cardiac MR were performed separately. A p value of less than 0.05 was considered statistically significant

4.3 Results

4.3.1 Patient and procedural data

Table 4.1 outlines the baseline study population demographics. Successful pulmonary vein isolation was achieved in all patients. Median follow-up time was 11 months (IQR 8 to 16 months). A three month blanking period was observed during which arrhythmia recurrences

were treated with antiarrhythmic drugs or DC cardioversion. No repeat ablation was performed within the blanking period. Clinical recurrence of AF was documented in 11(46%) patients with a median time to recurrence of 94days (IQR 45 to 166 days).Patients with recurrences had significantly larger LA size and longer duration of AF. Seven of 11 patients with recurrences underwent a re-do procedure; two patients are awaiting a redo procedure and two declined further intervention.Procedural complications include two femoral venous haematoma which did not require intervention. No stroke, tamponade or oesophageal fistula occurred in this study and no pulmonary vein stenosis was detected on follow up MRI.

Table 4-1Patient demographics categorized into no recurrences and recurrences at 6 month clinical follow-up.

	All Subjects n=25	No AF Recurrence n=14	AF Recurrence n=11	p Value
Age	58±10.7	49±12.4	55±10.8	0.46
Gender Male Female	 17(67%) 8(33%)	 11(78%) 3(22%)	 6(55%) 5(45%)	 0.60 0.68
Duration of AF, months	28±16 (12-60)	18±10 (12-48)	30±11 (18-60)	0.04
LA size, cm	3.7±0.5	3.4±0.2	4.2±0.3	0.03
LVEF, %	55±5	60	50	0.29
Hypertension	5	2	3	>0.10
Valve Disease	1	0	1	>0.10
History of smoking	1	1	0	>0.10
Thyroid disease	1(4%)	0	1(9%)	>0.10
Previous ablation Atrial Flutter	5(20%)	2(14%)	3(27%)	>0.10

4.3.2 Pre-ablation MRI

The circumferential burden of DE and T2 weighted signal detected prior to any ablation , was low in comparison with acute post-ablation imaging (figure 4.2 and figure 4.3) and did not occupy more than 5% of the PV circumference. Pre-ablation DE signal localised to the mitral annulus, a common finding due to the fibro-elastic nature of cardiac tissue at this site. T2 signal was largely observed around the atrial roof and this is likely explained by the imperfections arising from the MR-sequence. In Black-Blood sequence, residual bright blood signal is observed in areas of slow through-plane flow (e.g. in the apex of the ventricles). This problem has been reported in acute edema assessment in the ventricles following acute myocardial infarction [117]. Overall the amount of T2 signal pre-ablation was very small.

4.3.3 Post-ablation MRI

All acute imaging was performed between 18 and 24 hours following catheter ablation. Figure 4.2 demonstrates the typical T2-weighted and figure 4.3 typical DE appearances in two patients before and after catheter ablation. The left atrial burden of DE and T2-weighted signal was significantly increased following catheter ablation in comparison with baseline. On the acute scans, DE signal was concentrated in the PV antral region while T2 signal was more widely distributed in the atrium, remote from sites of ablation.

Individual analysis of the circumferential extent of both signal types revealed that T2-weighted signal occupied 100% of the antral circumference in 5/50 PV pairs while DE signal did not achieve complete encirclement of any vein pair. There was no significant difference between the circumferential extent of DE signal around the LPVs (63.0±8.6%)and the RPVs

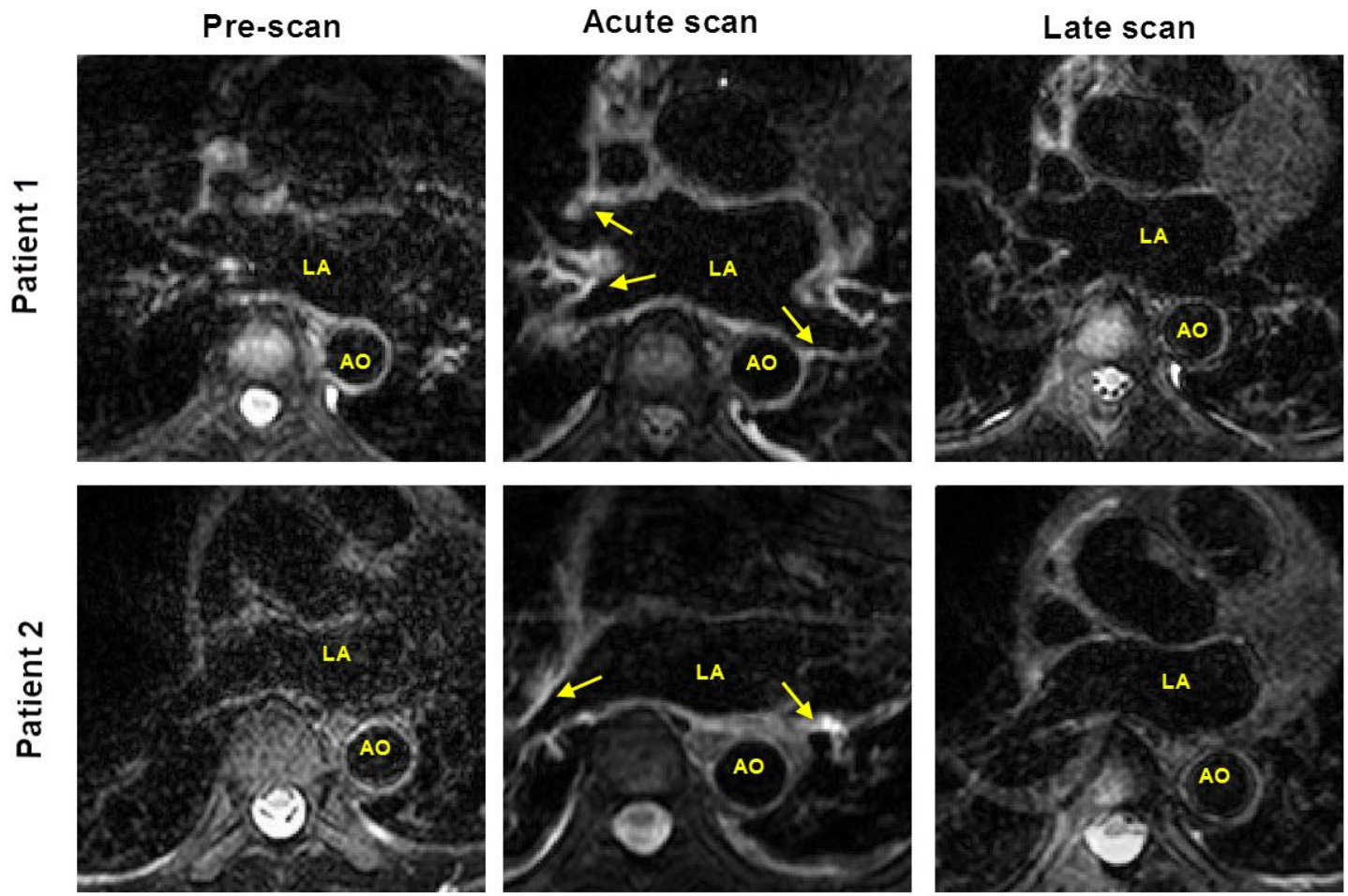

Figure 4-2: Demonstrates a series of T2 signal images of the left atrium and pulmonary veins in two patients with arrows pointing towards regions of hyper-enhancement in column 2. Baseline images in the first column show no significant T2 enhancement (tissue edema) compared to the acute post ablation images in the second column. The late scans in the third column shows the T2 signal becoming almost similar to baseline in the pre-ablation scans in column one.

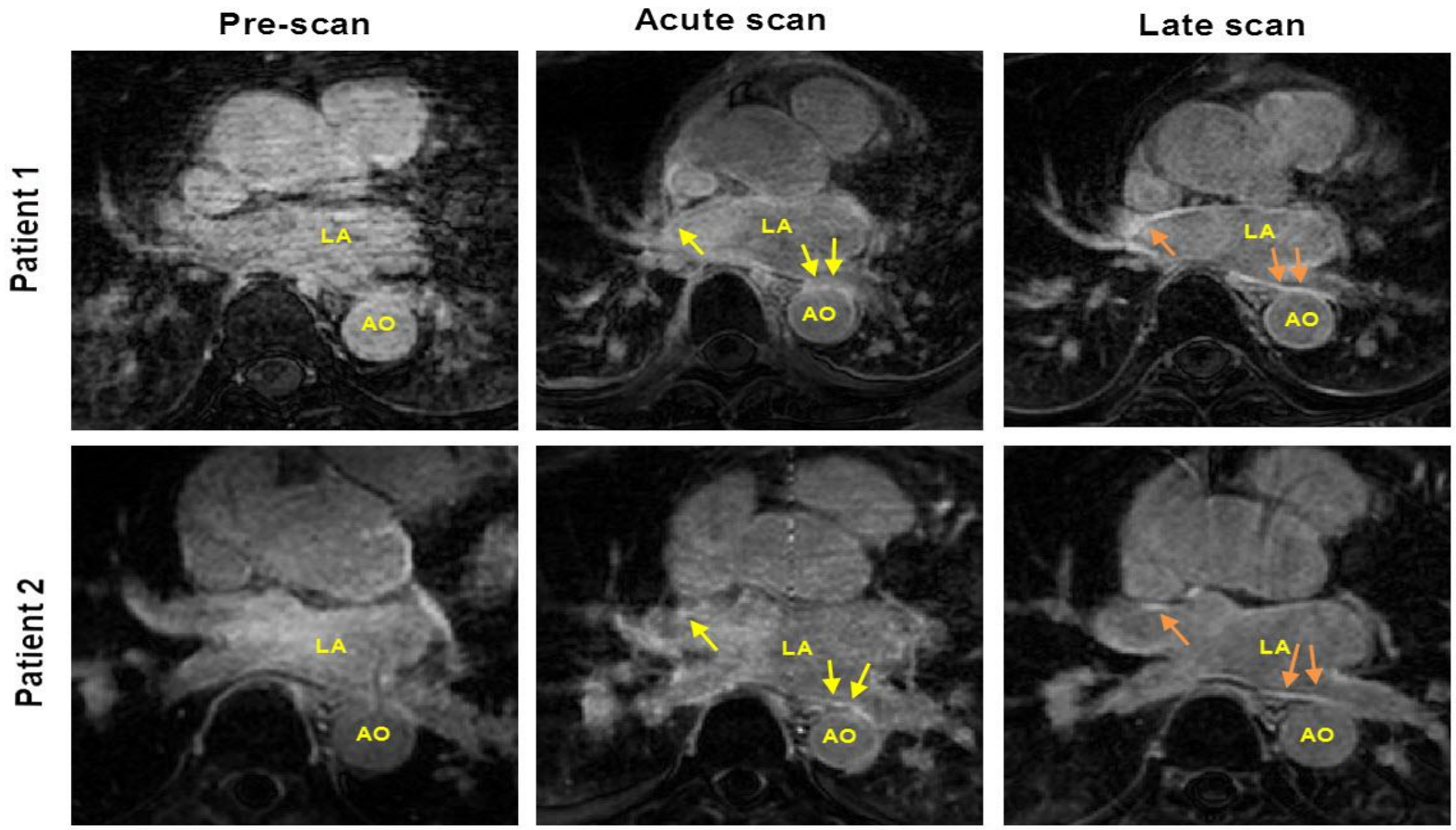

Figure 4-3: Demonstrates a series of DE images of the left atrium and pulmonary veins in 2 patients with arrows pointing towards regions of hyper-enhancement in both columns 2 and 3. Baseline images in the first column show no significant DE signal (tissue injury/necrosis) compared to acute post ablation images in the second column. The late scans in the third column shows that areas of DE signal become less diffuse and more defined with sharper borders in comparison to the acute scans.

Individual analysis of the circumferential extent of both signal types revealed that T2-weighted signal occupied 100% of the antral circumference in 5/50 PV pairs while DE signal did not achieve complete encirclement of any vein pair. There was no significant difference between the circumferential extent of DE signal around the LPVs (63.0±8.6%)and the RPVs (65.5±7.6%, p=0.67).Similarly, although the circumferential extent of T2 signal was greater, there was no significant difference between LPVs (82.8±8.4%) and RPVs (73.7±7.0%, p=0.31).

Combined analysis of DE and T2 signal, using reconstructed shells co-displaying both signal types, revealed areas of T2 enhancement to overlap and interdigitate with those areas of high DE signal intensity (figure 4.3). Hence the sum of DE and T2 is 100% or less. For the LPVs, the circumferential extent of DE signal alone, T2 signal alone and the combination of both signal types was 63.0±8.6%, 73.7±8.4% and 89.3±4.9% respectively. For the RPVs, the circumferential extent of DE signal alone, T2 signal alone and the combination of both signal types was 65.5±7.6%, 82.8±7.0% and 91.3±5.6%respectively. Compared to DE alone, the combined DE and T2 signal was significantly greater for both left (p=0.009) and right (p=0.027) PVs. Complete antral encirclement with combined DE and T2-weighted signal was seen in 17/50 (34%) PV pairs at the acute scan.

At the chronic follow-up scans, T2 signal had largely resolved (figure 4.4 and 4.5), while a decline in the extent of DE signal was seen. For the LPVs, the circumferential extent of DE signal decreased from 63.0±8.6% to 50.9±8.2% (p=0.016); for the RPVs, the circumferential extent of DE decreased from 65.5±7.6% to 47.6±8.5% (p=0.002). Discontinuities in areas of DE signal could be seen.

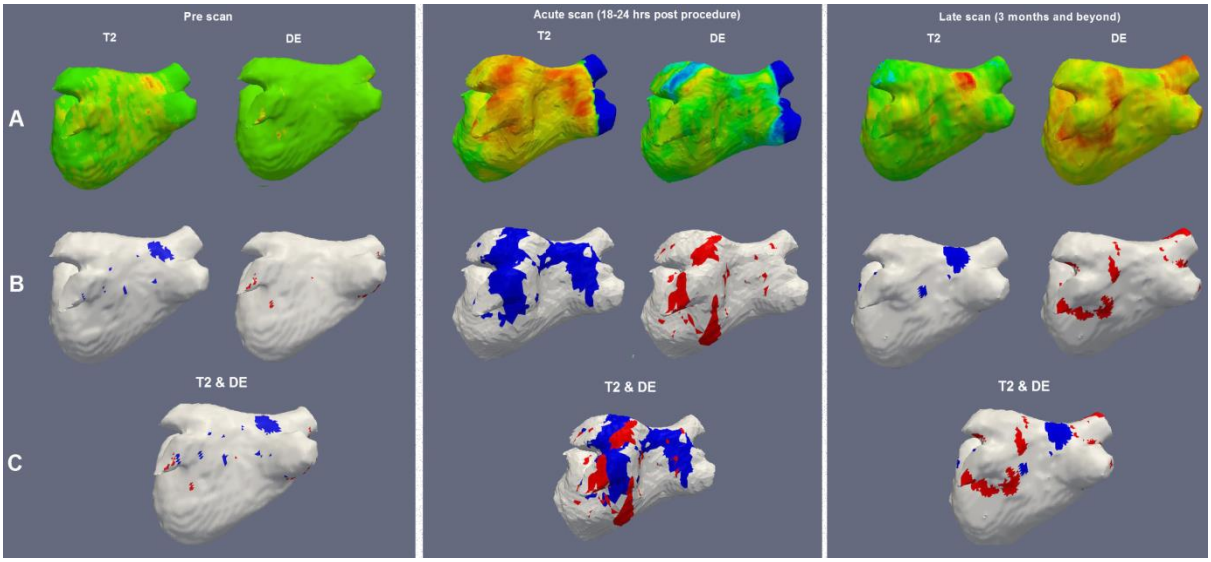

(i)

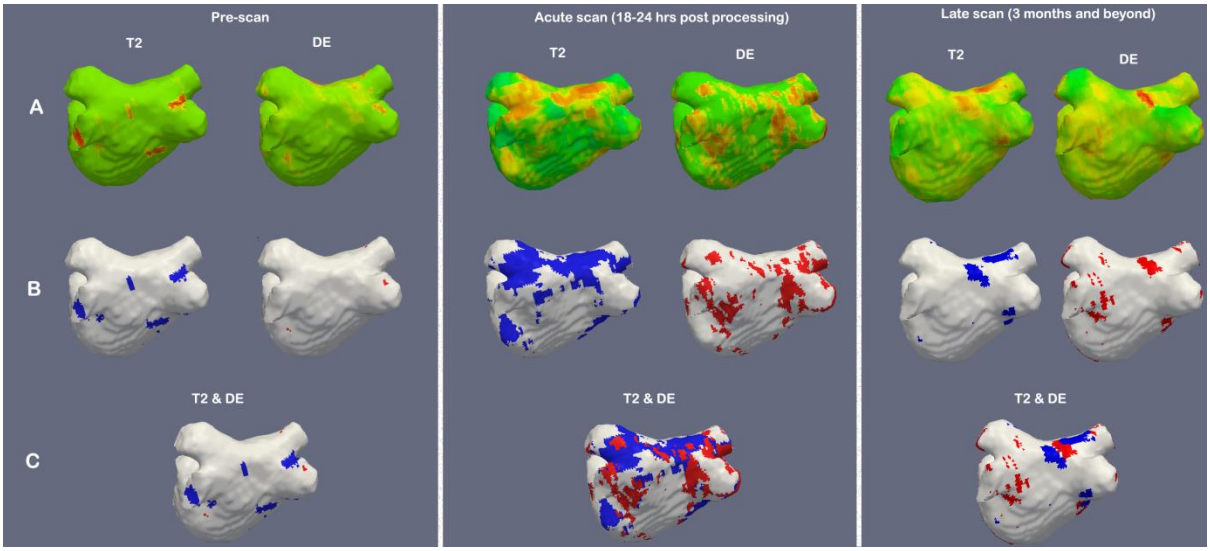

(ii)

Figure 4-4: (i)and (ii) demonstrate a series of reconstructed 3-D left atrial shells to visualise T2 and DE signal in the corresponding patients shown in figures 4.2 and 4.3. The 3 columns represent the 3 time points: pre-procedure scans (prescans, column 1), acute post procedure scans performed within 18 to 24 hours (column 2) and the late scans performed later than 3 months (column3). Quantification of these enhancements was performed as percentage encirclements of the left and right PV antra. Row A depicts the raw intensities mapped on to the shells from the T2 and DE MR scans. Row B shows the corresponding T2 and DE 3-D shells that have been thresh-holded semi-automatically. Red areas signify delayed-enhancement and blue areas signify T2 signal intensity. In row C, the combined enhancements of T2 and DE is seen together. On the acute scans seen in column 2, gaps present within areas of red (DE) are filled in by areas of blue (T2). In column 3, the blue (T2) and red (DE) signals resolve, with a greater effect seen for T2 versus DE signal.

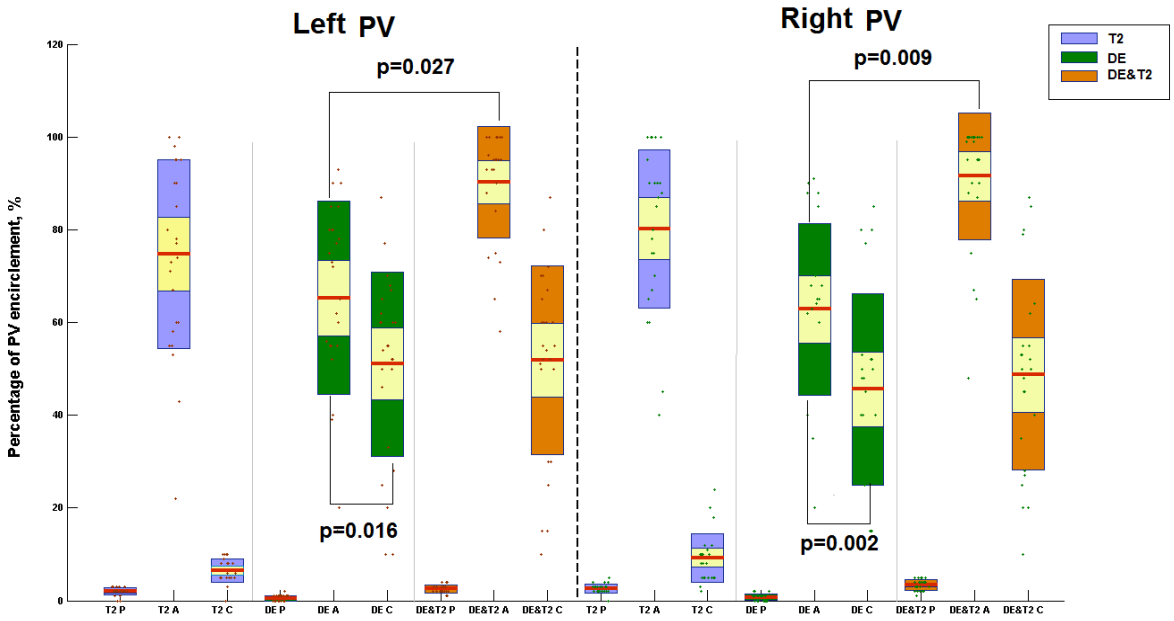

Figure 4-5: This scatter-boxplot shows a comparison of pre, acute and late T2, DE and combined T2&DE for both left and right pulmonary vein antrum. Each individual scatter plot represents the raw data for that specific group. The dots within each group have been dispersed horizontally to optimise visualisation and clarity. The boxplots on the other hand represent median (red line), 95% confidence intervals (yellow box) and 1 standard deviation (blue box) An overall higher enhancement is seen in all 6 groups on the acute scans compared to the 6 groups on the chronic scans. The % encirclement by T2 signal diminishes from above 75% to about 5% in keeping with reversible injury. The % encirclement by DE signal diminishes to a much lesser extent. Using a combination of DE and T2 signal, the % encirclement decreases from 90% at the acute scans to approximately 50% at the follow up scan

4.3.4 Recurrences of AF: relationship to MR assessment

Both acute and late scan data were analysed into two groups according to the respective clinical outcome – those with and without AF recurrences. 100 pairs of PVs (50 acute, 50 late) analysed previously were divided into two groups according to the presence or absence of a clinical recurrence of AF. Figure 4.6 summarises the percentage circumferential encirclement of DE, T2-weighted signal and the combination of DE &T2 around the left and right PV pairs by clinical outcome for both the acute and late scans.

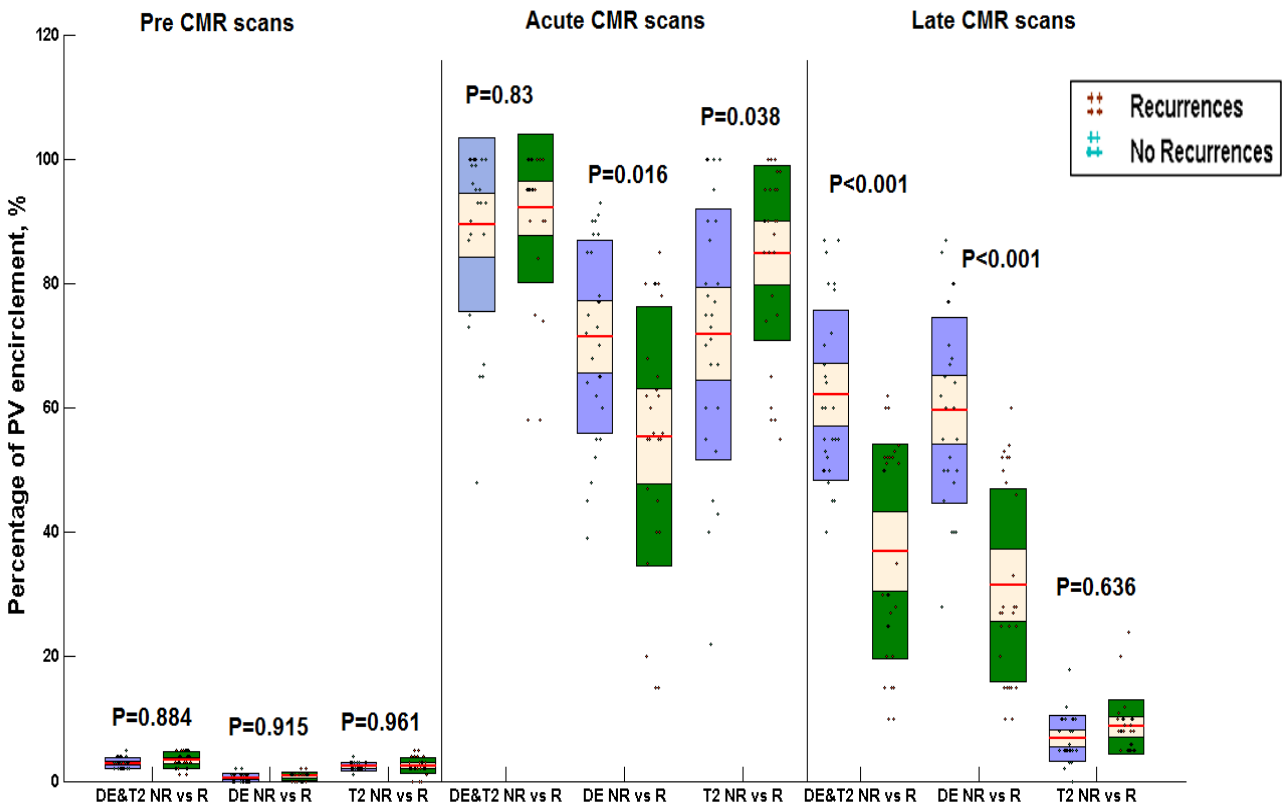

Figure 4-6 :.This scatter-boxplot shows a comparison of percentage of PV encirclement according to clinical outcome no recurrence (NR) v recurrence (R) of AF accounted for by T2 signal, DE signal and combined T2&DE at three time points: pre-ablation (Pre) immediately post (Acute) and follow up scans (Late). Each individual scatter plot represents the raw data for that specific group. The dots within each group have been dispersed horizontally to optimise visualisation and clarity. The boxplots on the other hand represent median(red line), 95% confidence intervals (yellow box) and 1 standard deviation (blue box). The absolute decline in DE is less for patients with no AF recurrence.

On the acute scans, there was no difference in the combined DE&T2 signal between both groups with mean % encirclement of 88.7±5.4% (no recurrences) and 93.3±4.8% (recurrences). When DE signal alone was analyzed, a significantly higher mean percentage encirclement was noted in the AF free group (n=14; 28 pairs of PVs) compared to the group with recurrences (means±CI, 73.1±6.0% vs 54.5±9.1% respectively, p = 0.016). Conversely, the T2 signal was noticeably lower in the AF free group compared to the group with recurrences (means ± CI, 70.3±7.8% vs 87.7±6.3% respectively, p = 0.038).With the combined areas of DE & T2 forming almost complete rings around the pulmonary veins,

ratios of DE to (DE &T2) were calculated (figure 4.7). Patients with no recurrences had a higher mean DE/(DE&T2) ratio compared to the recurrence group (0.82±0.12 vs 0.58±0.20; p=0.0001).

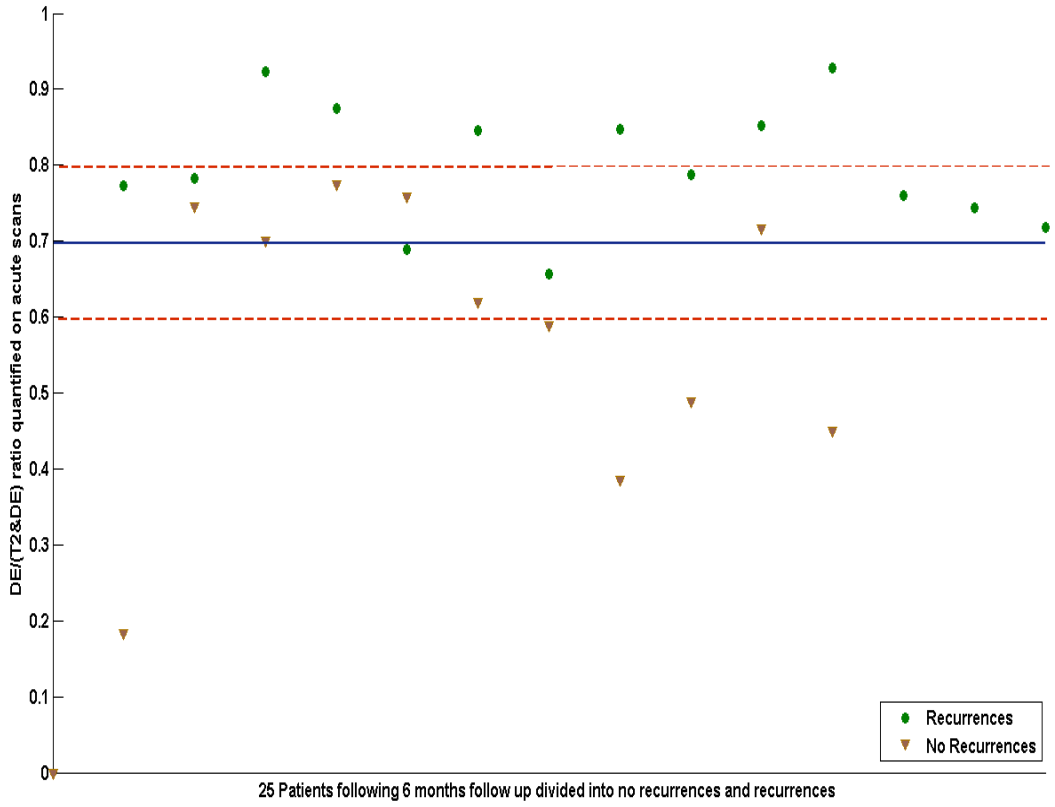

Figure 4-7: Mean DE/T2&DE ratios quantified on the acute scans for patients with no recurrences versus those with recurrences. An overall higher DE/T2&DE ratio is seen in patients free from AF.

On the late scans, DE was the predominant signal type seen and was significantly greater in the AF free group compared to the group with recurrences (61.0±5.7% vs 34.7±7.3% respectively, p <0.0001). A comparison of the acute and late scan DE data in both groups showed a lower regression of this signal type in the AF free group (from 73.1±6.0% to 61±5.7%, p=0.03) relative to the group with arrhythmia recurrences (from 54.5±9.1% to 34.7±7.3% p=0.01).

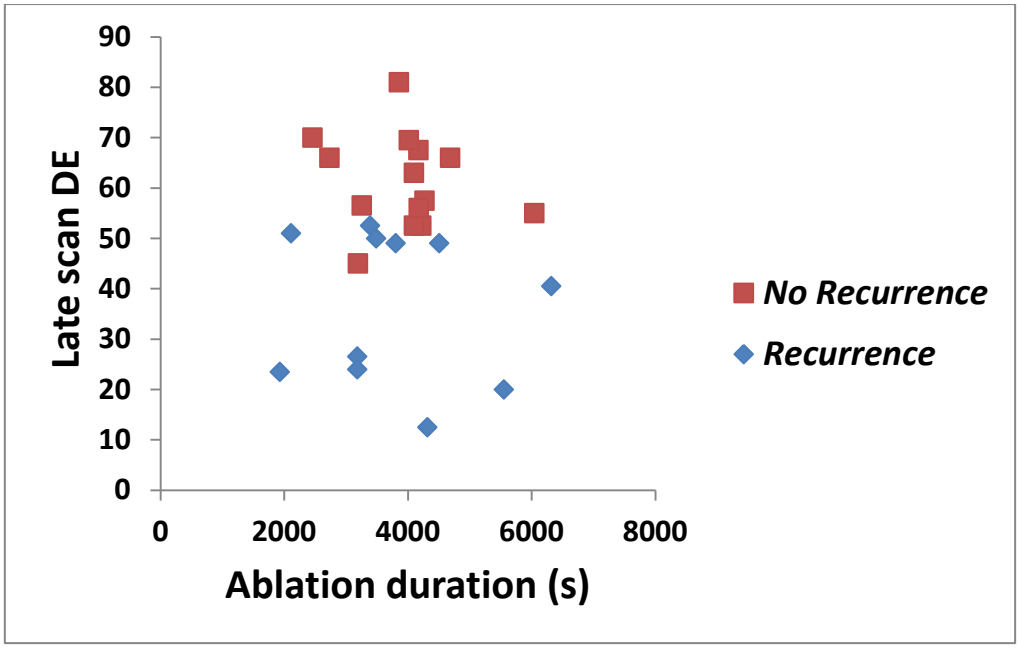
90
80
70
60
50
40
30
20
10
0
Late scan DE
0
2000
4000
6000
8000
Ablation duration (s)
No Recurrence
Recurrence

(a)

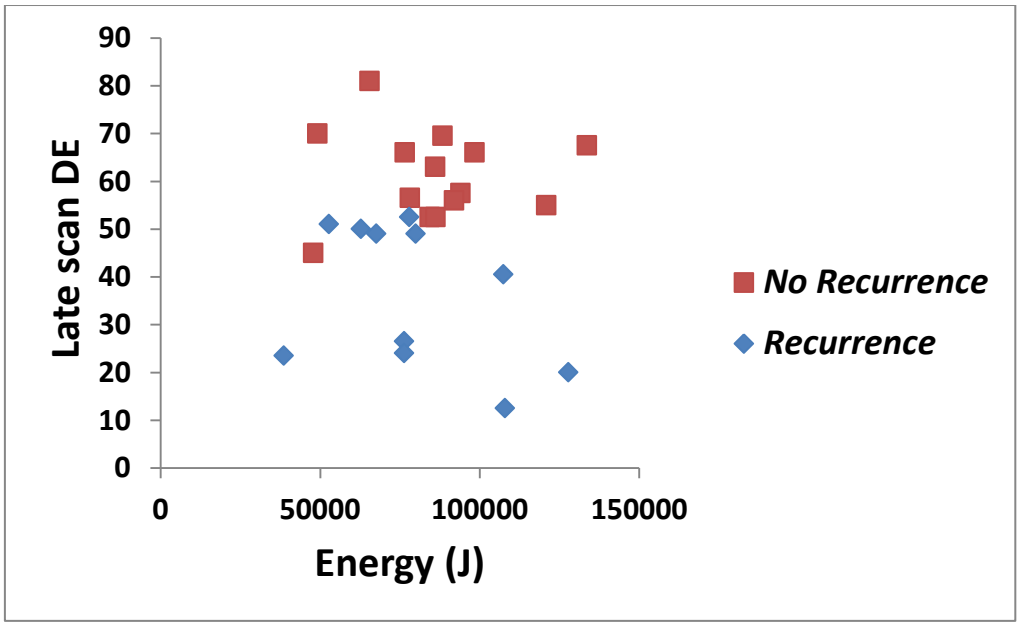
90
80
70
60
50
40
30
20
10
0
Late scan DE
0
50000
100000
150000
Energy (J)
No Recurrence
Recurrence

(b)

(c)

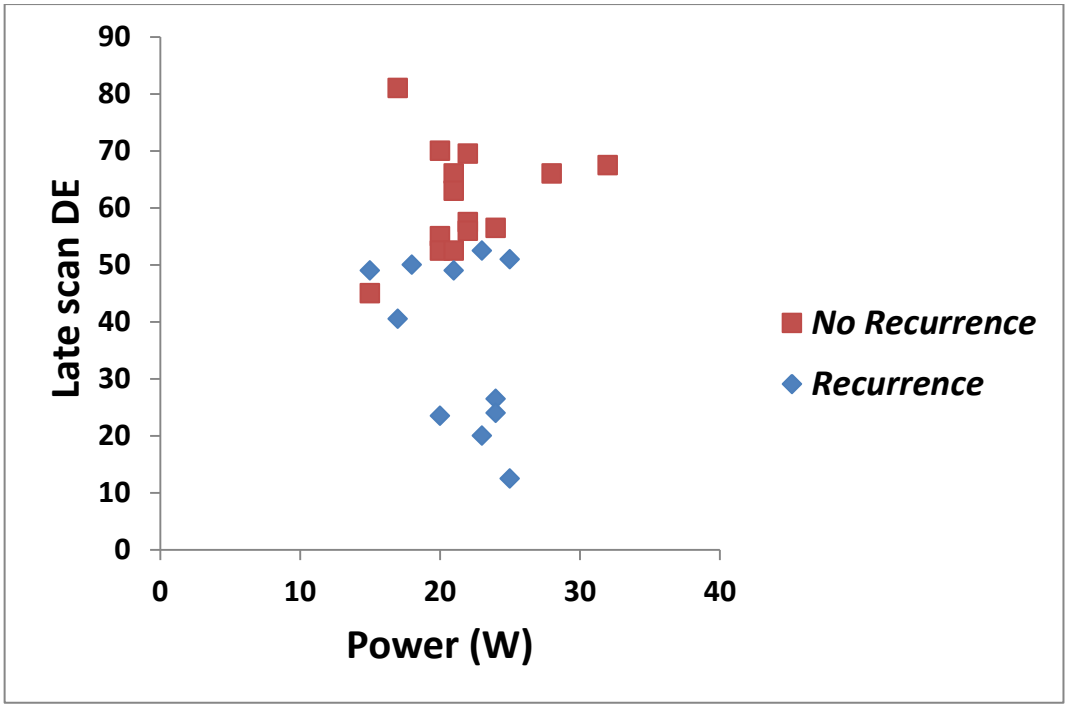

(d)

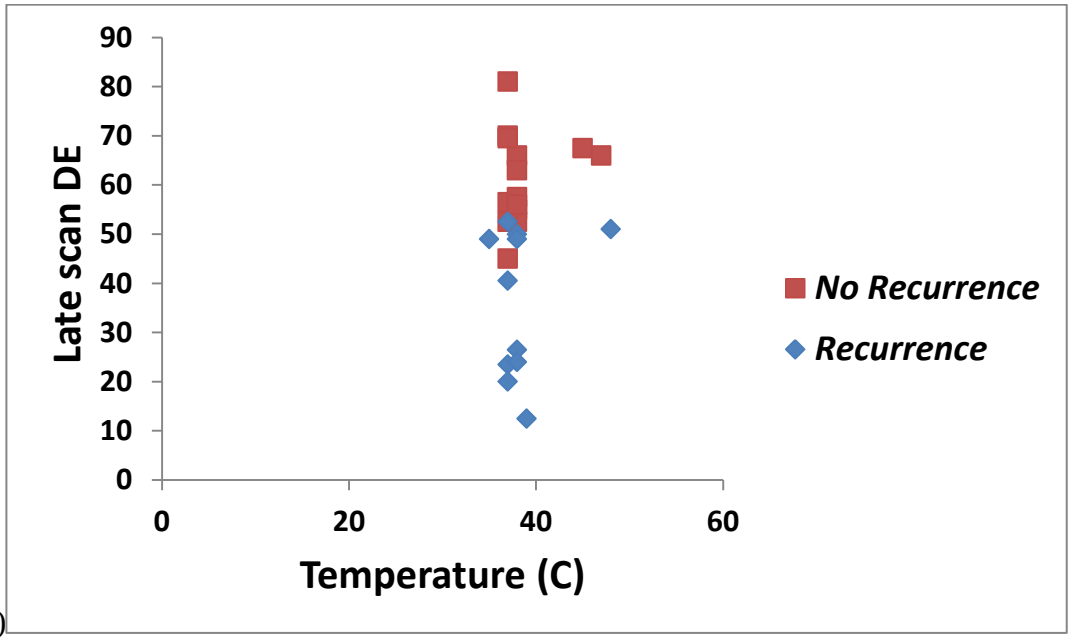

Figure 4-8 The relationship between late scan DE and individual ablation duration (a), energy delivered (b), average power (c) and temperature (d) settings has been divided here into no recurrences and recurrences. The absence of any trend between the individual parameter and the amount of late DE observed on CMR may be explained by catheter-tissue contact which in this study we were unable to assess.

4.4 Discussion

The findings of this paper are: (1) Acute pulmonary vein isolation is not associated with complete circumferential injury as determined by cardiac MR imaging; (2) Increased DE and T2-weighted signal are both seen within 24 hours of left atrial catheter ablation; (3) T2-weighted signal has largely resolved by 3 months of follow-up, supporting its use as a marker of acute, reversible atrial injury; (4) In patients with clinical recurrences, a greater proportion of the acute circumferential antral injury is accounted for by T2-weighted signal than in those patients who remain arrhythmia-free

Previous work evaluating the role of CMR in LA assessment post catheter ablation has focused on delayed enhancement imaging delineating areas of scar pre and post ablation. [98, 112, 118, 119] However MR imaging of acute, reversible atrial injury following catheter ablation has only been recently reported.[120, 121]There is evidence from animal studies that tissue edema causes right atrial wall thickening following linear ablation in the right atrium.[122]Left atrial edema most likely occurs during and immediately after AF ablation as evidenced by an increase in atrial wall thickness, and resolves within one month.[123] During late-gadolinium MRI performed immediately after ablation, both non-enhancing and hyper-enhancing tissue types are seen, the former of which is a poor predictor of scar visualized at 3 months follow-up.[121] This is likely to reflect ablated but not necessarily necrotic tissue confirming previous work, including that from our own laboratory, that DE MRI overestimates the acute extent of tissue injury following left atrial catheter intervention by virtue of the accumulation of gadolinium in extravascular water associated with acute inflammation. Although there is a good correlation between endocardial voltage-defined scar and T2 weighted signal immediately post ablation, there is a poor correlation with the DE MRI-defined scar at three months follow up [124], further supporting the transient nature of at least part of the ablation injury process.

T2 signal was found in the acute CMR scans remote form the ablation sites. Similar observations have previously been described. [124] This is most likely related to a cytokine (IL-6) mediated inflammatory response following radiofrequency ablation. [125] Another possible mechanism giving rise to this observation may be related to sheer/rotational force of the catheters against the atrial wall during catheter manipulation.

4.4.1 Acute PVI and atrial ablation injury

The data presented in this paper demonstrate a high circumferential extent of each of T2 and DE signal within 24hours of ablation. While this is consistent with a high degree of overlap of the two imaging signal types, there are also some areas where T2 signal can be detected in the absence of DE signal and vice versa . By overlaying DE and T2 weighted images on the same anatomical shell, we have demonstrated that the circumferential extent of ablation injury is greater when both signal types are summated, reaching approximately 90%. Although 100% circumferential extent of combined T2 and DE signal was seen in only 17 of 50 PV pairs, it is well known that acute PV isolation can be achieved using a segmental, electrogram-guided approach rather than a circumferential ablation approach, the former of which does not necessarily result in ablation of the entire PV circumference.[58] This may explain the finding that PV isolation can be readily achieved without circumferential MR evidence of ablation injury.

4.4.2 Atrial scar and arrhythmia recurrence

The MR data at the follow up scan demonstrate near-abolition of T2 signal while DE signal is reduced and continues to occupy only 60% of the circumferential extent of both pairs of pulmonary veins. This is in keeping with the finding that chronic pulmonary vein reconnection is ubiquitous following conventional wide area circumferential ablation and indeed was seen in all AF recurrences in this paper.[94, 96] In the present study, a greater extent of circumferential DE signal at the 24h scan was predictive of freedom from AF while the

extent of T2 signal was greater in the arrhythmia recurrence group. While there is a lack of clarity of what DE and T2 signals truly represent in the immediate aftermath of a catheter ablation procedure, the presence of DE signal beyond three months follow-up is likely to represent permanent atrial scar.[121, 126]

The decline in circumferential extent of DE signal between acute and follow up scans was less for patients with no AF recurrence than for those patients in whom AF recurred. This supports our hypothesis that the greater the contribution of T2 signal, representing reversible injury, to acute PVI, the higher the likelihood of PV reconnection following resolution of tissue edema.

Although preliminary work has demonstrated a qualitative correlation between discontinuities in areas of high DE signal and conduction gaps on electrophysiology study[98, 99], pulmonary vein reconnection also occurs in patients without clinical arrhythmia recurrence[95] and therefore caution must be exercised in relying on the use of MR-defined scar as a surrogate for electrophysiological reconnection.

4.4.3 Potential Clinical Significance

It has been previously shown that durable radiofrequency lesion formation is dependent on parameters including catheter tip electrode size, power, catheter tip temperature and contact force. The presented data suggest that there is an element of reversible myocardial injury during ablation. Ablation strategies and techniques which favourably alter the necrosis/edema ratio such as alternative energy sources, contact pressure sensing and improved catheter stability may minimise reversible myocardial injury.

4.4.4 Study limitations

There are significant limitations to MR imaging of the left atrium following catheter ablation with no widely accepted standardisation of technique between laboratories.

Whilst there is evidence from animal studies that gadolinium is predominantly a marker for tissue necrosis, by virtue of its kinetics, it also accumulates in extracellular water which is also seen in acute inflammation. In addition, while T2 MRI can preferentially represent myocardial edema, there is currently no robust histological evidence corroborating this in the atria following radiofrequency ablation.

Although the DE and T2 signal recorded acutely following ablation almost certainly include some "double counting" of edema and necrosis by both techniques, the near complete resolution of T2 signal at follow up indicates that at the very least, T2 predominantly represents some form of reversible atrial injury.

The annotation of lesions on an electroanatomic map is subjective and likely does not accurately reflect the site of atrial injury, which may explain in part the unanticipated MR finding of PV encirclement in only 36% of PV pairs. We attempted to mitigate this by using a point-by-point technique, with RF applications of 30 seconds and 1 tag per application.

Detection of asymptomatic recurrences of AF without the use of continuous monitoring is impossible. Because of the frequency of monitoring, it is likely that the incidence of asymptomatic AF is underreported in the current study.

This is a small, hypothesis-generating study and the utility of necrosis and edema imaging as a predictor of longer-term clinical outcome would require a larger study for validation.

4.5 Conclusion

Acute pulmonary vein isolation is achieved by a combination of reversible and irreversible circumferential tissue injury at the PV-LA junction. The greater the ablation extent accounted for by reversible injury, the higher is the incidence of AF recurrence.

5 Technology Assessment of Atrial Fibrillation Catheter Ablation by Cardiac Magnetic Resonance Imaging

5.1 Introduction

Arrhythmia recurrences following pulmonary vein isolation in paroxysmal atrial fibrillation is almost universally associated with electrical reconnection between the left atrium and pulmonary veins [94]. Acute PV electrical isolation achieved following energy delivery to the left atrial-pulmonary vein (LA-PV) junction or antrum[108, 109] does not always translate into long term clinical success with only 50-60% of patients being cured following a single procedure [110, 127]. The formation of durable transmural scar is critical to block electrical conduction between the LA and PV's and prevent spontaneous pulmonary vein ectopics from triggering AF.

Recent studies suggest that radiofrequency (RF) lesions within the left atrium can be visualised using delayed enhancement cardiac MR imaging[93, 98, 112, 115, 118, 119, 121] . A good correlation between greater amounts of delayed enhancement quantified following ablation and a successful clinical outcome has been demonstrated [93]. We have previously shown that acute cardiac injury following RF ablation comprises tissue necrosis (irreversible injury), inflammation (comprising both irreversible and reversible injury) and tissue oedema (reversible injury) [115]. Whilst T2-weighted imaging enables oedema visualisation, DE imaging in the acute setting is likely to represent both necrotic and inflamed tissue [114, 128]. In the chronic scans, it is likely that some of the areas of inflamed tissue recovers and other parts progress on to form scar and DE here is likely to represent true scar. The more complete the circle of tissue necrosis around the pulmonary vein, the less likely that LA to PV conduction will be restored.

It has been shown that RF lesion depth and dimensions are heavily influenced by catheter tip force [129]. The Hansen Robotic System (HRS) has an incorporated pressure sensing mechanism (IntelliSense, MV, CA) to determine the force exerted by the catheter tip upon the myocardium. This facility and the ability to maintain a stable catheter tip position should improve the delivery of RF energy and enhance the occurrence of a tissue necrotic lesion, in comparison with a manually applied lesion [130].

The present study examines the cardiac MR findings around the PVs following robotically guided ablation in comparison to manual lesion delivery and correlate this to the respective clinical outcomes.

5.2 Methods

5.2.1 Patient population

Forty patients (28 male, mean age 54±13.8 years) with symptomatic, drug refractory paroxysmal AF undergoing their first PVI completed the study. 45 patients were consented for the study but five were excluded (3 because of claustrophobia with failure to complete the scan and 2 due to an ineffective respiratory navigator). All scans used for the purposes of data analysis were deemed of adequate quality for analysis by an experienced CMR operator. Therapeutic anti-coagulation with an INR >2 for at least 4 weeks prior to the procedure was mandated. The study was approved by the Local Research Ethics Committee.

Acute procedural success was defined as PVI confirmed using a circumferential mapping catheter. Clinical outcomes are reported at 6 months follow-up. Patients were followed in clinic to assess symptoms. 24 hour Holter monitors were performed at 6 months. Recurrences were defined on the basis of 1) symptoms with ECG evidence of the presence of atrial

fibrillation/flutter/tachycardia or 2) the presence of symptomatic or asymptomatic episodes of atrial arrhythmia lasting for >30 seconds on ambulatory cardiac monitoring.

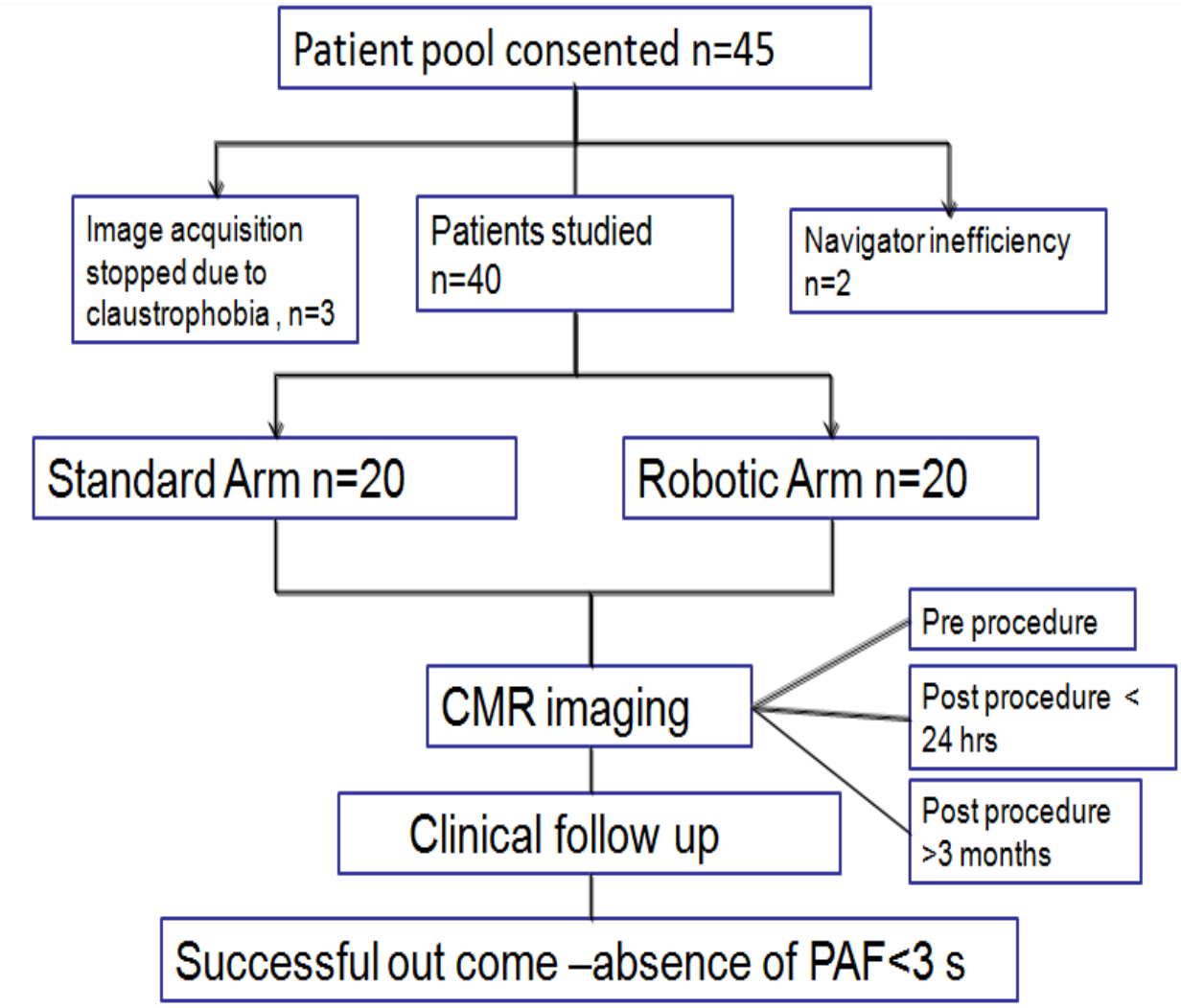

Figure 5-1: The above flow diagram describes this single centre study performed over 18 months. Of the 45 patients consented, 3 developed claustrophobia during CMR image acquisition and 2 had suboptimal images due to navigator inefficiency. The remaining 40 patient studied underwent the same catheter ablation strategy for paroxysmal atrial fibrillation and were imaged between 3-4 months post procedure. Both selected single inversion recovery, SSIR and non-selective dual inversion recovery, NSDIR sequences were performed following gadolinium contrast administration. The routine imaging time point for SSIR following a look-locker scan was performed at 25 minutes post contrast injection whilst NSDIR was performed at two earlier time points (15 and 20mins) and at one later time point (30mins) post contrast delivery. Of the 15 patients studied, 12 patients had 24 good images that were analysed.

5.2.2 MR Image acquisition

The CMR imaging technique utilised has been described previously in Chapter 4. In summary, T2-weighted images were acquired using a multi-slice Turbo Spin Echo (TSE) acquisition technique with a double inversion recovery (DIR) pre-pulse for black-blood imaging. Spatial pre-saturation with inversion recovery (SPIR) fat suppression was applied. The echo time used was set at 120ms with a linear profile ordering. This enabled the image resolution to be set at 1.5x1.5mm^2 with a slice thickness of 5mm. The number of slices was set to provide complete coverage of the left atrium (20-25 slices). Diaphragmatic motion was tracked and respiratory motion correction applied to minimize motion blurring and differences in respiratory phase between slices during image acquisition.

In order to visualize DE, a 3D ECG-triggered, free-breathing inversion recovery (IR) turbo field echo (TFE) scan with respiratory navigator motion correction was performed with a pixel resolution of 1.3x1.3x4mm^3, which was then reconstructed to 1.3x1.3x2mm^3. Data were acquired at mid-diastole with a 150ms acquisition window and a low-high k-space ordering as well as SPIR fat suppression. The IR delay time was determined from a Look-Locker sequence and was set at a TI intermediate between the optimal TIs to null myocardium and blood. Previous work has validated this method for reproducible visualization of the late enhancement signal from necrotic tissue.[115] DE scans were performed 20 minutes following contrast agent administration. The number of slices was set for complete atrial coverage (30-40 slices). To optimize visualization of the PVs, slice orientation was performed in the four-chamber view. Images obtained with this method appear to reflect the pulmonary veins at their maximal size. Similar MR sequences were used for images acquired (i) prior to ablation, (ii) within 24 hours of ablation and (3) 3-6 months following ablation.

5.2.3 Robotic Navigation System

The RNS (Sensei Robotic Catheter System, Hansen Medical, Inc, Mountain View, California) is an electromechanical system comprising a physician workstation with 3 components – instinctive motion controller, remote robotic catheter manipulation (RCM) arm and the artisan sheath (Figure 5.2). The latter sheath consists of an outer (14F) and an inner sheath (10.5F) which allows for the incorporation of any 7-French mapping or ablation catheter. Catheter navigation is performed by four pull wires in the internal sheath facilitating catheter insertion/de-insertion or deflection with an angle up to 360^{o}, and two further pull wires in the external sheath allowing for insertion/de-insertion rotation or deflection. The steerable sheath system is connected to the RCM that is attached to the X-ray procedure table. RCM navigation is realised by the instinctive motion controller (Figure 5.2) which is integrated within the physician workstation, placed remotely from the patient table. The operator moves a ball in the workstation and this movement is transmitted to the steerable Artisan sheath system. In the absence of tactile feedback for the operator, a special feature that indirectly estimates catheter contact force on the tissue (IntelliSense) is present to ensure ablation safety. This estimated contact force measure is displayed instantaneously on the workstation screen.

Figure 5-2: (Clockwise) The electrophysiologist's workstation with the instinctive catheter motion controller (top left and middle), the remote robotic catheter manipulator RCM (top right), the Artisan steerable sheath (bottom left) and the artisan sheath delivered through a short 14.5F sheath.

5.2.4 Ablation Procedure

A 6F decapolar catheter was placed in the coronary sinus to provide a reference for electroanatomic mapping and to enable LA pacing. Double transseptal puncture from the right femoral vein was performed manually and access to the left atrium was obtained using 8.5Fr non-deflectable long sheaths, (St. Jude Medical Inc., St. Paul, MN, USA). Following the first transseptal puncture, intravenous heparin was administered to achieve an activated clotting time of between 300 and 400 seconds. Both circular mapping catheter (Inquiry™Optima™, St. Jude Medical Inc.) and NaviStar® ThermoCool® 3.5 mm irrigated tip catheter (Biosense Webster Inc., Diamond Bar, CA, USA) were employed to create a 3-dimensional geometry of the left atrium with either NavX™ (St. Jude Medical Inc., St. Paul,

MN, USA) or CARTO XP (Biosense Webster Inc., Diamond Bar, CA, USA). Following this, the ablation catheter was withdrawn from the left atrium and inserted into the flushed Artisan sheath and subsequently connected to continuous irrigation. The Artisan RNS was placed within the right atrium via a short 14-Fr sheath in the right femoral vein and then manually introduced into the left atrium through the previous transeptal puncture. By leaving the ablation catheter out beyond the Artisan sheath, the ablation catheter functioned as a landmark under fluoroscopic guidance during the advancement of the Artisan sheath through the venous system and across over into the left atium. The Artisan tip was aligned with the fluoroscopy system and baseline force sensing pressure (Intellisense) was calibrated whilst the catheter was positioned in the middle of the left atrium with minimal electrical signal spikes being recorded on the ablation catheter.

The circular mapping catheter was then placed in each pulmonary vein in turn while the corresponding LA-PV antrum was targeted with wide area circumferential ablation. The ablation catheter irrigation flow was set at 15 ml/min, power limited to 25 W on the anterior wall and 20 W on the posterior wall and temperature 40^0C. Ablation lesions were marked on the LA geometry when there had been an 80 % reduction in the local electrogram voltage or after 30 seconds of energy delivery. One tag was applied to the shell per 30s RF energy delivery and a standard tag size was used throughout the study. If LA-PV conduction persisted despite wide area circumferential ablation, additional lesions were delivered at sites of earliest activation on the circular mapping catheter until entry block in all 4 veins was confirmed by observing the elimination or dissociation of pulmonary vein potentials. Exit block was not routinely assessed. Neither adenosine nor isoprenaline was routinely administered to test the integrity of PVI or to search for non-PV triggers of AF

The technical aspects of the ablation were identical in both robotic and standard approach apart from the different navigational approach and ablation settings - flow limited to 17 ml/min, power limited to 30W on the anterior wall and 25W on the posterior wall and temperature 50^0C.

5.2.5 Image processing and analysis

T2 and DE signal circumferential quantification was performed by reconstructing all CMR scans into individual left atrial shells using a semi-automated 3-D visualization method previously described in chapter 3 [115]. Areas of DE or high T2 signal intensity were defined as being more than three standard deviations above the mean signal intensity of an area of healthy ventricular myocardium. This threshold was chosen based on work assessing cardiac injury following ablation or myocardial infarction[90, 113]. The LA surface was colour coded according to the MIP values, ranging from green (minimum) to red (maximum).

For the acute post ablation scan and chronic follow up scan, PVs were analyzed as ipsilateral pairs for each of the 40 patients, permitting analysis of 240 PV pairs (80 pre ablation pairs, 80 acute scan pairs and 80 chronic follow-up scan pairs). For each PV pair, T2 and DE was quantified as occupying a percentage of the antral circumference. The % delayed gadolinium enhancement (DE), high T2-weighted signal (T2) and combination of delayed gadolinium enhancement and T2 (DE+T2) encircling the pulmonary veins was quantified. All 3D MR reconstructions were analyzed twice independently by two experienced readers, blinded to clinical outcome and to the timing of the scan following catheter ablation. A high degree of interobserver agreement was seen on a Bland Altman test with a maximum observed difference of 10% seen. The mean±SD inter-observer error for DE, T2 and DE&T2 was 1.5±2.5%, 1.5±3.5% and 0.8±2.2% which was acceptable for the purposes of data analysis.

5.2.6 Statistical analysis

Summaries for continuous variables are expressed as mean ± confidence interval. Follow-up times are reported as the median and interquartile range (IQR).Categorical variables were compared among recurrences and non-recurrences groups using a chi-square test. The % circumferential encirclement by DE, T2 and DE&T2 groups were compared to test for differences between group means. Statistical analyses were performed using Stata (StataCorp 2009). A linear regression model with predictor (code 1 for no recurrence and 0 for recurrence) and outcome T2, DE, T2&DE, DE/(T2&DE) respectively was applied and run in Stata. We used the vce (cluster subject) option in Stata[116] to allow for inter-subject dependence (left and right pulmonary vein measurements from the same patient). Analyses for acute and chronic pulmonary vein findings on cardiac MR were performed separately. A p value of less than 0.05 was considered statistically significant.

5.3 Results

5.3.1 Patient and procedural data

Table 5.1 outlines the clinical characteristics of the study population in both groups. Successful pulmonary vein isolation was achieved in all patients. Means for RF application, energy delivered and fluoroscopic time in the robotic group were 141±34, 88390J±38583J and 43±11.5min in comparison to 126±79 (p=0.52), 80011J±42757J (p=0.50) and 55±18.5min (p=0.04) in the standard group. At 6 month follow-up, 12 (60%) in the robotic group versus 11 (55%) in the standard group were arrhythmia free. Median time to recurrence was 78days (range 32 to 146 days) for the robotic group versus 96 days (range 68 to 167days).Patients with recurrences in both groups were listed for a re-do ablation. In the arrhythmia free. In the standard group, 2 patients declined a further ablation, 2 pending and of the 5 patients (PAF) undergoing a second procedure, only 1 has remained arrhythmia free.

Overall success in the robotic group was 75% following 1.2 procedures compared to 60% following 1.25 procedures. Procedural complications include two femoral venous haematoma which resolved on its own and 1 pseudoaneurysm that did not require surgical intervention. No stroke, tamponade or oesophageal fistula occurred in this study and no pulmonary vein stenosis was detected on follow up MRI.

Table 5-1: Baseline Characteristics

	Total Population (N=40)	Robotic Navigation (N=20)	Standard Catheter Ablation (N=20)	P Value
Male, n (%)	28 (70)	15 (75)	13 (65)	0.53
Age (years)	54+-13.8	54+-14.3	55+-11.2	0.86
AFduration (months)	30+-11.2	32+-9.1	30+-12.6	0.78
LA size, cm	3.4+-3.5	3.4+-0.3	3.5+-0.2	0.92
LVEF, %	56±8	58±6	56±8	0.86
Hypertension	11	7	4	>0.10
Diabetes	1	0	1	>0.10
Coronary Artery Disease	1	1	0	>0.10
Thyroid	2	2	0	>0.10
Smoking	6	4	2	>0.10
Fluoroscopy time (minutes)	48.9+-14.1	43.1+-8.6	54.8+-16.4	0.04
Procedure time (hours)	210+-26.1	220+-21.4	199+-27.7	0.06
Number of applications	134+-42	141+-33	126+-58	0.63
Energy delivered (Joules)	84201+-28855	88391+-28519	80011+-28338	0.46

5.3.2 Cardiac MR evaluation

Baseline circumferential burden of DE and T2 weighted signal prior to any ablation were similar in both groups (Figure 5.3) and did not occupy more than 5% of the PV circumference. Post-ablation acute imaging was performed between 18 and 24 hours following catheter ablation. Figure 5.3 demonstrates the typical T2-weighted (figure 5.3 a) and DE (figure 5.3 b) appearances in two patients before and after catheter ablation. The left atrial burden of DE and T2-weighted signal was significantly increased following both catheter ablation approaches in comparison with pre-ablation (Figure 5.3). In general, DE signal was concentrated in the PV antral region while T2 signal was more widely distributed in the atrium, remote from sites of ablation.

Combined analysis of DE and T2 signal, using reconstructed shells co-displaying both signal types, revealed areas of T2 enhancement to overlap and interdigitate with those areas of high DE signal intensity (figure 5.3). Hence the total combined DE and T2 percentage PV encirclement on the combined overlay shells were 100% or less.

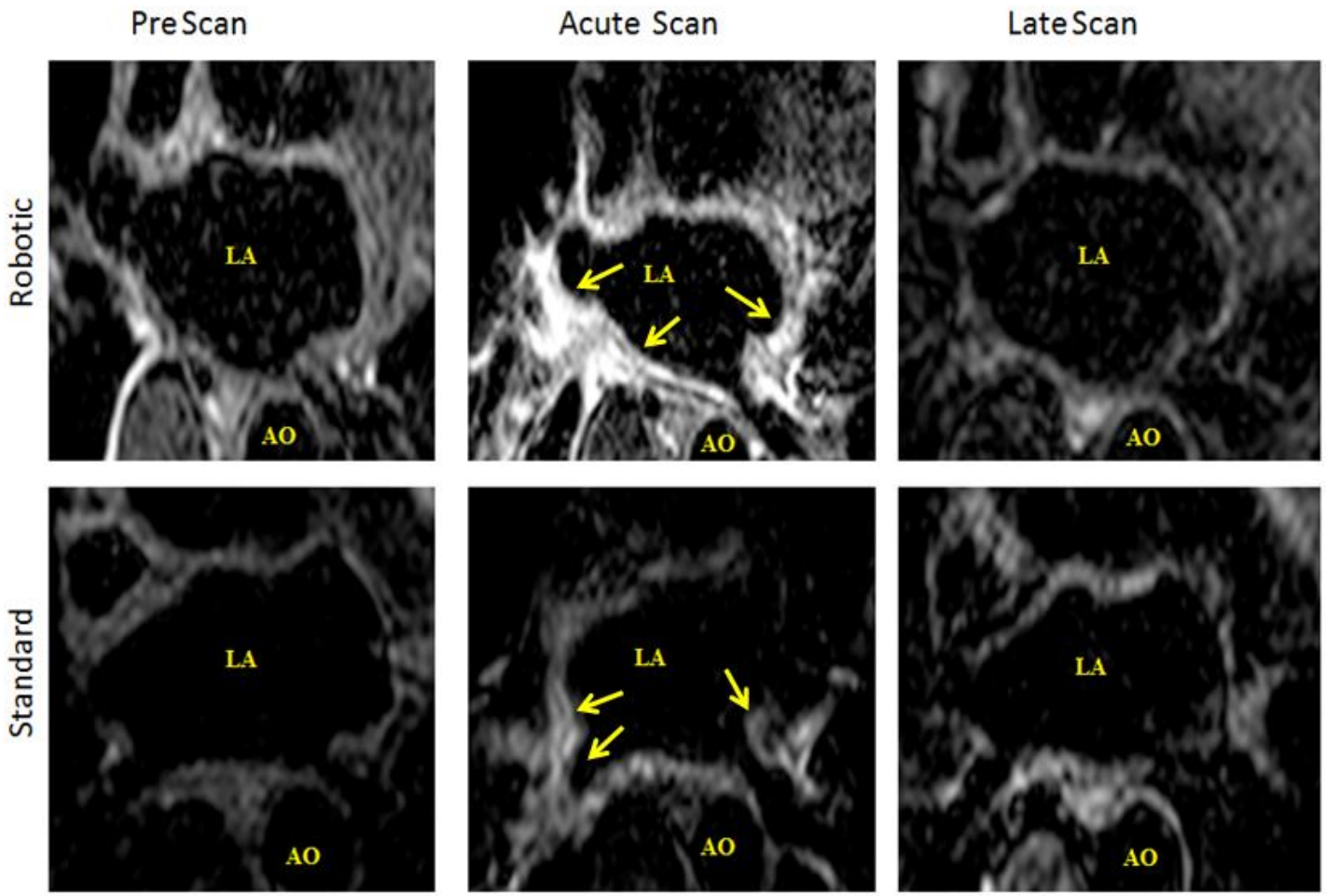

(a)

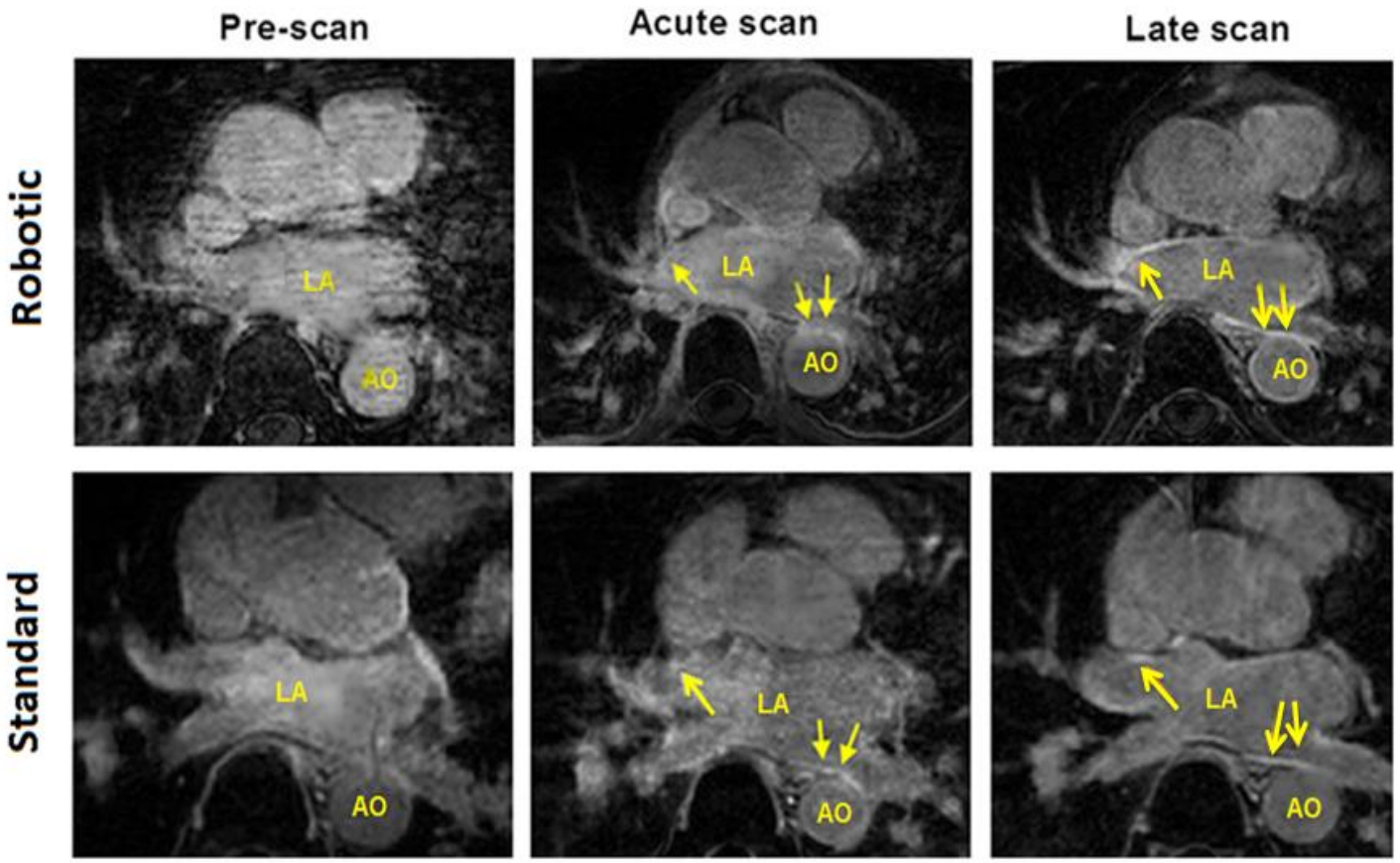

(b)

Figure 5-3 : (a) Serial T2 CMR scans performed on a single patient following robotic and standard navigated catheter ablation at 3 time points.(b) Serial DE CMR scans performed on a single patient following robotic and standard navigated catheter ablation at 3 time points.

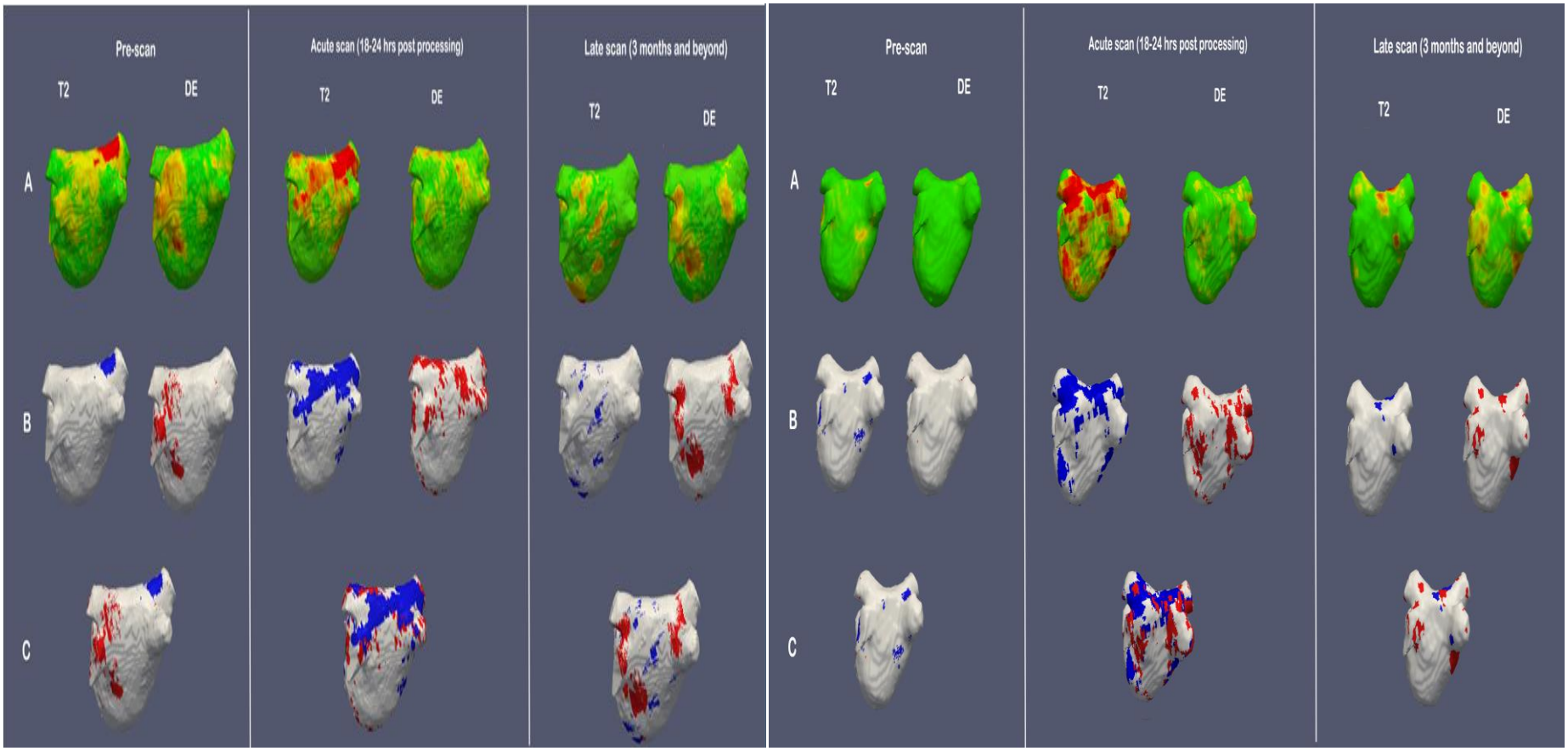

(a) (b)

Figure 5-4 : Depicts an example of a series of 3-D LA reconstructed shells (at 3 time points) in two patients to compare robotic (3a) versus standard catheter ablation (3b). Blue represents areas of T2 signal whilst red represents DE. Greater 'islands' of red is seen in the robotic assisted LA shell.

In the robotic group, the LPV circumferential extent of DE signal alone, T2 signal alone and the combination of both signal types was 72±13%, 80±19% and 94±10% respectively. For the RPVs, the circumferential extent of DE signal alone, T2 signal alone and the combination of both signal types was 71±13%, 78±30% and 95±10%respectively. Compared to DE alone, the combined DE and T2 signal was significantly greater for both left ($p<0.0001$) and right ($p<0.0001$) PVs. Complete antral encirclement with combined DE and T2-weighted signal was seen in 14/30 (47%) PV pairs at the acute scan.

In the standard group, the LPV circumferential extent by DE signal alone, T2 signal alone and the combination of both signal types was 60±18%, 71±35% and 87±11%respectively. For the RPVs, the circumferential extent of DE signal alone, T2 signal alone and the combination of both signal types was 58±23%, 81±15% and 89±13%respectively. Compared to DE alone, the combined DE and T2 signal was significantly greater for both left ($p<0.0001$) and right ($p<0.0001$) PVs. In contrast to the robotic group, complete antral encirclement with combined DE and T2-weighted signal was seen in half of the PV pairs at the acute scan, 7/30 (23%).

Follow-up CMR scans were performed between 3 and 6 months post procedure. Here, T2 signal had largely resolved (Figure 5.4), while a decline in the extent of DE signal was seen in both groups. In the robotic group, the circumferential extent of DE signal in the LPV decreased from 72±13% to 58±22% ($p=0.002$); for the RPVs, the circumferential extent of DE decreased from 71±13% to 53±22% ($p=0.001$). In the standard group, the circumferential extent of DE signal in the LPV decreased from 60±18% to 47±32% ($p=0.09$); for the RPVs, the circumferential extent of DE decreased from 58±23% to 44±30% ($p=0.09$). Discontinuities in areas of DE signal could be seen in both groups. Overall, a higher mean

percentage encirclement was consistently observed in the robotic group in both acute and late scans with a 10% higher margin encirclement observed on the chronic scans by DE.

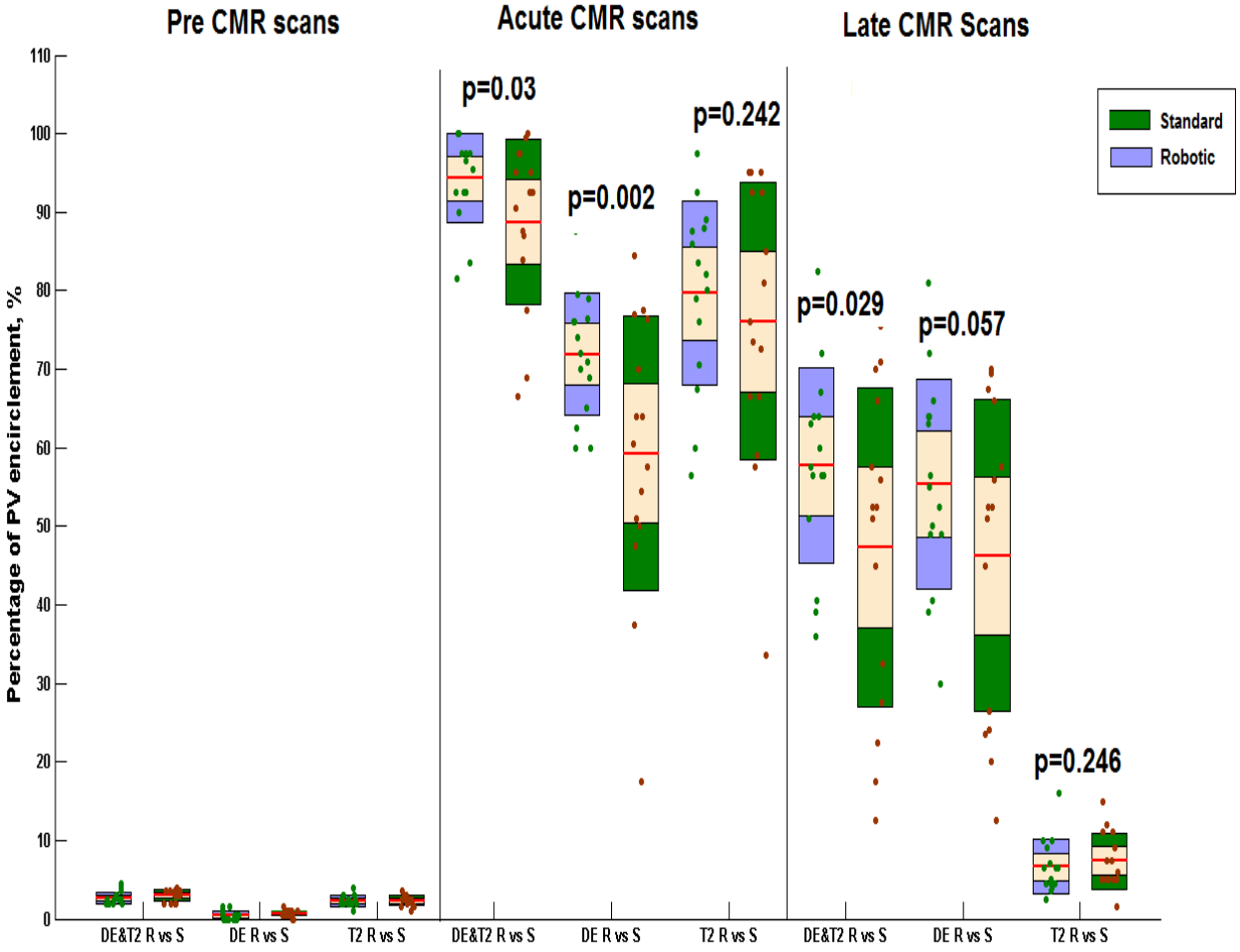

Figure 5-5: This scatter-boxplot shows a comparison of pre, acute and late T2, DE and combined T2&DE for both robotic and standard ablation. Each individual scatter plot represents the raw data for that specific group. The dots within each group have been dispersed horizontally to optimise visualisation and clarity. The boxplots on the other hand represent median (red line), 95% confidence intervals (yellow box) and 1 standard deviation (blue box). An overall higher enhancement is seen post procedure in the robotic group compared to the standard group

5.3.3 Outcome in relation to CMR assessment

In both robotic and standard groups, acute and late scan data were analysed into two groups according to the respective clinical outcome – those with and without AF recurrences. 160 pairs of PVs (80 robotic, 80 standard) analysed previously were divided according to the

presence or absence of arrhythmia recurrences. Figure 5.5 summarises the percentage circumferential encirclement of DE, T2-weighted signal and the combination of DE &T2 around the left and right PV pairs by clinical outcome for both the acute and late scans.

In the robotic group, the acute CMR findings in the arrhythmia free versus recurrences by DE alone, T2 alone and a combination of DE&T2 was 74±13%, 76±16% and 93±13% versus 68±14%, 82±16% and 96±5%. Similarly, in the standard group, the percentage encirclement by DE alone, T2 alone and a combination of the two in the arrhythmia free versus recurrences group was 70±25%, 71±33% and 90±13% versus 46±19%, 81±24% and 87±14%.

recurrences, DE was higher in the robotic group (43±19% vs 30±35%, p=0.02). A comparison of energy delivered, DE quantified on late CMR scans and clinical outcome between the two groups is presented in Figure 5.6. In contrast to the standard group, the points on the robotic scatter plot are less spread and more close together with DE values being above 40%. Furthermore, at energy values ranging between 40000J - 90000J, greater numbers of points are observed with higher DE in the RNS group.

On the late scans, DE was the predominant signal type seen and was significantly greater in both groups for arrhythmia free versus recurrences (robotic 64±18% versus 43±19% and standard 60±14% vs 30±35% respectively, p <0.0001). Arrhythmia free patients had an almost similar mean DE encirclement (robotic 64±18%, standard 60±14%, p=0.45) but in

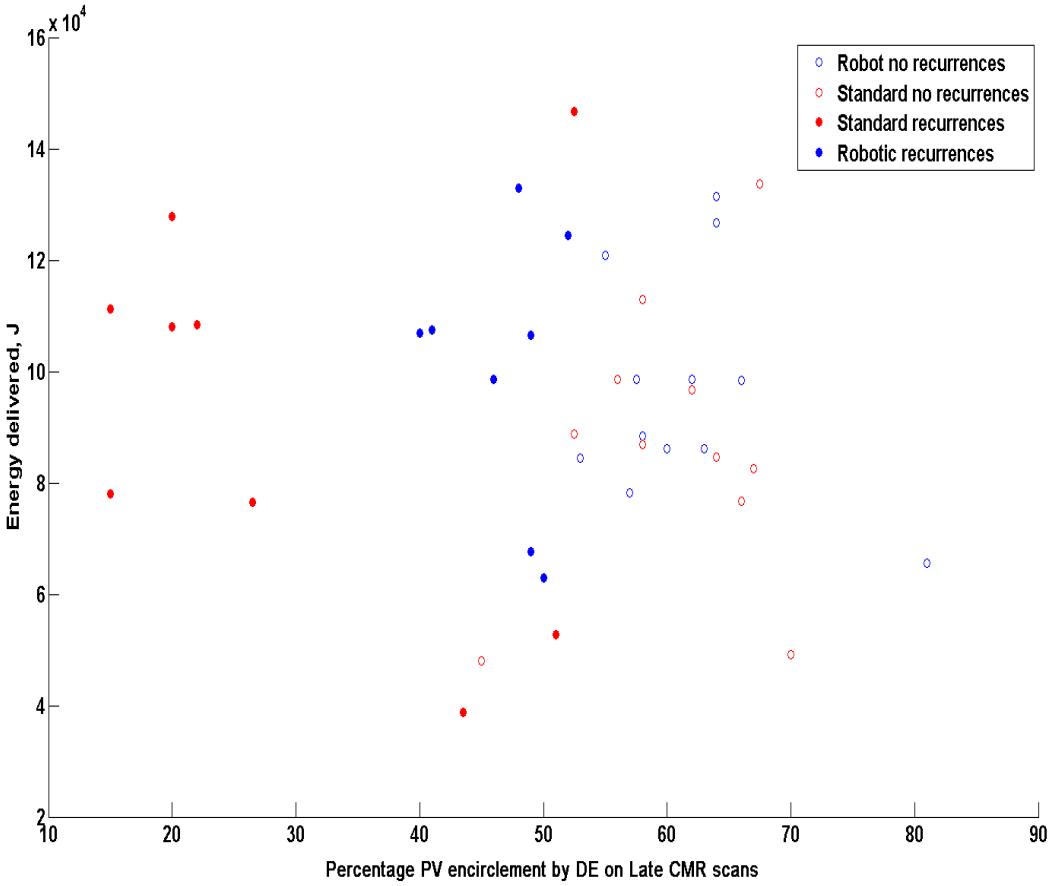

Figure 5-6: This scatter plot describes the relationship between energy delivered and scar created as quantified on DE-CMR by percentage PV encirclement. Both robotic and standard ablation datasets have been categorised into no recurrences versus recurrences. The blue circles representing robotic procedures appear less dispersed and have a minimum DE value of around 40%. The red circles representing standard catheter ablation are widely dispersed and have a minimum DE value of 15% to 30% despite high total energy delivery. This suggests better catheter-tissue contact conferred by the robotic system yielding higher percentages of PV antrum scar.

5.4 Discussion

This is the first report to compare robotic and standard catheter ablation lesions using cardiac MR and correlate the findings to clinical outcome. The main findings of this single-centre study are as follows – (1) electromechanic robotic assisted lesion delivery results in greater percentages of PV encirclement quantified on CMR, (2) CMR atrial shell analysis of the lesion patterns reveal a more contiguous encirclement around the PV in the robotically

navigated RF ablation group in comparison to a scattered pattern observed in the standard group, (3) a significantly less regression in acute versus late scan DE in the robotic recurrences group suggest that energy delivery with this approach favourably results in more longer term robust lesions, (4) the more closely placed points observed on the robotic scatter plot suggests better consistency and higher reproducibility in lesion delivery with an overall greater minimum scar formation (DE > 40%).

The challenges during AF ablation arise from not only the importance of precision in catheter movement, catheter stability and tissue contact [129, 131] but also the variable heterogeneity in PV anatomy, chamber size, tissue thickness [132]. Several studies have previously reported that robotically navigated catheter ablation can be performed effectively in achieving acute electrical isolation of PV potentials and mid-term freedom from arrhythmia with complication rates comparable to conventional procedures (Table 5.2). This study extends the clinical experience on both feasibility and safety of the robotic navigation catheter ablation and also reports on the clinical outcome. Former studies have showed that robotic navigated catheter ablation can be performed safely with a marked reduction in fluoroscopic time and achieve a high acute success rate. Recently, mid-term success rates described in Hlivak's study demonstrates a 63% first procedure success rate and a 86% success rate following 1.21 procedures per patient at 15 months follow-up [133]. Natale's group in the largest single centre RNS study achieved an overall 85% success rate at 14.1±1.3months [132]. Both the introduction of the Intellisense contact force evaluation and RNS procedural experience over the last 5 years recommending cautious power settings especially during LA posterior wall ablation have reduced the overall complication profile. The recent study involving 100 RNS procedures reported only 2 small haematomas at the puncture site, a pseudoaneurysm that resolved following manual pressure and no other adverse events [133].

Table 5-2:Summary of Robotic Navigation System studies that outline procedural characteristics and clinical outcome

No	Authors	Paper Title	Patients Studied	Procedure Time	Fluoroscopy time	Clinical Outcome (Freedom from AF)	Complications	Study Conclusion
1	Saliba W, Reddy VY, Wazni O et al 2008	Atrial fibrillation ablation using a robotic catheter remote control system: initial human experience and long-term follow-up results	40	2.8 ± 1.5 hours	64 ± 33 minutes	98% at 12 months	5% (tamponade 5%)	This preliminary human experience suggests that mapping and ablation of AFL and AF using this novel robotic catheter with remote control system is feasible with similar results to conventional approach.
2	Kautzner J, Peichl P, Cihak R, Wichterle D, Mlcochova H et al 2009	Early experience with robotic navigation for catheter ablation of paroxysmal atrial fibrillation	22	3.5 ± 0.5 hours	15 ± 5 minutes	91% at 5 ± 1 month	0%	Early clinical experience in using robotic navigation to achieve pulmonary antrum isolation was safe, effective and associated with shorter procedural and fluoroscopic times than standard approach
3	Schmidt B, Roland R, Ouyang F et al 2009	Remote Robotic Navigation and Electroanatomical Mapping for Ablation of Atrial Fibrillation	65	3.3 ± 0.7 hours	17 ± 7 minutes	73% at 8 months	5% (1.5% tamponade)	PVI using the novel RN system can be performed safely and effectively with one third of the operator's fluoroscopy exposure time reduced.
4	Di BiaseL,Wang Y, Natale A et al 2009	Ablation of atrial fibrillation utilizing robotic catheter navigation in comparison to manual navigation and ablation: single-center experience.	193	3.1± 0.8 hours	48.9 ± 24.6 mins	85% at 14 ± 1 month	1.5% , (1% tamponade)	Robotic navigation and ablation of atrial fibrillation is safe and effective. Fluoroscopy time decreases with experience

5	Wazni O, Natale A, Saliba W et al 2009	Experience with the Hansen Robotic System for Atrial Fibrillation Ablation—Lessons Learned and Techniques Modified: Hansen in the Real World	64	3.1± 0.8 hours	24±10mins	81% at 12 months	0%	The suggested modifications- Intellisense incorporation and tailored power and force settings may make the system easier to use with the potential to reduce complications.
6	P Hlivak, H Milcochova, J Kautzner et al 2011	Robotic Navigation in Catheter Ablation for Paroxysmal Atrial Fibrillation: Midterm Efficacy and Predictors of Postablation Arrhythmia Recurrences	100	3.7 ± 0.9 hours	11.9 ± 7.8 mins	63% at 6 months following first procedure and 86% at 15months, after 21 patients had a repeat procedure	0%	This study demonstrates feasibility and safety of robotic navigation in catheter ablation for paroxysmal AF. Midterm follow-up documents success rate comparable to other technologies and potential for improvement in more extensive ablation along the ridges with thicker myocardium.
7	Arujuna A, Razavi R, Rinaldi A, O'Neill M, Gill J et al 2012	Remote Robotic Navigation versus Standard Catheter Ablation: A Cardiac MR Comparison with Clinical Outcomes	20	3.8 ± 0.9 hours	43.1 ± 8.6 mins	60% at 6 months following first procedure and 75% at 12months, after 4 patients had a repeat procedure	0%	The cardiac MR findings suggest that robotic navigation systems permit greater long term scar. This is likely to be a function of increased catheter stability with better navigation control allowing for greater tissue contact.

In the context of cardiac MR assessment of catheter ablation lesions, delayed enhancement MRI (DE-MRI) following the administration of gadolinium-containing contrast agents has been used to visualize the atrial tissue injury following catheter ablation [93, 98, 112, 115, 118, 119, 121,

[124]. The poor washout kinetics of gadolinium in areas of damaged cells results in contrast agent accumulation, thus highlighting areas of tissue injury. In viable myocardial tissue, gadolinium washes out faster resulting in reduced areas of enhancement [134-136]. A good correlation between greater amounts of DE on late scan imaging and better procedural outcome has been documented [93]. On the other hand, T2 weighted magnetic resonance imaging has been used to visualize myocardial oedema following radiofrequency ablation. Left atrial oedema is thought to be common following AF ablation. Okada et al used electron beam tomography to show that an increase in LA wall thickness occurred immediately following AF ablation and resolved within one month [137]. This increase in wall thickness was attributed to atrial wall oedema. Recently, Marrouche et al using CMR demonstrated the presence of T2 enhancement alongside DE in patients following catheter ablation. A correlation between low voltage areas (<0.05mV mapped on Carto) and areas of T2 enhancement was shown here. A comparison between acute and 3 month CMR scans performed by this group showed loss of T2 enhancement areas suggesting resolution of oedema.

This study reports the cardiac MR findings comparing robotic navigated catheter ablation lesions to standard catheter ablation. The higher mean percentage encirclement consistently observed in the robotic group in both acute and late scans is likely a function of both catheter stability and tactile feedback with Intellisense conferring better catheter control. Improved lesion delivery resulted in an overall 10% higher margin encirclement observed on the RNS late scans. Whilst almost similar % encirclements were observed on late scan DE between the two groups with no recurrences, a significantly higher amount of DE was noted in the robotic group. This lower regression of DE between the acute and late scans in the robotic recurrences group suggests an overall better quality lesion created using the RNS. Anova

comparisons between the two groups demonstrate a narrower range in % encirclements in the robotic group confirming less variability in lesion delivery, suggesting better tissue contact.

The overall more contiguous lesion set appearance on qualitative examination of the 3-D CMR atrial shells in the robotic group is again attributable to better catheter control and greater stability. More circular shaped encirclement patterns observed in the RNS group suggests that the system allows for a more accurate and precise catheter movement along the PV antrum with sufficient tissue contact creating better adjoining lesions. The association between energy delivered and scar formation analysed on late DE CMR scans was examined. At a set range of energy delivery, more points with higher DE was observed on the robotic scatter plot. This is likely to be a function of better catheter stability conferred by the RNS. The better consistency and higher reproducibility inferred from both the smaller standard deviation and more closely placed points on the scatter plot implies a relatively a higher precision in lesion delivery in the robotic group in comparison to the standard.

5.4.1 Potential Clinical Significance

On average, patients with atrial fibrillation undergo between 2 to 3 ablation procedures to become arrhythmia free. Repeat procedures incur cost, utilizing further health resources and more importantly inconveniencing the patient by subjecting them to another ablation. The creation of more durable ablation lesions will benefit the patient greatly alongside optimising and saving on healthcare resources which is becoming a necessity, more so in the present economic climate.

RNS confers greater catheter stability, better control and improved tissue contact allowing for the creation of more durable contiguous lesions around the PV antrum. The reduced DE variance and overall higher percentage encirclement observed on CMR quantification in the robotic recurrence group suggests both a higher consistency in lesion delivery and greater

atrial tissue injury. This is evidenced by the overall 75% success rate following 1.2 procedures in comparison to a 60% success following 1.40 procedures in the standard group. The recurrence arrhythmia pattern of atrial tachycardia which was greater in numbers in the RNS group suggests that the index ablation had successfully modified the arrhythmia into a more organised rhythm which was successfully ablated during the subsequent procedure.

5.4.2 Study limitations

This is a small, hypothesis-generating study and the role of Robotic Navigation Syetem assisted catheter ablation in conferring overall better mid to long-term clinical outcome would require a larger study for validation. With regards to cardiac MR tissue injury quantification, there are some limitations with no widely accepted standardisation of technique between laboratories.

Whilst there is evidence from animal studies that gadolinium is predominantly a marker for tissue necrosis, by virtue of its kinetics, it also accumulates in extracellular water which is also seen in acute inflammation. In addition, while T2 MRI can preferentially represent myocardial oedema, there is currently no robust histological evidence corroborating this in the atria following radiofrequency ablation.

Detection of asymptomatic recurrences of AF without the use of continuous monitoring is impossible. Because of the frequency of monitoring, it is likely that the incidence of asymptomatic AF is underreported in the current study.

5.5 Conclusion

The cardiac MR examination findings in this study suggest that remote robotic assisted navigation systems permit the creation of more contiguous, durable scar around the PV

antrum. This is likely to be a function of increased catheter stability improving tissue contact and better catheter control allowing for more accurate lesion delivery.

6 Novel Dual Inversion Recovery Pre-Pulse for Improved Blood Suppression to Better Visualise Scar

6.1 Introduction

Pulmonary vein disconnection following atrial tissue necrosis is the principal mechanism by which patients with paroxysmal atrial fibrillation benefit from catheter ablation therapies. To assess the efficacy of catheter ablation, it is useful to determine and quantify areas of atrial injury created by measuring the final scar size. The recent few years have seen the use of delayed enhancement cardiac magnetic resonance imaging, DE-CMR in visualising areas within the left atrium following catheter ablation [90, 93, 98, 112, 115, 118, 119, 121, 124, 126, 138]. Studies have confirmed that the higher the degree of atrial scar created, the better the clinical outcome[93, 98]. Furthermore, DE-CMR imaging has been used to guide re-do procedures by identifying gaps between lesion sets and thus providing a potential road map to guide target areas of ablation [98].

However the present method of atrial scar visualisation and quantification is affected by the presence of some contrast remaining within the atrial blood pool. The presence of this increased signal intensity can lead to an overestimation of scar presence during quantification. Furthermore, the difference in circulating atrial blood pool contrast between individuals may affect quantification analysis in a cohort study. In addition, imaging has to be performed following the washout of gadolinium contrast from the blood pool which can be up to 30 minutes following contrast injection.

Recently, the dual-IR pre-pulse technique was shown to achieve improved blood suppression in delayed enhancement images of ventricular scar [139]. In this study, we aimed to examine the application of this sequence in imaging atrial scar following radiofrequency catheter ablation

6.2 Methods

6.2.1 Study population

This prospective study was conducted between July 2011 and December 2011 at a single tertiary centre. Figure 6.1 outlines the study design. Patients with paroxysmal atrial fibrillation undergoing follow-up CMR scans, median 5months (IQR 4-7months) post catheter ablation

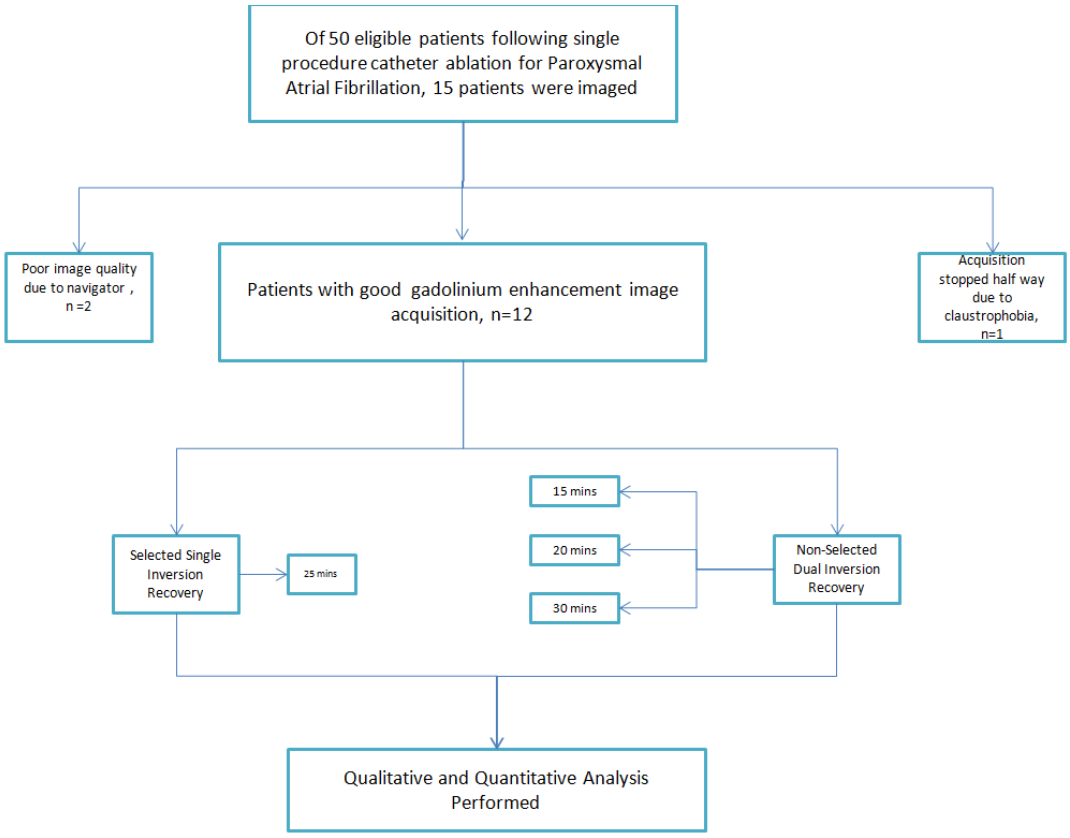

Figure 6-1: This flow diagram describes this single centre study design performed over 6 months. All patients recruited underwent the same catheter ablation strategy for paroxysmal atrial fibrillation and were imaged between 3-4 months post procedure. Both selected single inversion recovery, SSIR and non-selective dual inversion recovery, NSDIR sequences were performed following gadolinium contrast administration. The routine imaging time point for SSIR following a look-locker scan was performed at 25 minutes post contrast injection whilst NSDIR was performed at two earlier time points (15 and 20mins) and at one later time point (30mins) post contrast delivery. Of the 15 patients studied, 12 patients had 24 good images that were analysed.

were recruited. To ensure that the CMR findings reflected atrial scar following the index catheter ablation, patients were not enrolled if they had a previous left atrial ablation. Further exclusion criteria included contraindications to DE-CMR (i.e metallic intracranial implants, poor renal function, pacemakers) and general anxiety/claustrophobia. Therapeutic anti-coagulation with an INR >2 for at least 4 weeks prior to the procedure was mandated. All patients provided written informed consent to participation in the study which was part of a larger CMR study aimed at quantifying areas of delayed enhancement within the left atrium following catheter ablation and corroborating this to clinical outcome. The study was approved by the Local Research Ethics Committee.

6.2.2 Catheter Ablation

This has been previously described in chapter 4. In summary, two transseptal punctures were made and access to the left atrium was obtained using 8.5Fr non-deflectable long sheaths, (St. Jude Medical Inc., St. Paul, MN, USA). A 3-dimensional geometry of the left atrium was created using either NavX™ (St. Jude Medical Inc., St. Paul, MN, USA) or CARTO XP (Biosense Webster Inc., Diamond Bar, CA, USA). A circular mapping catheter (Inquiry™Optima™, St. Jude Medical Inc.) was then placed in each pulmonary vein in turn while the corresponding LA-PV antrum was targeted with wide area circumferential ablation. Energy was delivered through a NaviStar® ThermoCool® 3.5 mm irrigated tip catheter (Biosense Webster Inc., Diamond Bar, CA, USA) with flow limited to 17 ml/min, power limited to 30 W on the anterior wall and 25 W on the posterior wall and temperature limited to 50^0C.

6.2.3 CMR

Areas of post ablation left atrial scar was imaged using a 1.5 Tesla Philips Achieva MR system (Philips Healthcare, Best, Netherlands) with a 32 channel surface coil (Invivo,

Orlando, Florida, USA). The standard CMR imaging technique utilised has been described previously in Chapter 4. In summary, the conventional LGE imaging was performed using a 3D free breathing, respiratory-navigated, ECG-triggered gradient echo (GE) sequence (2). Image acquisition was timed at end diastole using a preceding b-SSFP cine image. Imaging parameters included: TE/TR=2.6/5.4ms, TR effective=1 heartbeat, navigator window=5-7mm, flip angle=25°, voxel size=1.3x1.3x4mm^3 (reconstructed=1.3x1.3x2mm^3). The navigator restore was removed and a delay of 100ms was applied between the navigator and image acquisition to avoid the pulmonary vein inflow artifact (x4). The traditional IR-GE pre-pulse (Figure 6.2a) was employed with the TI set to null normal myocardium using a preceding Look Locker scan. Previous work has validated this method for reproducible visualization of the late enhancement signal from necrotic tissue [115]. The dual-IR-GE sequence (Figure 6.2b) employed two non-selective inversion pre-pulses separated by time delays TI1 and TI2. These delays were optimized to achieve signal suppression in a T1 range 250 - 1400ms. The aim of the dual IR sequence is to simultaneously suppress both normal atrial wall and blood signal whilst maintaining high signal in atrial scar.

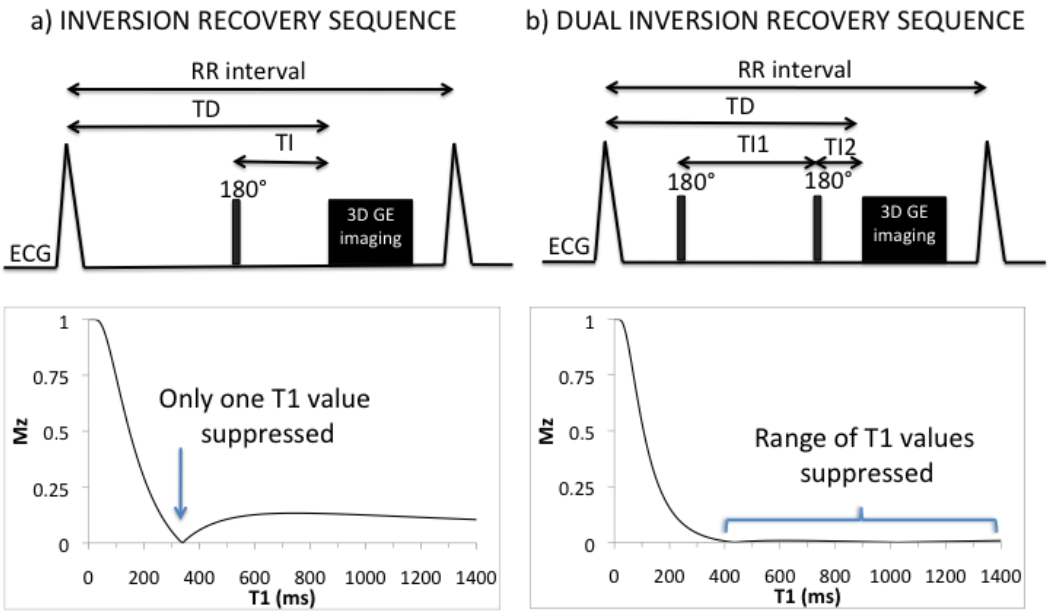

Figure 6-2: Inversion recovery and (b) Dual inversion recovery pre-pulses with corresponding signal versus T1 plots. The IR pre-pulse only suppresses the T1 of normal atrial wall whereas both the atrial wall and blood are suppressed with the dual-IR pulse.

6.2.4 Image Analysis

6.2.4.1 CNR and SNR Image analysis.

Regions of interest were manually defined in 5 slices in the blood pool and in right superior pulmonary vein scar. Blood and scar signal-to-noise (SNR) and scar-to-blood contrast-to-noise (CNR) values were measured in all images using Osirix medical imaging software.

6.2.4.2 Qualitative Visual Image analysis

Images were assessed and scored by 5 experienced CMR readers. Five categories were assessed - atrial blood pool nulling, scar visualization, noise, artefact, and blur with a score of 0-4 conferred. Individual categories were scored as following. For blood pool nulling, 0= no nulling, 1=inadequate nulling, 2=adequate nulling, 3 good nulling and 4 very good nulling. For scar visualization, 0= no scar seen, 1= scar visible with poor demarcation of borders or edges, 2=scar visible with moderately blurred borders or edges, 3= scar visible with mildly blurred borders or edges and 4= scar visible with sharply demarcated borders or edges. Signal

noise, artifact and noise respectively graded as 1= great amount, 2=moderate amount, 3= mild amount and 4= none. Observers were blinded to the type of sequence used.

6.2.4.3 Quantitative Delayed Enhancement analysis

Areas of delayed enhancement around the pulmonary veins were manually segmented out by two experienced CMR readers that were blinded to both clinical outcome and acquisition sequence used. Quantification was performed in Osirix.

6.2.4.4 Statistical Analysis

Summaries for continuous variables are expressed as mean ± confidence interval. Follow-up times are reported as the median and interquartile range (IQR).Categorical variables were compared among recurrences and non-recurrences groups using a chi-square test.

6.3 Results

Of the 50 patients participating in the initial CMR study, 15 patients were enrolled into this study where 12 good quality scans were acquired. Two scans were suboptimal due to navigator inefficiency and 1 scan had to be stopped as the patient became claustrophobic.

6.3.1 Patient characteristics

Demographics and clinical characteristics are shown in Table 6.1. The baseline characteristics include mean age 58 ± 10.7 years, 10 male patients (67%) with a mean LA size of 3.7±0.5, AF duration of 28±16 months and BMI of 23.2 ± 1.8. Successful acute pulmonary vein isolation was achieved in all patients.

Table 6-1: Patient demographics categorized into no recurrences and recurrences at 6month clinical follow up.

	All Subjects n=12	No AF Recurrence n=7	AF Recurrence n=5	p Value
Age	58±10.7	49±12.4	55±10.8	0.46
Gender **Male** **Female**	 10(67%) 2(33%)	 11(78%) 3(22%)	 6(55%) 5(45%)	 0.60 0.68
Duration of AF, months	28±16 (12-60)	24±10 (12-48)	30±11 (18-60)	0.24
LA size, cm	3.7±0.5	3.5±0.2	3.7±0.3	0.14
LVEF, %	55±5	60	50	0.29
Hypertension	5	2	3	>0.10
Valve Disease	1	0	1	>0.10
History of smoking	1	1	0	>0.10
Thyroid disease	1(4%)	0	1(9%)	>0.10
Previous ablation	none	None	none	N/S

AF, atrial fibrillation; LA, left atrium; LVEF, left ventricular ejection fraction

6.3.2 CMR

Dual-IR images achieved superior blood suppression at an earlier time point (Figure 6.3). At 15 minutes effective nulling of the atrial blood pool is achieved with the NSDIR sequence in comparison to 25-30 minutes in the SSIR sequence .

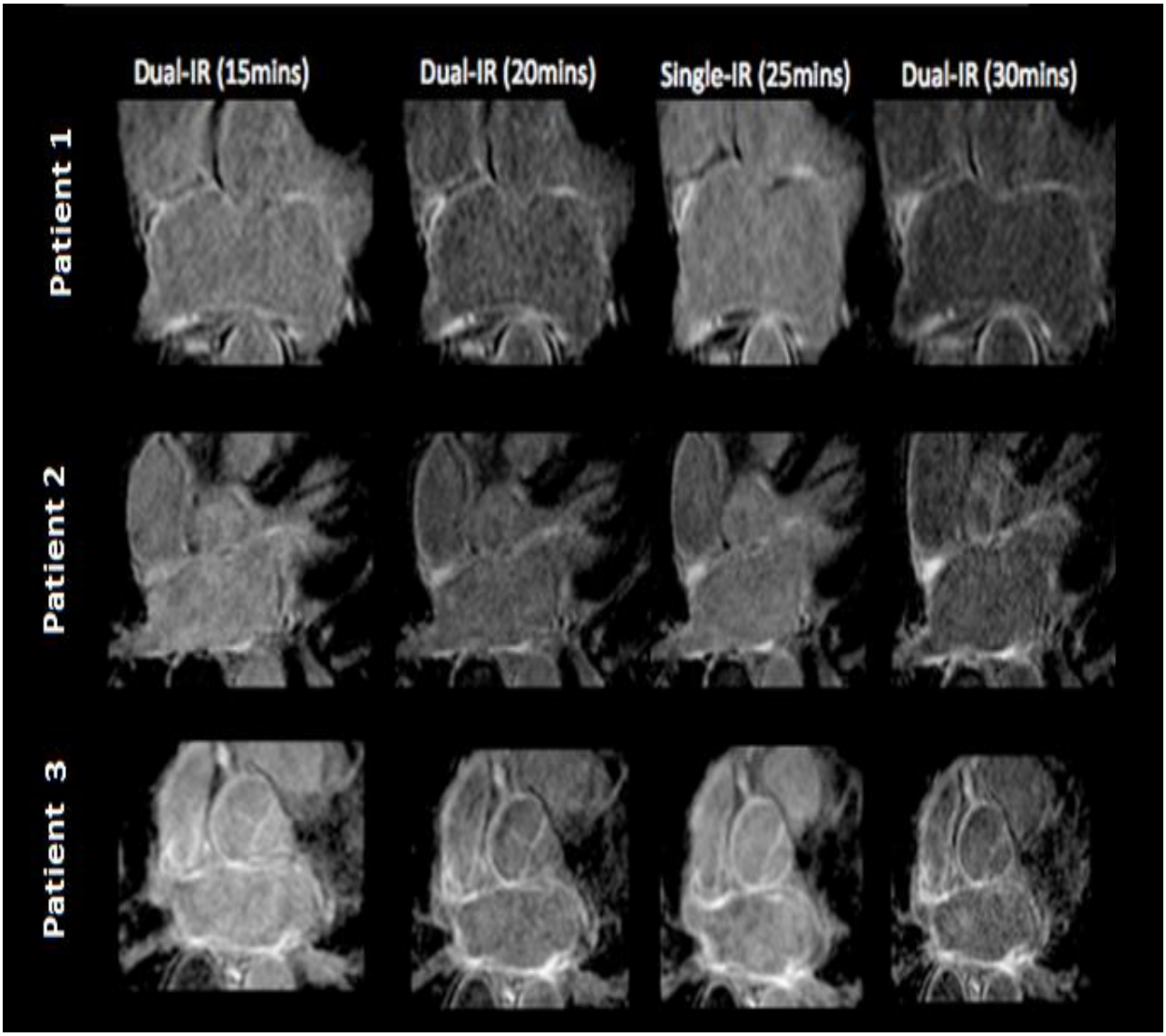
Dual-IR (15mins)
Dual-IR (20mins)
Single-IR (25mins)
Dual-IR (30mins)
Patient 1
Patient 2
Patient 3

(a)

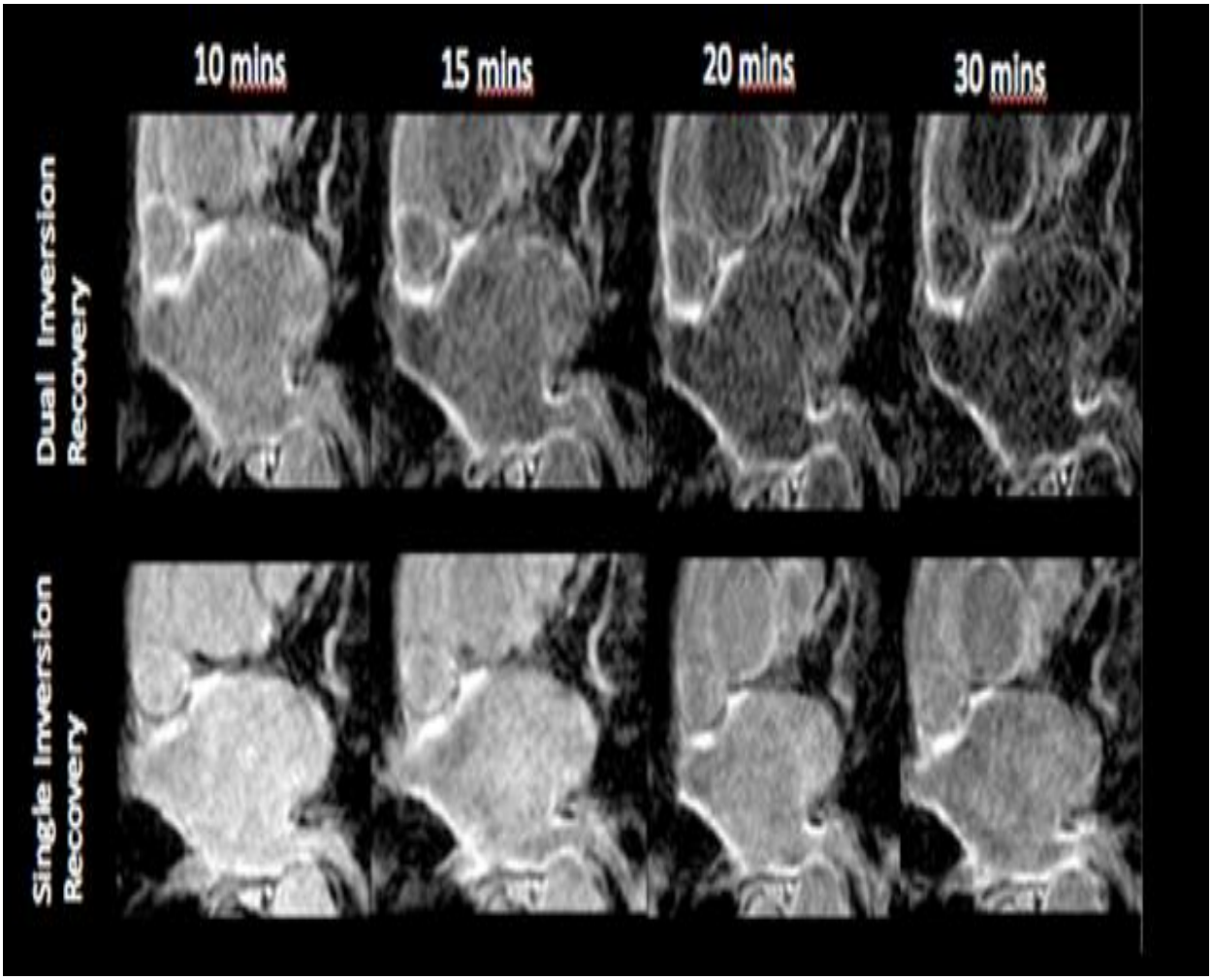

(b)

Figure 6-3: (a) Three patients undergoing both dual inversion recovery imaging (at 15mins, 20 mins and 30 mins) and single inversion recovery (at 25 mins) following contrast administration are depicted here. (b) This series depicts the images acquired from a single patient undergoing single inversion recovery followed by dual inversion recovery 2 weeks later. Effective nulling of the atrial blood pool is achieved at an earlier time point, 15 minutes with the NSDIR method in comparison to 30 minutes in the SSIR sequence.

Blood SNR values were significantly reduced at all time points compared to IR images (Figure 6.4a) whereas there was no significant difference in scar SNR (Figure 6.4b). Scar-to-blood SNR values were significantly improved with dual-IR after 20 and 30 minutes compared to IR at 25 minutes

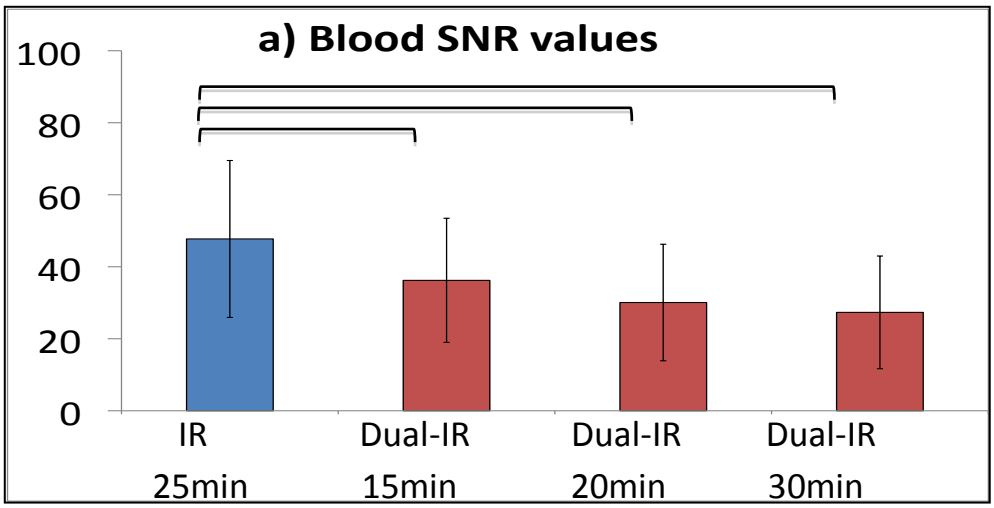

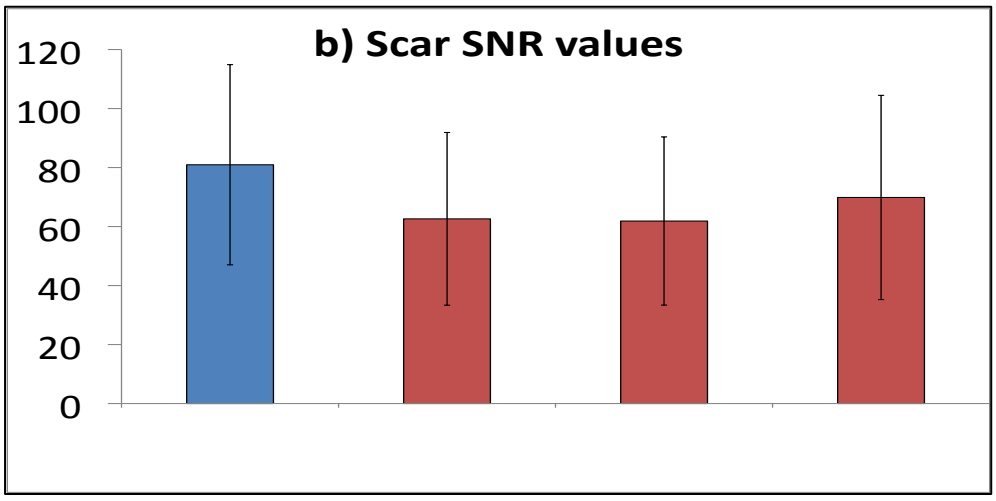

Figure 6-4 : (a) Blood SNR, (b) scar SNR and (c) scar to blood CNR measurements for both selective single inversion recovery and non-selected dual inversion recovery images. The horizontal bars indicate statistical significance (<0.05) in a paired t-test

6.3.3 Qualitative visual CMR assessment

Table 6-2: Qualitative Visual Assessment of Left Atrial Gadolinium Enhanced Scans following Pulmonary Vein Encirclement for Paroxysmal AF.

	SIR	DIR
Blood Pool Nulling	Score (range 2-3) Adequate to good nulling	Score(range3-4) Good to very good nulling
Scar Visualization	Score (range 1-3) Scar visible, ranging from poor to mildly blurred border demarcation	Score(range3-4) Scar visible, mildly blurred to sharp border demarcation
Signal Noise	Score(range3-4) Mild amount to no noise	Score(range 1-3) Mild to moderate amount of noise
Artifact	Score(range3-4) Mild amount to none	Score(range3-4) Mild amount to none
Blurring	Score(range3-4) Mild amount to none	Score(range3-4) Mild amount to none

6.3.4 DE quantification by hand-segmentation

Quantification of scar was performed by manual segmentation of areas of atrial enhancement slice by slice in all patients. Figure 6.5 shows a scatter plot comparing quantified areas of SIR against DIR in all patients. The total sum of enhancement regions segmented was 104cm^2 versus 78cm^2 respectively for standard inversion recovery versus dual inversion recovery. The linear regression in the scatter plot comparing SIR versus DIR yields a value of 0.69. A slope close to 1.0 would imply an almost similar range of values between the two groups. However a value of 0.69 implies that quantification performed on the DIR images were lower in comparison to the SIR.

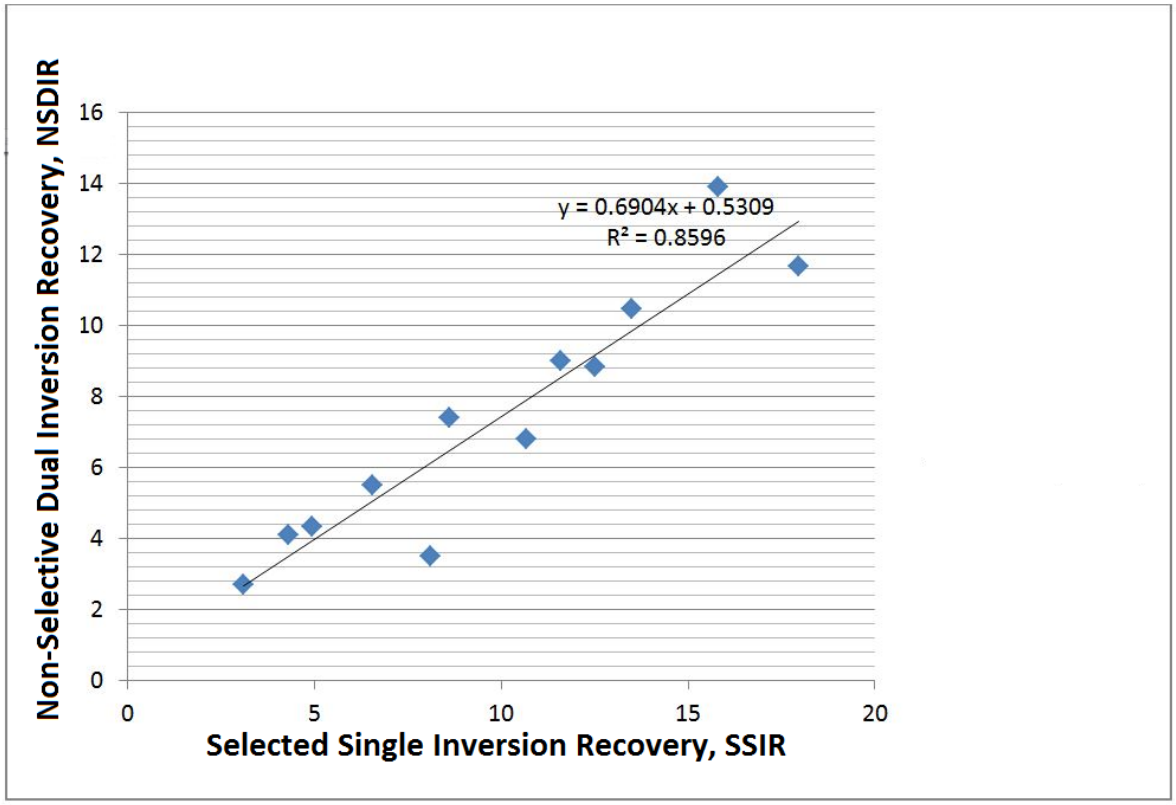

Figure 6-5: A comparison between atrial enhancement regions quantified in the non-selective dual inversion recovery (NSDIR) images versus areas quantified in the selected single inversion recovery (SSIR) images in 12 patients is demonstrated in this scatter plot. The linear regression in the scatter plot yields a value of 0.69 implying that quantification performed on the DIR images were lower in comparison to the SIR images.

6.4 Discussion

Main findings are 1) NSDIR achieves better atrial blood pool suppression conferring improved delayed enhancement visualisation 2) patient time within the scanner is reduced 3) improved visualisation enables more accurate and precise scar quantification.

Targets for atrial substrate modification have evolved from ablating anywhere within the pulmonary vein to wide encircling lesions around the pulmonary vein antrum and additional RF energy applications targeting anatomic areas (left atrial roof line, mitral isthmus lines, right atrial structures) and electrophysiological parameters (complex fractionated atrial electrograms, CFAEs) [77]. Nevertheless, single procedure success rates are modest, suggesting that the factors which contribute to acute electrical isolation are not well understood [110]. This has subsequently led to a need for an effective tool in assessing catheter ablation lesions in patients. Understanding the nature of these radiofrequency lesions (full thickness versus partial thickness) assessing their distribution in relation to anatomic landmarks and following-up these lesions over time may help improve our knowledge in understanding the variation in catheter ablation outcome results and possible underlying mechanisms responsible for AF initiation and maintenance. Previously parameters affecting lesion creation have been assessed in animal models looking at temperatures achieved, power delivered, tissue contact force, catheter orientation, duration of energy delivery and blood flow within the cardiac chambers[140]. However, there are technical limitations in extrapolating this data directly into patients as catheter orientation, catheter stability, blood flow and exact tissue contact force achieved has been difficult to assess.

The recent advancement in novel cardiac magnetic resonance imaging sequences has allowed for the visualisation, quantification and characterisation of post-procedural radiofrequency lesions in vivo[90, 93, 98, 112, 115, 118, 119, 121, 124, 126]. This tool is rapidly proving to be an invaluable

commodity for researchers, electro physiologists and patients offering numerous benefits in improving the quality and standards of care delivery [124]. Table 6.3 summarises the present contemporary CMR studies evaluating post-ablation atrial scar. Improved visualisation of scar is important in correctly identifying areas that have been successfully ablated. More importantly, delayed enhancement atrial imaging has recently been utilised to guide repeat procedures and identify gaps between areas of previous ablation [98].

This novel technique confers an overall better visualisation of left atrial delayed enhancement areas with improved atrial blood pool nulling and better definition of the edges and boundaries of DE areas. Shoulders of the DE areas are better demarcated enabling areas of gaps to be better visualised.

The linear regression of 0.69 in Figure 6.5 is likely to correlate with the improved atrial blood nulling achieved in the NS-DIR technique, thus reducing the likelihood of the quantification process incorporating enhancement within the blood pool adjacent to the previously ablated tissue.

6.4.1 Post Ablation Atrial Scar assessment by CMR

Adequate catheter-tissue contact is integral in creating durable ablation lesions in order to maintain long term sinus rhythm [141]. At present all available data during the development of catheter ablation technology stems from animal work [140]. Clinical use and effectiveness is determined by follow-up outcomes. The utility of post ablation CMR of lesions allows for in vivo scar assessment of areas within the left atrium following energy delivery. This may help in both understanding mechanisms of recurrences and improving present ablation techniques. Key catheter ablation research areas including contact force, catheter stability, type of energy delivered and materials used in catheter design can be assessed in vivo. Furthermore, the effectiveness of electronic anatomical navigation systems in guiding catheter ablation through

the sometimes challenging heterogenous LA-PV junction anatomy can be evaluated by correlating ablation lesion points on the EAM shells to areas of delayed enhancement on the left atrial CMR shells[104].

6.4.2 Clinical implications

This new technique enables an overall improvement in image quality with the added bonus of a shorter acquisition time. The latter is important in improving patient journey and experience within the MR scanner and optimising resources by reducing scan duration time whilst the former ensures quality control. It is important to note the standard inversion recovery method relies on a Look-Locker sequence to be performed and the time delay to be ascertained by the individual operator to ensure optimum nulling to visualise areas of delayed enhancement. NS-DIR on the other hand mitigates this step, by-passing the element of operator variability in choosing the trigger delay for nulling. In the setting of a research study, this becomes pertinent as the imaging technique is more reproducible.

6.5 Study Limitations

The study sample population utilised here is small. Nevertheless the images acquired suggest good clinical potential and a larger study is currently being planned.

6.6 Conclusion

The application of dual-IR CMR sequence achieves high quality delayed enhancement images earlier following contrast administration. There is a demonstrable improvement in scar contour visualization and boundary definition achieved within a shorter time span.

Table 6-3: Summary of Left Atrial CMR studies following Catheter Ablation to-date

No	Authors	Paper Title	Patients studied	Scanner and contrast agent used; clinical outcome	Findings / Conclusion
1	Peters, Wylie, Hauser, Kissinger, Botnar, Essebag, Josephson, Manning , 2007	Detection of Pulmonary Vein and Left Atrial Scar after Catheter Ablation with Three-dimensional Navigator-gated Delayed Enhancement MR Imaging: Initial Experience	23 AF patients imaged pre and post-ablation	1.5-T Achieva MR scanner (Philips Healthcare Best, the Netherlands); 0.2mmol/kg Magnevist; 16/18(88%) patients were AF free at 149±72 days follow-up	A comparison of pre and post ablation DE CMR scans showed new regions of delayed enhancement (i.e scar) within the LA and ostia of the PVs in all patients following radiofrequency ablation.
2	Wylie, Peters, Essebag, Manning, Josephson, Hauser , 2008	Left Atrial function and scar after catheter ablation of atrial fibrillation	33 AF patients (24PAF,9nonPAF) imaged pre and post-ablation	1.5-T Achieva MR scanner (Philips Healthcare Best, the Netherlands); 0.2mmol/kg Magnevist; 6 month outcome not stated.	An association between decreased LA size and reduced atrial systolic function on CMR was observed following catheter ablation of AF. A strong linear correlation between the change in LA EF and scar volume was documented.
3	Peters, Wylie, Hauser, Nezafat, Josephson, Manning et al 2009	Recurrence of Atrial Fibrillation Correlates With the Extent of Post-Procedural Late Gadolinium Enhancement	35 AF patients (17PAF,18 nonPAF) imaged 30 to 60 days post ablation	1.5-T Achieva MR scanner (Philips Healthcare Best, the Netherlands); 0.2mmol/kg Magnevist; 22/35 (63%) were AF free at 6.7±3.6 months.	Post ablation quantification of extent of scar by DE CMR , especially RIPV enhancement predicted AF recurrences. Overall the LIPV displayed the most circumferential enhancement, followed by the RIPV, the LSPV and the RSPV.
4	Oakes, Badger, Kholmovski, Akoum, Marrouche et al, 2009	Detection and Quantification of Left Atrial Structural Remodeling With Delayed-Enhancement Magnetic Resonance Imaging in Patients With Atrial Fibrillation	81 AF patients (40PAF,41 nonPAF) imaged pre procedure and 6 healthy volunteers	1.5-T Avanto MR scnner (Siemens Medical Solutions);0.1mmol/kg Multihance ; 56/81 (69.1%) were AF free at 9.6±3.7 months	Pre-ablation DE CMR provides a non-invasive metric of overall disease progression (mild, moderate and extensive) and distribution of pathological regions (septum, anterior and posterior wall) within the LA. Predictors of ablation success were dependent on the extent and location of LA enhancement.
5	Taclas, Nezafat, Wylie, Josephson, Manning, Peters et al,	Relationship between intended sites of RF ablation and post-procedural scar in AF patients, using	19 AF patients imaged at > 30 days post ablation	1.5-T Achieva MR scanner (Philips Healthcare Best, the Netherlands); 0.2mmol/kg Magnevist; 10/19 (53%) were AF	Whilst both visual and quantitative correlation was observed between areas of enhancement on post ablation DE CMR and points marked on the

	2010	late gadolinium enhancement cardiovascular magnetic resonance		free at 4.9±2.8 months.	Carto map, about 20% of the Carto ablation sites did not have corresponding enhancement points on the DE scan and 5% of DE regions were without Carto ablation points.
6	Badger, Daccarett, Akoum, Adjei-Poku, MacLeod, Marrouche et al 2010	Evaluation of Left Atrial Lesions After Initial and Repeat Atrial Fibrillation Ablation	144 AF patients imaged at > 3months post ablation;	1.5-T Avanto MR scnner (Siemens Medical Solutions);0.1mmol/kg Multihance ; 102/144 (71%) were AF free at 10.2±5.1 months	Using post ablation quantification of extent of scar by DE CMR, both the number of complete circumferential PV antrum lesions and the extent of total LA scar correlated with procedure success. Whilst individual complete circumferential PV lesions were not always observed, achieving all four complete PV encirclement was infrequently seen; an important endpoint to maintaining durable pulmonary vein isolation. Identification of breaks in ablation lesions which correlate with electrical conduction on these scans can be used as targets in subsequent procedures.
7	Akoum, Daccarett, McGann, Segerson, Vergara, MacLeod, Marrouche et al, 2010	Atrial Fibrosis Helps Select the Appropriate Patient and Strategy in Catheter Ablation of Atrial Fibrillation: A DE-MRI Guided Approach	120 AF patients imaged at two time points: pre and >3 months post ablation;	1.5-T Avanto MR scnner (Siemens Medical Solutions);0.1mmol/kg Multihance ; 83/120 (69%) were AF free at follow-up	A corroboration between extent of pre-ablation staging of scar quantified on DE CMR scans (Utah stage 1 <5% DE, Utah stage 2, 5-20% DE Utah stage 3, 20-35% DE and Utah stage 4, >35% DE) and post ablation clinical outcome identified 2 subgroups – excellent(minimal fibrosis) or poor (extensive fibrosis) prognosis following energy delivery.
8	Mahnkopf, Badger, Burgon, Daccarett, Haslam,	Evaluation of the left atrial substrate in patients with lone atrial fibrillation using	333 AF patients (40 lone AF; 293non-lone AF) imaged pre-procedure;	1.5-T Avanto MR scnner (Siemens Medical Solutions);0.1mmol/kg Multihance ; 27/40 (68%) lone AF and	Pre-ablation scar quantification as a measure of extent of LA structural remodeling on DE-CMRI did not differ

	Macleod, Marrouche et al , 2010	delayed-enhancement MRI: Implications for disease progression and response to catheter ablation		170/293 (58%) non-lone AF patients were AF free at 10.8±7.8 months	between patients with lone AF and non-lone AF.
9	Vergara, Marrouche , 2010	Tailored Management of Atrial Fibrillation Using a LGE-MRI based Model: From the Clinic to the Electrophysiology	387 AF patients (187PAF, 200nonPAF) imaged pre and post procedure ;	Either 1.5-T Avanto or 3-T Verio MR scanner (Siemens Medical Solutions);0.1mmol/kg Multihance. Outcome not stated.	Immediately postablation, T2 signal was seen not only in regions subject to RF energy but also distant regions whilst the >3 month post ablation scans showed a resolution of the signal. Acute oedema defined as these T2 areas correlated with low voltage areas (defined as <0.05mV) and was much larger than areas covered by DE on acute CMR scans. DE was present on both acute (representing a combination of tissue oedema, other reversible changes and areas that will scar completely) and late scans (scar).
10	McGann, Kholmovski, Blauer, Vijayakumar, Marrouche et al, 2011	Dark Regions of No-Reflow on Late Gadolinium Enhancement Magnetic Resonance Imaging Result in Scar Formation After Atrial Fibrillation Ablation	37 AF patients imaged at three time points – pre, immediately post and at 3 months post procedure	3-T Verio MR scanner(Siemens Medical Systems) ; 0.1mmol/kg Multihance; 29/37(78.4%) were AF free at 12 months	DE CMR findings immediately post ablation(IPA) can be categorized as regions of hyperenhancement(HE-representing a spectrum of injuries from inflammation to necrosis) and nonenhancement(NE –representing areas of no-reflow); the latter being a better early predictor of final scar at 3 months.
11	Daccarett, Badger, Akuom, Burgon, MacLeod, Marrouche et al , 2011	Association of Left Atrial Fibrosis Detected by Delayed Enhancement Magnetic Resonance Imaging and the Risk of Stroke in Patients With Atrial Fibrillation	387 AF patients (187PAF, 200 nonPAF) imaged pre procedure	Either 1.5-T Avanto or 3-T Verio MR scanner (Siemens Medical Solutions);0.1mmol/kg Multihance ; 36/387 (9.4%) patients incurred a stroke (time from to DE CMR 22.7±8.8months)	Significantly higher levels of LA fibrosis was quantified on DE CMR scans in patients who suffered an ischaemic stroke. The amount of enhancement representing extent of LA structural remodeling could be a valuable clinical tool to be used in conjunction with the

					CHADS2 index as a marker for both stroke risks and anticoagulation risk stratification.
12	Arujuna, Rhodes, Razavi, ONeill, Gill et al ,2012	Acute Pulmonary Vein Isolation is Achieved by a Combination of Reversible and Irreversible Atrial Injury following Catheter Ablation: Evidence from Magnetic Resonance Imaging	25 PAF patients imaged at three time points – pre, immediately post and at 3 months post procedure	1.5-T Achieva MR scanner (Philips Healthcare Best, the Netherlands); 0.2mmol/kg Magnevist; 14/25 (56%) were AF free at 6.5±2.8 months.	Acute pulmonary vein isolation is achieved by a combination of reversible and irreversible circumferential tissue injury at the PV-LA junction. A greater decline observed from acute to chronic DE in patients with recurrences in comparison to no recurrences. This suggests the presence of more reversible tissue injury, providing a potential mechanism for PV reconnection resulting in arrhythmia recurrence.

7 Assessment of an Automatic Segmentation Tool for Left Atrial Delayed-Enhancement CMR analysis following Radiofrequency Catheter Ablation

7.1 Introduction

Gaining insights into the understanding of the mechanisms resulting in PV reconnection following catheter ablation and improving present AF ablation strategies is important. Magnetic resonance imaging (MRI) has been shown to be an effective tool in assessing tissue injury following energy application. In particular, delayed enhancement (DE) CMRI has the potential to detect changes that take place in the LA when performed pre and post catheter ablation. DE-MRI has been extensively used to detect myocardial scarring in the ventricles following ischaemic injury [142]. This technique has recently been extended to be used in patients with AF to detect the degree of LA fibrosis prior to ablation[90]; to detect acute (<24hrs) post-ablation LA tissue injury [115]; and to detect chronic (>3 months) postablation LA fibrotic scarring caused by tissue injury[112, 118].

See Fig. 7.1 for examples of chronic DE-MRI imaging.

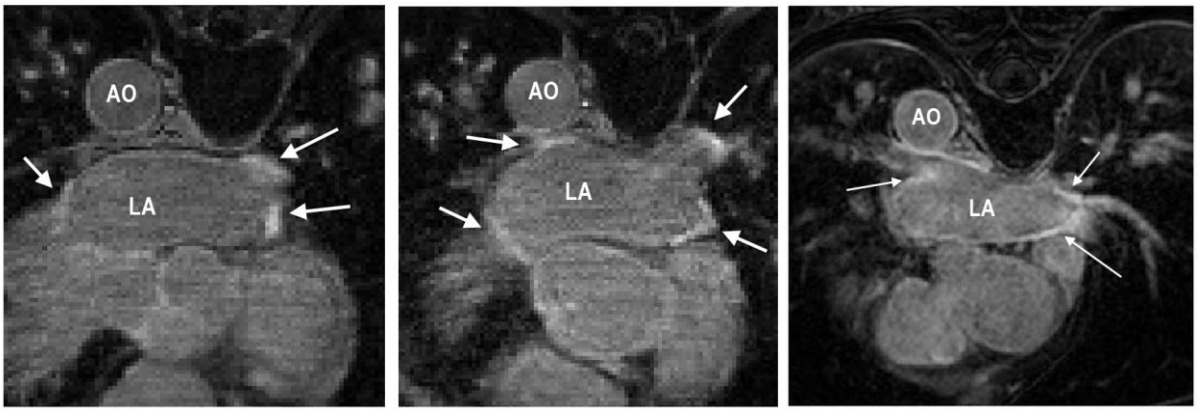

Figure 7-1: DE-MRI images from three patients taken 3 months post-ablation. Arrows indicate areas of enhancement. Abbreviations: AO - aorta, LA – left atrium

Quantification and segmentation of ventricular scar from DEMRI images is not un-common. For ventricular scar, classifying scar into its core and periphery (i.e. grey-zone) has important applications. Several studies [143-145]have employed the fullwidth- half-maximum (FWHM) approach, for segmenting the core of the infarct. The FWHM is a straightforward method for determining a threshold for the core infarct. It defines core as 50% of the maximum signal intensity within a user selected region-of-interest (ROI), which is usually within a hyper-enhanced scar in the image. The next step is normally thresholding, but some works have also employed region growing with thresholding[144]. Patients requiring LA imaging often have an irregular heart rate rendering precise cardiac-gated image acquisition a challenge. As a result, the image quality in LA DE-MRI can sometimes be sub-optimal. This, alongside the relatively thin walled left atrial, makes LA DE-MRI segmentation more of a challenge compared to ventricular DE segmentation and analysis.

Quantification of LA enhancement in DE-MRI has been proposed using thresholding techniques for either endocardial surface-based segmentation[115] or volumetric segmentation[90, 112, 146] . In the former method[115], the maximum intensity projection (MIP) of the DE-MRI signal intensity on the segmented LA shell is first computed for visualizing post-ablation injury. The MIP is then thresholded based on a user-selected ROI inside healthy myocardium to give a binary segmentation for injury. The selection of the threshold is based on the number of standard deviations healthy myocardium is from injury, usually ranging from 3 to 8. This technique has two important drawbacks: 1) it does not provide a volumetric segmentation of injury, and 2) it relies on the correct selection of the threshold which in-turn is often dependent on the ROI selected by the user. In the volumetric method [90], the authors describe a technique for the volumetric segmentation of pre-ablation LA fibrosis. Here the LA wall is first manually segmented from the DE-MRI image. Next, the intensity histogram

of the segmented DE-MRI wall is analysed by assuming it to be bi-modal and the two means are obtained.

Finally, fibrosis is thresholded as 2-4 standard deviations from the lower mean of the histogram. This technique requires a laborious manual task of delineating the LA wall from DE-MRI images. Moreover, the LA wall is not always clearly visible in these images, especially the epicardial boundary. A similar patient-specific thresholding technique for measuring post-ablation chronic scar was also proposed previously [146], where the threshold level was chosen on visual inspection of an experienced user. The average threshold was 3 to 6 standard deviations above the blood signal. In[93]the threshold level was chosen as the minimum threshold which eliminates most blood pool pixels. However, thresholding in this manner can fail to exclude normal myocardium with intensity levels above that of blood pool. All the existing techniques described above are essentially thresholding techniques that can have major limitations. They suffer from poor reproducibility of segmentations especially when the correct threshold level is not selected and often requiring the level to be set by an expert user. They also fail to preserve the continuity of shape in structures. With a certain level of noise expected in MR images, thresholding often generates holes in structures that it segments. Also, employing a global threshold for the entire image leads to segment disconnected islands of segmented regions that are not likely to be related to fibrosis/tissue injury/scar.

This study examines a novel segmentation method for LA DE-MRI. It is based on a probabilistic tissue intensity model of DE-MRI data, which is derived both from training and data. The algorithm uses a Markov random field (MRF)-based energy formulation that is solved using graph-cuts[147]. The method of graph-cuts has shown high accuracy, simultaneous ROI detection, and scalability to three dimensions in segmenting structures [148]. It has been applied in a wide variety of segmentation problems arising in computer vision and medical

image processing [149, 150]. We use it to efficiently solve our MRF model. The automatic method was previously validated using digital phantoms by our department in Kings's College London This further preliminary work has been performed on 11 patients who underwent ablation treatment for AF and were imaged at approximately 6 months post-procedure. The segmentations are compared to expert manual segmentations and existing semi-automatic approaches [90, 115]. This study focuses on segmentation of post-ablation chronic scar from DE-MRI but the algorithm could equally be applied to pre-ablation fibrosis or post-ablation acute tissue injury if different training data were used.

7.2 Clinical and Imaging Protocols

7.2.1 Patients

11 patients were followed up at 6 months following their first ablation for the treatment of paroxysmal AF. The procedures were carried out in the cardiac catheterization laboratory at St. Thomas Hospital, London, U.K. All patients gave written permission to take part in this local ethics committee approved study.

7.2.2 Ablation procedure

This section has been described more elaborately in Chapter 4. In summary, two trans-septal punctures were made to access the left atrium using standard long sheaths (St. Jude Medical, MN, USA). A three-dimensional (3D) LA geometry was created using either EnsiteNavX (St. Jude Medical, MN, USA) or CARTO XP (Biosense Webster, Diamond Bar, CA, USA). A circular mapping catheter was then placed in each PV in turn while the corresponding LA-PV ostium was targeted with wide area circumferential ablation. Energy was delivered through a 3.5 mm irrigated tip catheter with flow limited to 17 ml/min, power limited to 30 W on the anterior wall and 20 W on the posterior wall and temperature limited to 50 _C. Ablation

lesions were marked on the LA geometry when there had been an 80% reduction in the local electrogram voltage or after 30seconds of energy delivery.

7.2.3 Postablation MRI procedure

The CMR protocol used has been described previously in Chapter 4. The scan sequence utilised for the visualization of delayed-enhancement was a 3D ECG-triggered, free breathing inversion recovery (IR) turbo field echo (TFE) with respiratory-navigated and cardiac-gated with whole heart coverage. The pixel resolution was reconstructed to 1.3x1:3x 2mm^3. Please refer to Chapter 4 section 3 for a full description of the CMR imaging technique utilised.

7.2.4 Computational Analysis

A summary of the steps involved in the proposed segmentation technique utilised by the automatic.software is presented in Fig. 7.2 Starting with the training images of manually-segmented scars, the intensity energy model for scar is trained on the scar-to-blood-pool ratios of voxels labelled as scar. The neighbourhood model is also obtained from the training images, where a value for the scale _ in the Lorentzian norm is derived by sampling intensity gradients within tissues surrounding scar.

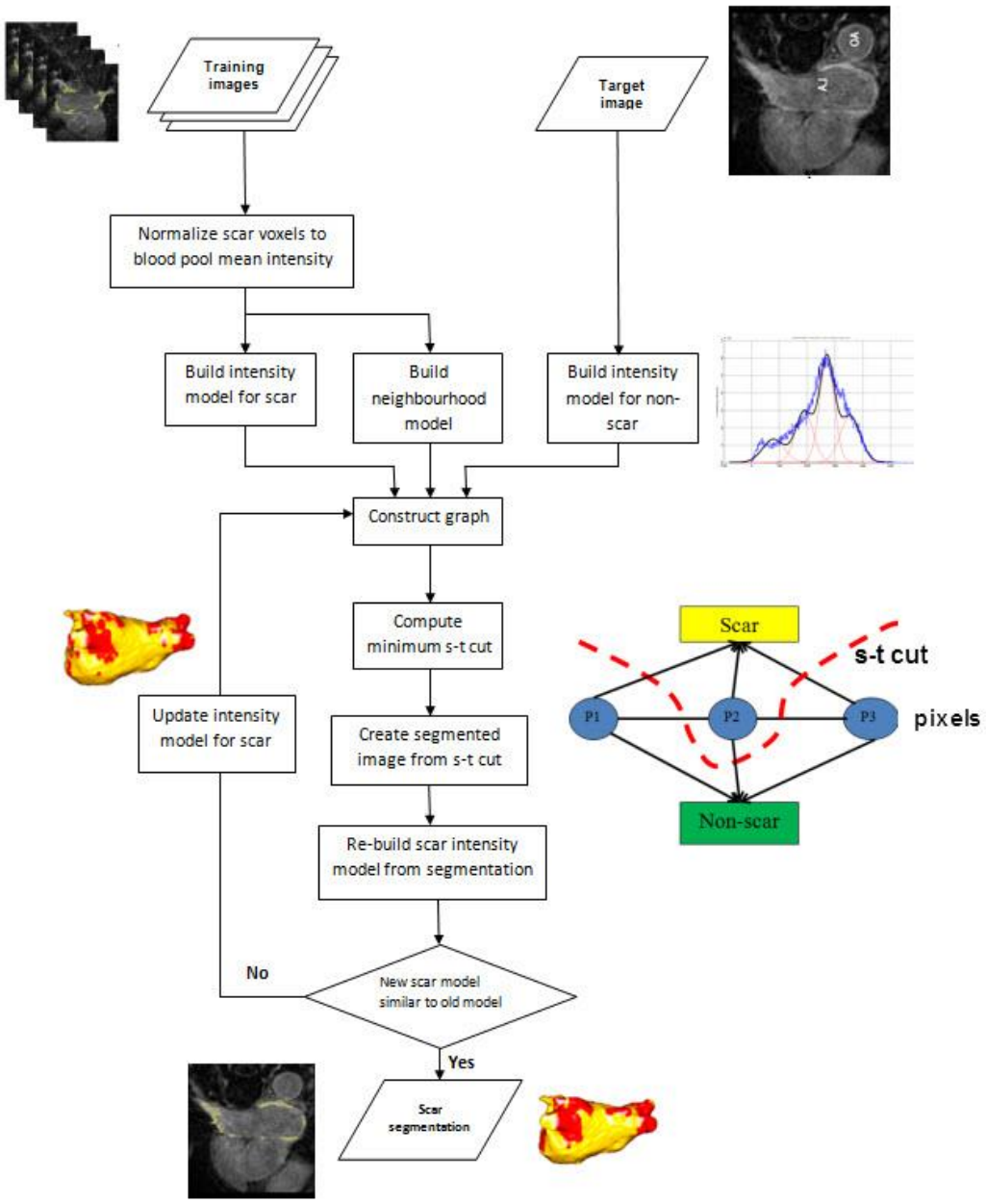

Figure 7-2: An overview of the steps involved in the graph-cut segmentation.

The intensity energy model for non-scar is obtained from the target image by locating regions of blood-pool, atrial wall and pericardium. This is accomplished by fitting a multi-modal Gaussian with the EM-algorithm. The above intensity models allow a graph to be constructed where each voxel of the target image denotes a node in the graph. The edge weights for each

node are derived from the intensity models, based on its intensity. The minimum s-t cut is computed resulting in the optimal segmentation of the target image into foreground (i.e.scar) and background. Following segmentation, the intensity model for scar is updated based on the obtained segmentation.

If the new model is sufficiently close to the old model in terms of its mean and variance, the segmentation process is terminated; otherwise the entire process (starting with graph construction) is repeated with this new model for scar. This feedback strategy is important as it allows to obtain the optimal scar model for the target image, which is often not the model obtained from the training. Nevertheless, the training model provides with a good initial starting estimate.

7.2.5 Clinical data

Here, segmentations from the proposed algorithm and the manual segmentations of three observers were compared. For manual segmentations, the observers were blinded to the results from the automatic and semi-automatic segmentations. Regions of scar were located and marked using ITK Snap in the manual segmentations. All experiments were run on a 2.8 GHz PC.

In a separate set of experiments, we obtained volumetric segmentation of scars from 3 observers. These observers had prior experience looking at scars in DE-MRI. The observers were blinded to the results from the automatic and semiautomatic segmentations. Each observer was provided with DE-MRI scans from the 11 patients. Scars in the images were segmented slice-by-slice using ITK-Snap (www.itk-snap.org) using a simple digital paint-brush tool with a variable tip width. Each patient took approximately 15-45 minutes depending on the amount of scar in the image. The agreement between observers was analyzed by comparing their segmentations using the Dice overlap measure.

It is also important to note that segmentations from the proposed approach were obtained automatically without any user interaction necessary at any step of the algorithm. The total time to obtain segmentations from the proposed approach was less than a minute on a 2.5 GHz PC. For semi-automatic segmentations, the expert observer was required to carefully select the correct threshold levels, often requiring an additional 2-3 minutes depending on the user's level of experience.

7.3 Results

Segmentations from the algorithm on clinical datasets can be seen in Fig. 7.3. Both the raw MR data and the corresponding segmented scar area is presented in this figure. These findings were then presented as maximum intensity projection (MIPs) onto the corresponding 3-D atrial surface shells. Manually segmented areas of scar was presented in the similar way,

A good correspondence was found between the segmentations.. Fig.7.4 shows some of these visualizations confirming the good correspondence.

Results comparing manual segmentations of three different observers are given in Table 7.1. A relatively low degree of agreement was found, especially with the third observer (mean Dice = 0:2; 0:3). All observers found the task of manually segmenting scars difficult, time consuming and laborious. In many patients, scars were not as distinctly visible as others, owing to the poor signal-to-noise and scar-to blood- pool ratios. Also, sometimes scars appeared as thin lined structures in the image and as a result made the labelling task increasingly difficult. In most cases where observers labelled thin lined scar regions, the labelling would normally spill into neighbouring regions as it was difficult to draw along scar.

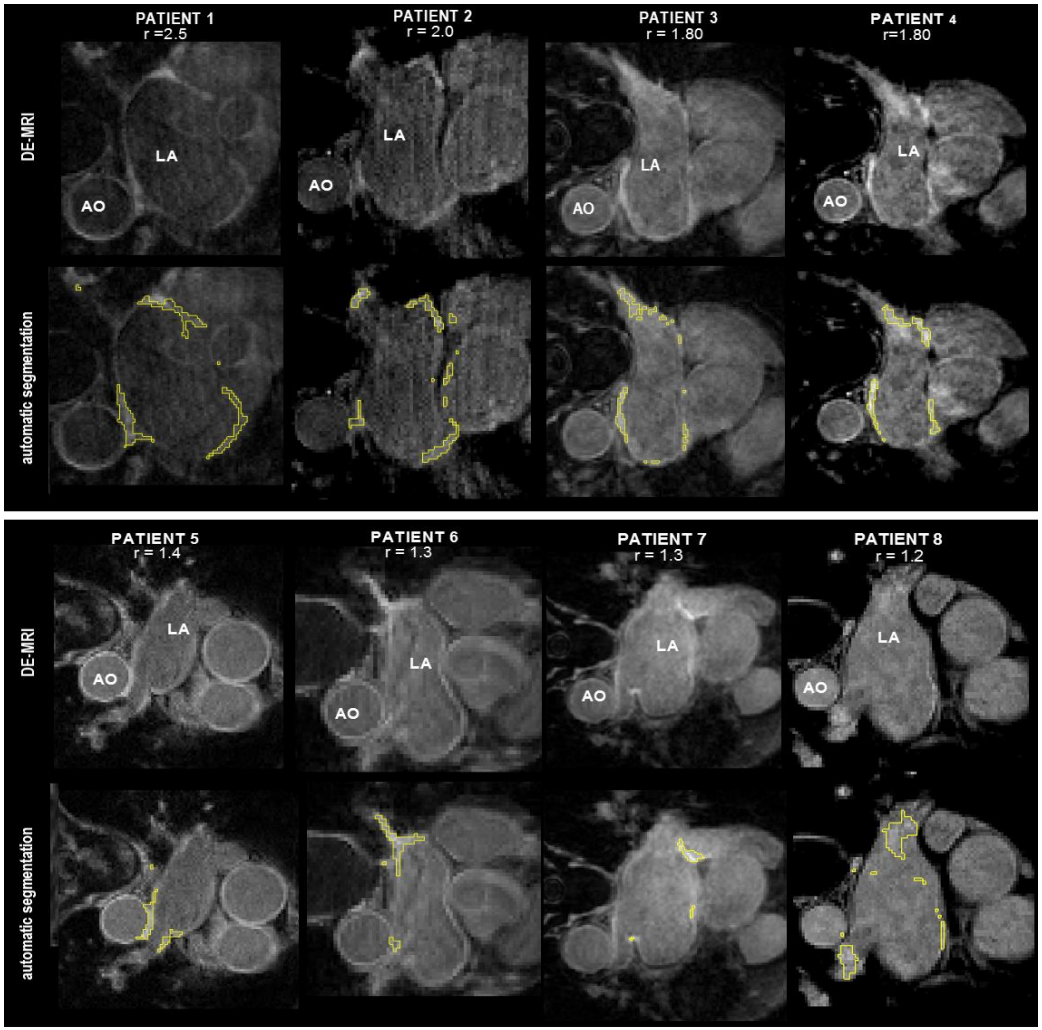

Figure 7-3 : Original DE-MRI slices (top-row) and automatic segmentation(bottom-row) from eight patients.

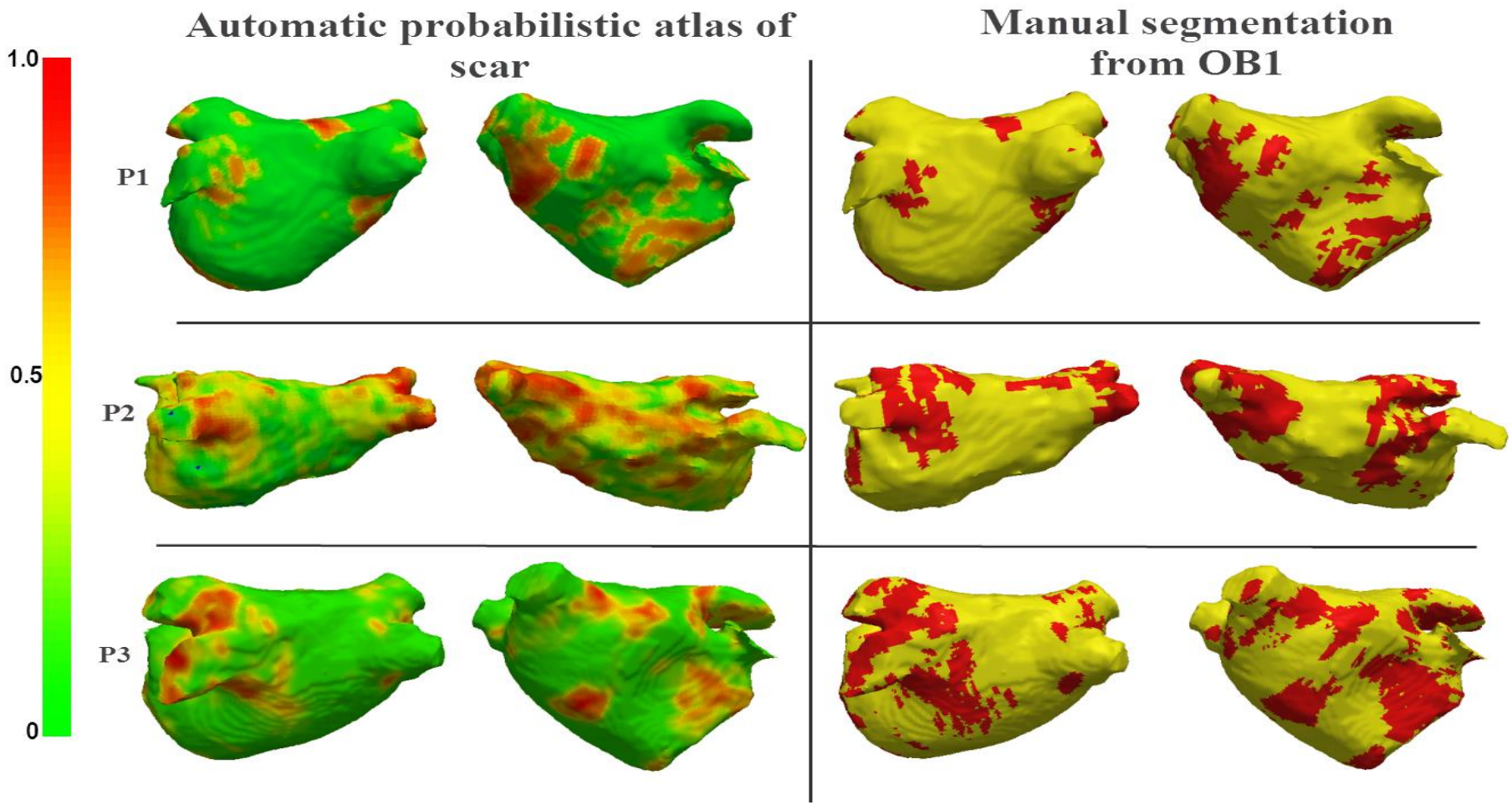

Figure 7-4 : Probabilistic map of scar for three patients shown alongside their manual segmentations from an observer. The probabilistic map is obtained by combining segmentation labellings from each iteration of the segmentation process.

Table 7-1 The degree of agreement between observers.

Patients	(OB1 / OB2)	(OB1 / OB3)	(OB2 / OB3)
P1	0.4	0.3	0.2
P2	0.1	0.1	0.3
P3	0.2	0.1	0.1
P4	0.4	0.1	0.2
P5	0.5	0.1	0.2
P6	0.5	0.4	0.3
P7	0.3	0.4	0.3
P8	0.3	0.2	0.3
P9	0.3	0.2	0.3
P10	0.4	0.2	0.3
P11	0.4	0.2	0.4
Mean	0.4	0.2	0.3

Moreover, an observer is often reluctant to repeatedly change the width of the tip of the brush to adapt to the size of the scar. This exaggerated the extent of scar in some regions and explains to some extent the inter-observer variability in the segmentations.

7.4 Discussion

The results presented in this work demonstrate that the fully automatic technique is well suited for segmenting scars in the LA from DE-MRI images. With good overlap with three expert manual segmentations and two established semiautomatic techniques, the proposed technique was able to segment scars with good accuracy. Because of the absence of ground truth for scar in real patient DE-MRI datasets, it becomes difficult to evaluate segmentations of scar from the algorithm. The next best approach is to compare it to manual segmentations and we have demonstrated that there is a high degree of inter-observer variability, primarily due to low image quality often encountered in LA DE-MRI scans.

It was shown that the proposed approach is suitable for extracting scar from post-ablation clinical MRI data. It overcomes many of the limitations of existing semi-automatic approaches. A major limitation is the high inter-observer variability, especially in the threshold selection stage, making it difficult to reproduce the segmentations. Also as it is

technically challenging to achieve good nulling of the myocardium and blood-pool, the intensity ranges for non-scar tissues are bound to overlap with scar. Since all existing approaches essentially rely on thresholding, a single intensity cut-off for scar is insufficient. The proposed method overcomes this by considering not only a voxel's intensity alone but also its intensity in relation to its neighbours and its intensity in relation to the training data. It then computes a global optimal solution using a well established optimization technique.

A second major advantage over existing approaches is that it is fast and fully automatic requiring no expert user interaction. On a 2.8 GHz PC, the graph-cuts stage generating the scar segmentation takes less than 1 minute.

The proposed technique has some limitations. The quality of the LA segmentation can affect the algorithm's output. Since the technique utilizes the LA segmentation as a base-line to identify regions of blood pool, myocardium and pericardial regions, a mis-segmentation of the LA can cause regions of the myocardium to overlap with other tissues. This is generally not an issue as the algorithm is well-equipped to discard tissues that are dissimilar to its training data. However, this becomes an issue when the aortic wall, which is almost always hyper-enhanced in DE-MRI images, overlaps with the myocardium and is segmented as scar. This can be overcome if a segmentation of the aortic wall is also available.

A second limitation that can cause the algorithm to sometimes oversegment is a diffused high-signal intensity artefact almost always present in the right superior PV. This is caused due to the respiratory navigator used during scans. The algorithm is not yet equipped to ignore this artefact. However, incorporating spatial information about each vein and exclusively training it on the intensity levels of the artefact will make it possible to avoid segmenting these regions. More importantly, the work from chapter 6 utilising a novel dual inversion recovery sequence assists in improving image acquisition quality with good blood pool suppressions and less artefactual signal intensities .This has a role in facilitating the use

of this software As both projects were running in parallel, we intend to evaluate the scar segmentation utilising this software on the images acquired using the new sequence.

7.5 Conclusion

The use of DE-MRI for imaging RF ablation lesions has allowed a more in depth characterization of lesions. This study presents an automatic segmentation approach for segmenting lesions from DE-MRI. It is envisaged that user-independent lesion segmentation with low computational cost will allow for standardization of DE-MRI as a marker for cardiac injury. Future work will focus on improved training and validation using a larger patient cohort with more expert segmentations per data set. It will also be interesting to adapt the algorithm to segment fibrosis in pre-ablation DE-MRI and acute tissue injury using 24-hours imaging.

8 Discussion

8.1 Characterisation of post ablation lesions and an assessment of the temporal relationship between DE and T2 signal

8.1.1 CMR left atrial tissue injury assessment : Reversible and irreversible tissue injury

Serial CMR scans performed immediately following catheter ablation (within 18 to 24 hours post procedure, acute scans) and at 3-5 months post procedure (late scans) has enabled CMR evaluation of the nature of left atrial tissue injury. Based on the two observations made- that firstly areas of DE regressed to varying levels in all patients on the late scans whilst T2 signal reduced to near baseline pre procedural levels and secondly the association between greater acute T2 signal and a higher DE regression on the chronic scans suggest the presence of reversible and irreversible acute tissue injury. This is likely to reflect ablated but not necessarily necrotic tissue confirming previous work, including that from our own laboratory, that acute DE MRI overestimates the acute extent of tissue injury following left atrial catheter intervention by virtue of the accumulation of gadolinium in extravascular water associated with acute inflammation. Although there is a good correlation between endocardial voltage-defined scar and T2 weighted signal immediately post ablation, there is a poor correlation with the DE MRI-defined scar at three months follow up [124], further supporting the transient nature of at least part of the ablation injury process.

8.1.2 Atrial scar and arrhythmia recurrence

The significance of both acute and late CMR scan findings were evaluated by correlating the DE and T2 encirclement to clinical outcome. We observed that a greater extent of circumferential DE signal at the 24h scan was predictive of freedom from AF while the extent of T2 signal was greater in the arrhythmia recurrence group. On the late scans, patients

with greater initial DE and a lower acute T2 had a lower subsequent DE regression which correlated well with being arrhythmia free. The clinical significance of this has been further elaborated in the discussion section of Chapter 4.

8.2 CMR comparison of lesions created using robotic navigated systems against lesions created in the conventional way

8.2.1 PV encirclement by DE: more versus less

This work reports the first cardiac MR findings comparing robotic navigated catheter ablation lesions to standard catheter ablation. The higher mean percentage encirclement consistently observed in the robotic group in both acute and late scans is likely to be a function of both catheter stability and tactile feedback with Intellisense conferring better catheter control. Improved lesion delivery resulting in an overall 10% higher margin encirclement was observed on the robotic navigated late scans. Whilst almost similar % encirclements were observed on late scan DE between the two groups with no recurrences, a significantly higher amount of DE was noted in the robotic group. This lower regression of DE between the acute and late scans in the robotic recurrences group suggests an overall better quality lesion created using the Robotic Navigation System (RNS). The clinical significance and a comparison of contemporary robotic assisted procedures against standard catheter ablation has been commented upon in the discussion section of chapter 5.

8.2.2 Lesion set appearance: more versus less contiguous

The overall more contiguous lesion set appearance on qualitative examination of the 3-D CMR atrial shells in the robotic group is again attributable to better catheter control and greater stability. More circular shaped encirclement patterns observed in the RNS group suggests that the system allows for a more accurate and precise catheter movement along the PV antrum with sufficient tissue contact creating better adjoining lesions.

8.3 DE imaging sequence optimization: A comparison between non-selective dual inversion recovery (NSDIR) versus standard selective single inversion recovery (SSIR)

8.3.1 CNR and SNR Image analysis

The need for better image acquisition is important to enable better visualization of scar boundary which in return allows for better localization of areas of tissue injury and a more accurate quantification of scar burden. The novel scan sequence acquisition using non-selective dual inversion recovery imaging has shown to achieve superior blood suppression at an earlier time point. There is effective atrial blood pool nulling that is achieved within 15 minutes with this NSDIR sequence in comparison to 25-30 minutes with the conventional sequence. A more than adequate atrial blood pool nulling was achieved without the compromise of scar visualization. This scanning sequence enables an overall improvement in image quality with the added bonus of a shorter acquisition time. The latter is important in improving patient journey and experience within the MR scanner and optimising resources by reducing scan duration time whilst the former ensures quality control. The potential clinical significance of this is elaborated in the discussion section of Chapter 6.

8.4 Novel automatic delayed enhancement lesion segmentation tool

8.4.1 Motivation behind developing an automatic tool

Delayed enhancement assessment by CMR has several potentials within the research and clinical domain. In the former, its role as a biophysical marker in studies can proof to be a useful surrogate. Quantifying total areas and distribution of these areas following energy delivery is useful in the development of and assessment of newer ablation technology – ranging from novel energy sources (laser, cryo) to delivery systems to modern catheters

(force sensing catheters , gold tip catheters). In the clinical domain, a potential role of DE CMR imaging maybe in the guidance and planning of re-do ablation procedures.

In order to achieve the above, a robust reproducible system is required in segmenting out areas of delayed enhancement. With respect to this, we examined a novel systems platform that automatically segments out areas of DE from the raw scan data.

8.4.2 Advantages conferred by the automatic segmentation technique

A comparison between segmentations performed manually by hand by three experienced CMR readers against DE segmentations performed by the automatic alogorithm. Zones of enhancement were relatively similar between the two groups. Importantly, this suggests that the tool was able to correctly identify regions of DE and perform the segmentation at much quicker rate. Furthermore, a standardised technique would negate the inter-observer variability, thus increasing reproducibility, accuracy and precision.

As mentioned above, this tool overcomes a major limitation in the existing semi-automatic technique by minimising inter-observer variability, especially in the thresholding selection stage. Moreover in some instances, it is technically challenging to achieve good nulling of the myocardium and blood-pool,with intensity ranges for non-scar tissue areas overlapoing with areas deemed as scar. Since all current existing approaches rely on thresholding, a single intensity cut-off for scar is insufficient. Here, the proposed method overcomes this by considering not only a voxel's intensity alone but also its intensity in relation to its neighbours and its intensity in relation to the training data. It then computes a global optimal solution using a well established optimization technique.

A second major advantage over existing approaches is that it is fast and fully automatic requiring no expert user interaction. On a 2.8 GHz PC, the graph-cuts stage generating the scar segmentation takes less than 1 minute. The volumetric segmentations generated allow both visualization of scar on the original image volume and through MIP on the LA shell.

This is advantageous as scar visualizations on LA shells can be used for assessing lesion gaps. Also, volumetric segmentations are vital for computing scar thickness especially for the assessment of transmurality which is becoming an important domain in understanding mechanisms of PV reconnection in AF recurrence.

8.5 Future Work: Novel Hybrid Imaging Platform for Real-Time Image Guidance in Catheter Ablation

CMR has a role in assessing post ablation tissue injury for both research in ablation technology development and in clinical use by providing a road map of in vivo lesions created within the atrium. The potential role in providing real time image guidance is currently being developed. Mapping and ablating catheters compatible within the magnetic scanner are undergoing phase 1 studies alongside electro-anatomic mapping systems and other equipment being designed to function within the magnetic field environment. One important consideration is the materials used for the measurement of intra-cardiac potentials such that electrical information is not affected by the magnetic field and simultaneously, the electrical flow does not create image artefacts within the scanner.

Translating CMR into a real-time image guidance tool for catheter ablation within patients may take some time to be perfected. However, the combination of fluoroscopy and echocardiography imaging modalities to provide real time catheter – tissue information is within reach and does not require a high capital investment to be set up. With this in mind we assessed a novel platform that integrates the echo matrix into the fluoroscopy matrix.

8.5.1 Novel System for Real-Time Integration of 3D Echo and Fluoroscopy for Image Guidance: Systems Overview

The scanning setup comprises a Philips AlluraXper FD10 C-arm X-ray system and a Philips iE33 3D ultrasound system with an X7-2t 3D TEE probe. Data is streamed in real-time from

each system to a PC running the visualisation software. The software displays a 2D projection view in the coordinates of the X-ray image, overlaid with a projection of the echo volume. Figure 8.1 illustrates an example of an X-ray view and an echo volume integrated to obtain the hybrid view.

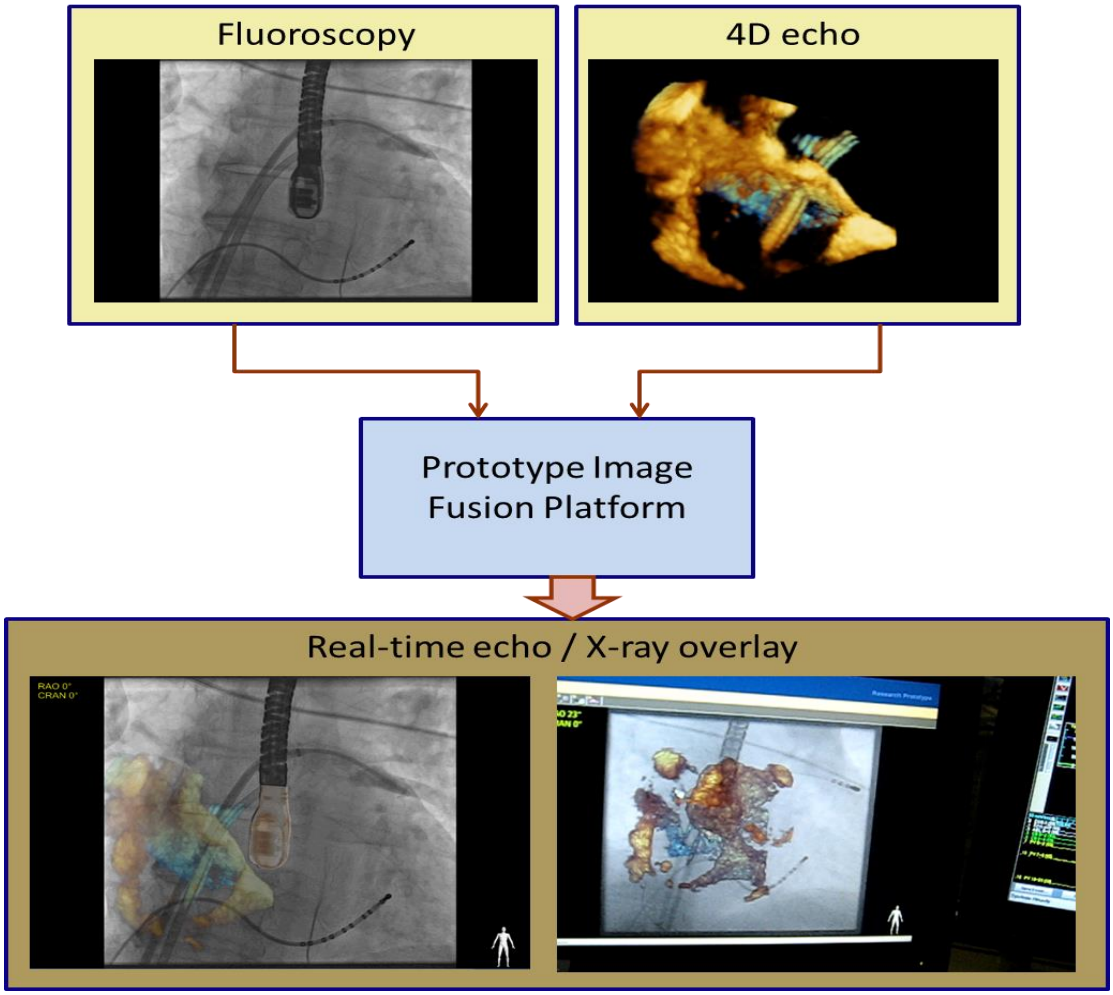

Figure 8-1: Both the X-ray fluoroscopic image and echocardiogram image are acquired separately and streamed into the visualisation platform that allows for the real-time integration of the two matrices

The two views are registered using the projection image of the TEE probe in the X-ray using our previously described method[10]. In brief, the registration is initialised manually to approximately the correct position and orientation before running an automatic 3D-2D registration algorithm. Following the manual registration,2 different X-ray views (ie AP and LAO 30 or RAO 30) are acquired and the automatic registrationis repeatedly rerun to track changes in the probe position due to cardiac and

respiratory motion. The automatic GPU (Graphic Processing Unit, NVIDIA GeForce 8800GTX)-accelerated registration updates in this way at a rate of 1–2Hz. Figure 8.2 shows a typical X-ray view, the probe model and a registration of the two. The study was divided into 2 phases. The preclinical phase involved data acquisition during a porcine experimental study. The clinical phase, involved data acquisition following software application during AF ablation (9 patients) and TAVI (2 patients) following approval from the Local Research Ethics Committee. The preliminary results of the use of this prototype software is shown in the following figures 8.2 to 8.4..

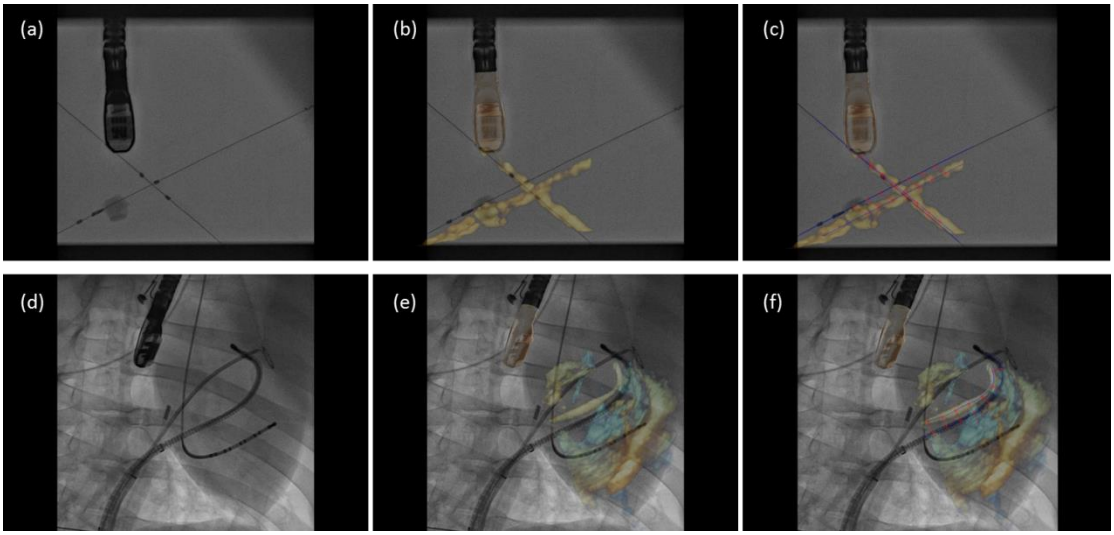

Figure 8-2: (a-c) Phantom model experimental overlay of fluoroscopic and echocardiographic images. Errors were measured between automatically defined landmarks on straight line models of the crossed wires. (d-f) Porcine experimental study overlay. Errors are measured as the shortest distance from landmarks on the echo catheter image to a spline model of the X-ray catheter.

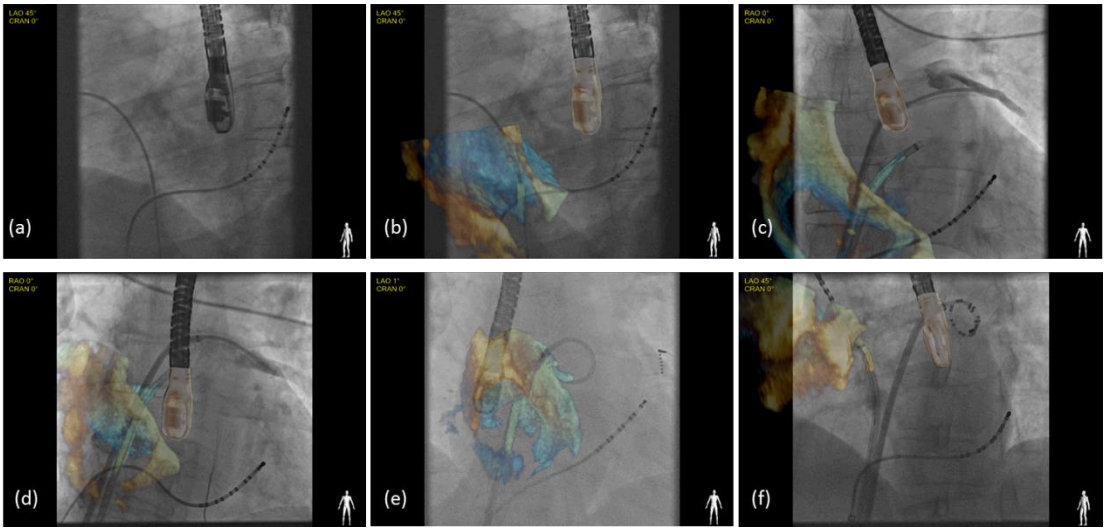

Figure 8-3: Clinical study to document feasibility in an AF ablation case. Real-time hybrid views were generated during the trans-septal puncture and subsequent placement of circular mapping and ablation catheters within the left atrial chamber.

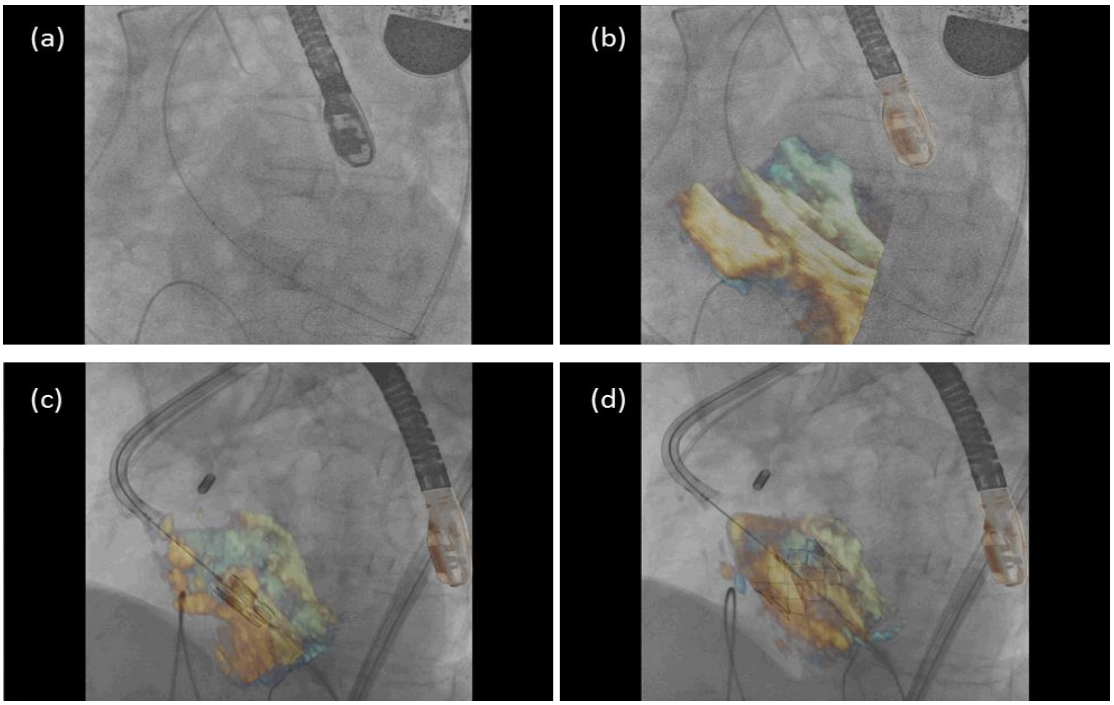

Figure 8-4: Clinical study to document feasibility in a TAVI case. Real-time hybrid views were generated during the placement of the Edwards core valve within the native aortic valve followed by the deployment of the prosthetic valve.

8.5.2 Real-time hybrid X-ray fluoroscopy and 3D echo visualisation in patients

Successful real-time integration was achieved in all 11 clinical cases. Figures 8.3 and 8.4 show typical examples of overlays from the catheter ablation and TAVI cases.. One of the potential advantages of the hybrid echo-fluoro imaging modality is increased and more precise control of the catheter/ guide-wire. Visualization of catheter direction in relation to the anatomical structures facilitates faster and more accurate catheter movement to the intended anatomical site.

An echo volume on its own can be difficult to interpret because of its limited field of view and lack of context for the echo coordinate system relative to the patient. Catheters and devices tend to produce artefacts in the ultrasound data reducing the clarity of the images. In the overlay view, the echo volume is displayed in a coordinate system that can be more easily related to the patient. Also, the highly visible catheters in the X-ray image help with identifying the catheters in the echo and so can be related to the cardiac anatomy via the echo image. During an ablation procedure, the precise location of the catheter tip and electrodes on the mapping catheter in relation to atrial tissue permits better targeted lesion delivery than just visualizing the catheter as a whole on fluoroscopy. Similarly during a TAVI procedure, being able to visualize both the native valve and the prosthesis on a single image will facilitate delivery and deployment of the prosthetic valve.

The accuracy requirement for a clinically useful image guidance system depends on many factors including the patient and the type of procedure being performed[151, 152].

Ultimately, randomized comparisons of real-time hybrid X-ray fluoroscopy and 3D echo image-guided therapy with standard visualization approaches are necessary to definitively establish its clinical utility and translate it from an experimental method to a clinical routine.

8.5.3 Present Limitations

It is important to recognize that one of the main objectives of this prelimary study was to assess the clinical feasibility of the proposed method. Although all the porcine experimental and clinical data were acquired specifically for this study, the data analysis was performed off-line. Our future work will focus on evaluating the accuracy of the live system and further improving the co-registration.

In addition our approach of measuring to the closest point accounts for 2-D in plane errors does not necessarily capture the complete error as there can also be misalignment tangentially to the catheters.

The clinical case numbers in this study at present time is small. Further studies involving larger patient groups are required to demonstrate that this novel technique translates into reduced fluoroscopy time, reduced complications and better overall patient outcome.

In this study, the practicability of real-time hybrid X-ray fluoroscopy and 3D echo visualisation was demonstrated in both a phantom model and a porcine experimental study, followed by a clinical series demonstrating work-flow feasibility. Further clinical validation and a randomized comparison between real-time hybrid echo-fluoro image-guided therapy versus standard visualization approach is needed to translate this tool into routine clinical practice.

9 Conclusion

Cardiac Magnetic Resonance Imaging in Atrial Fibrillation has a number of significant roles. The examination of tissue injury on cardiac CMR allows for the characterisation of lesions created following energy delivery. Serial delayed enhancement and T2 signal quantification around the PV antrum performed following catheter ablation demonstrated both a range of percentage encirclement and heterogeneity in the ratios of DE and T2 combination contributing towards the encirclement. Whilst on the acute scans both DE and T2 were observed, DE remained the predominant signal on the late scans. T2 generally resolved to near baseline levels. A comparison between acute and late scans demonstrated that DE resolved to varying degrees. Importantly DE associated with higher T2 signal on the acute scans had greater amount of signal regression and hence lesser amount of PV percentage encirclement. The clinical significance of this became apparent following the correlation of CMR findings to procedural outcome was assessed. Arrhythmia free patients had lower amount of initial T2 signal with higher amounts of DE quantified on both acute and late scans. Conversely, patients with recurrences had greater amounts of T2 and a larger regression in DE encirclement. The latter CMR findings allows for the potential categorisation of acute in vivo lesions into reversible and irreversible tissue injury. The continued trend of patients with higher DE and lower T2 signal on the acute scans having no AF recurrences at 6 months follow up suggests that CMR left atrial imaging has a role as an adjunct tool in clinical work to further understand recurrences of AF following catheter ablation.

The cardiac MR comparison between robotic assisted and standard catheter ablation suggest that remote robotic assisted navigation systems permit the creation of more contiguous, durable scar around the PV antrum. These CMR findings are the first to examine, report and

correlate in vivo lesion patterns created by robotic assisted catheter ablation to clinical outcome. On the whole, greater amounts of delayed enhancement was observed in the robotic group with an overall 75% success rate following 1.2 procedures in comparison to a 60% success following 1.40 procedures in the standard group. The recurrence arrhythmia pattern of atrial tachycardia which was greater in numbers in the RNS group suggests that the index ablation had successfully modified the arrhythmia into a more organised rhythm which was successfully ablated during the subsequent procedure.

Left atrial CMR delayed enhancement important an assessing the extent of post ablation tissue injury. A pilot study within this research has established that non-specific dual inversion recovery achieves better atrial blood pool suppression conferring improved delayed enhancement visualisation whilst reducing patient time within the scanner. The correlation between clinical outcome and improved visualisation enabling more accurate and precise scar quantification needs to be assessed in a larger clinical series.

The precision of left atrial scar quantification performed is important and requires a technique conferring high reproducibility. The comparison of a novel automatic segmentation tool to hand hand segmented lesions from DE-CMR images demonstrated a good correlation. This suggests that the tool is able to automatically identify the required pixels and segment out areas of atrial scar. Operator-independent lesion segmentation allows for greater reproducibility achieved over shorter time periods in addition to time and cost optimisation. Further work on improving software training and validation using a larger patient cohort is currently in progress.

In light of the above findings, CMR left atrial lesion imaging has a potential role as a surrogate biophysical marker in assessing newer catheter ablation technology to improve

lesion delivery. Catheter stability, good tissue contact force and adequate force time integral are important in creating better ablation lesions.

Bibliography

1. Moe GK. A conceptual model of atrial fibrillation. *Journal of electrocardiology*. 1968;1:145-146
2. Moe GK. Evidence for reentry as a mechanism of cardiac arrhythmias. *Reviews of physiology, biochemistry and pharmacology*. 1975;72:55-81
3. Cheung DW. Electrical activity of the pulmonary vein and its interaction with the right atrium in the guinea-pig. *The Journal of physiology*. 1981;314:445-456
4. Masani F. Node-like cells in the myocardial layer of the pulmonary vein of rats: An ultrastructural study. *Journal of anatomy*. 1986;145:133-142
5. Hou Y, Scherlag BJ, Lin J, Zhou J, Song J, Zhang Y, Patterson E, Lazzara R, Jackman WM, Po SS. Interactive atrial neural network: Determining the connections between ganglionated plexi. *Heart rhythm : the official journal of the Heart Rhythm Society*. 2007;4:56-63
6. Arruda MS, Armaganijan L, Di Biase L, Rashidi R, Natale A. Feasibility and safety of using an esophageal protective system to eliminate esophageal thermal injury: Implications on atrial-esophageal fistula following af ablation. *Journal of cardiovascular electrophysiology*. 2009;20:1272-1278
7. Morillo CA, Klein GJ, Jones DL, Guiraudon CM. Chronic rapid atrial pacing. Structural, functional, and electrophysiological characteristics of a new model of sustained atrial fibrillation. *Circulation*. 1995;91:1588-1595
8. Kaseda S, Zipes DP. Contraction-excitation feedback in the atria: A cause of changes in refractoriness. *Journal of the American College of Cardiology*. 1988;11:1327-1336
9. Wijffels MC, Kirchhof CJ, Dorland R, Allessie MA. Atrial fibrillation begets atrial fibrillation. A study in awake chronically instrumented goats. *Circulation*. 1995;92:1954-1968
10. Haines D. Biophysics of ablation: Application to technology. *Journal of cardiovascular electrophysiology*. 2004;15:S2-S11
11. Haines DE. The biophysics of radiofrequency catheter ablation in the heart: The importance of temperature monitoring. *Pacing and clinical electrophysiology : PACE*. 1993;16:586-591
12. Haissaguerre M, Jais P, Shah DC, Takahashi A, Hocini M, Quiniou G, Garrigue S, Le Mouroux A, Le Metayer P, Clementy J. Spontaneous initiation of atrial fibrillation by ectopic beats originating in the pulmonary veins. *N Engl J Med*. 1998;339:659-666
13. Calkins H, Brugada J, Packer DL, Cappato R, Chen SA, Crijns HJ, Damiano RJ, Jr., Davies DW, Haines DE, Haissaguerre M, Iesaka Y, Jackman W, Jais P, Kottkamp H, Kuck KH, Lindsay BD, Marchlinski FE, McCarthy PM, Mont JL, Morady F, Nademanee K, Natale A, Pappone C, Prystowsky E, Raviele A, Ruskin JN, Shemin RJ. Hrs/ehra/ecas expert consensus statement on catheter and surgical ablation of atrial fibrillation: Recommendations for personnel, policy, procedures and follow-up. A report of the heart rhythm society (hrs) task force on catheter and surgical ablation of atrial fibrillation developed in partnership with the european heart rhythm association (ehra) and the european cardiac arrhythmia society (ecas); in collaboration with the american college of cardiology (acc), american heart association (aha), and the society of thoracic surgeons (sts). Endorsed and approved by the governing bodies of the american college of cardiology, the american heart association, the european cardiac arrhythmia society, the european heart rhythm association, the society of thoracic surgeons, and the heart rhythm society. *Europace : European pacing, arrhythmias, and cardiac electrophysiology : journal of the working groups on cardiac pacing, arrhythmias, and cardiac cellular electrophysiology of the European Society of Cardiology*. 2007;9:335-379
14. Lewis T. Report cxix. Auricular fibrillation: A common clinical condition. *British medical journal*. 1909;2:1528

15. Fuster V, Ryden LE, Cannom DS, Crijns HJ, Curtis AB, Ellenbogen KA, Halperin JL, Le Heuzey JY, Kay GN, Lowe JE, Olsson SB, Prystowsky EN, Tamargo JL, Wann S, Smith SC, Jr., Jacobs AK, Adams CD, Anderson JL, Antman EM, Hunt SA, Nishimura R, Ornato JP, Page RL, Riegel B, Priori SG, Blanc JJ, Budaj A, Camm AJ, Dean V, Deckers JW, Despres C, Dickstein K, Lekakis J, McGregor K, Metra M, Morais J, Osterspey A, Zamorano JL. Acc/aha/esc 2006 guidelines for the management of patients with atrial fibrillation: A report of the american college of cardiology/american heart association task force on practice guidelines and the european society of cardiology committee for practice guidelines (writing committee to revise the 2001 guidelines for the management of patients with atrial fibrillation): Developed in collaboration with the european heart rhythm association and the heart rhythm society. *Circulation*. 2006;114:e257-354
16. Lip GY, Beevers DG. Abc of atrial fibrillation. History, epidemiology, and importance of atrial fibrillation. *BMJ*. 1995;311:1361-1363
17. Norman JN. William withering and the purple foxglove: A bicentennial tribute. *Journal of clinical pharmacology*. 1985;25:479-483
18. Mines GR. On dynamic equilibrium in the heart. *The Journal of physiology*. 1913;46:349-383
19. Moe GK, Abildskov JA. Atrial fibrillation as a self-sustaining arrhythmia independent of focal discharge. *American heart journal*. 1959;58:59-70
20. Moe GK, Rheinboldt WC, Abildskov JA. A computer model of atrial fibrillation. *American heart journal*. 1964;67:200-220
21. GK M. On the multiple wavelet hypothesis of atrial fibrillation. *Archives of Internal Pharmacodynamic Therapy*. 1962:6
22. M A, Lammers W, J,E,P., Bonke F, I,M., Hollen S, J. Experimental evaluation of moe's multiple wavelet hypothesis of atrial fibrillation. *Cardiac electrophysiology and arrhythmias*. 1985:11
23. M A, W L, J S, F B, J H. Total mapping of atrial excitation during acetylcholine-induced atrial flutter and fibrillation in the isolated canine heart. *Atrial fibrillation*. 1982:16
24. Engelmann T W. Ueber den einfluss der systole auf mororische leitung in der

herzkammer, mit bernerkungen zur theorie allorhythmischer herzstorungen. *Arch Gesamte Psychol*. 1896:24
25. H W. Ueber herzflimmern und seine beeinflussung durch kampher. *Z Exp Pathol Ther*.27
26. Rothberger C J, Winterberg H. Ber vorhofflimmern und vorhofflattern. *Pflugers Arch Gesamte Physiol Menshen Tiere*. 1915:49
27. Scherf D. Studies on auricular tachycardia caused by aconitine administration. *Proc Soc Exp Biol Med*. 1947;64:233-239
28. Scherf D, Romano F, J. , Terranova R. Experimental studies on auricular flutter and fibrillation. *American heart journal*. 1958:11
29. Scherf D, Terranova R. Mechanism of auricular flutter and fibrillation. *The American journal of physiology*. 1949;159:137-142
30. Goto M, Sakamoto Y, Imanaga I. Aconitine-induced fibrillation of the different muscle

tissues of the heart and the action of acetylcholine. 1967:11
31. Azuma K, Iwane H, Ibukiyama C, Watabe Y, Shin-Mura H, Iwaoka M, Wakatsuki T, Saito K, Shimizu K, Takada S, N: Y. Experimental studies on aconitine-induced atrial

fibrillation with microelectrodes. *Isr J Med Sci*. 1969:5
32. Jais P, Hocini M, Macle L, Choi KJ, Deisenhofer I, Weerasooriya R, Shah DC, Garrigue S, Raybaud F, Scavee C, Le Metayer P, Clementy J, Haissaguerre M. Distinctive electrophysiological properties of pulmonary veins in patients with atrial fibrillation. *Circulation*. 2002;106:2479-2485
33. Jais P, Haissaguerre M, Shah DC, Chouairi S, Gencel L, Hocini M, Clementy J. A focal source of atrial fibrillation treated by discrete radiofrequency ablation. *Circulation*. 1997;95:572-576

34. Hwang C, Wu TJ, Doshi RN, Peter CT, Chen PS. Vein of marshall cannulation for the analysis of electrical activity in patients with focal atrial fibrillation. *Circulation*. 2000;101:1503-1505
35. Shah DC, Haissaguerre M, Jais P, Clementy J. High-resolution mapping of tachycardia originating from the superior vena cava: Evidence of electrical heterogeneity, slow conduction, and possible circus movement reentry. *Journal of cardiovascular electrophysiology*. 2002;13:388-392
36. Tsai CF, Tai CT, Hsieh MH, Lin WS, Yu WC, Ueng KC, Ding YA, Chang MS, Chen SA. Initiation of atrial fibrillation by ectopic beats originating from the superior vena cava: Electrophysiological characteristics and results of radiofrequency ablation. *Circulation*. 2000;102:67-74
37. Allessie MA, Boyden PA, Camm AJ, Kleber AG, Lab MJ, Legato MJ, Rosen MR, Schwartz PJ, Spooner PM, Van Wagoner DR, Waldo AL. Pathophysiology and prevention of atrial fibrillation. *Circulation*. 2001;103:769-777
38. Allessie M, Ausma J, Schotten U. Electrical, contractile and structural remodeling during atrial fibrillation. *Cardiovascular research*. 2002;54:230-246
39. Kopecky SL, Gersh BJ, McGoon MD, Whisnant JP, Holmes DR, Jr., Ilstrup DM, Frye RL. The natural history of lone atrial fibrillation. A population-based study over three decades. *N Engl J Med*. 1987;317:669-674
40. Salmon D R, McPherson D, D. , Augustine D, E. , Holida M, D., White C, W. A canine model of chronic atrial fibrillation: Echocardiographic and electrocardiograhic validation. 1985:1
41. Konings KTS WM, Dorland R, Mast F, MA A. Mapping of electrically induced atrial fibrillation in humans. 1999:25
42. Smeets JL, Allessie MA, Lammers WJ, Bonke FI, Hollen J. The wavelength of the cardiac impulse and reentrant arrhythmias in isolated rabbit atrium. The role of heart rate, autonomic transmitters, temperature, and potassium. *Circulation research*. 1986;58:96-108
43. Rensma PL, Allessie MA, Lammers WJ, Bonke FI, Schalij MJ. Length of excitation wave and susceptibility to reentrant atrial arrhythmias in normal conscious dogs. *Circulation research*. 1988;62:395-410
44. Wang Z, Page P, Nattel S. Mechanism of flecainide's antiarrhythmic action in experimental atrial fibrillation. *Circulation research*. 1992;71:271-287
45. Wiener N, Rosenblueth A. The mathematical formulation of the problem of conduction of impulses in a network of connected excitable elements, specifically in cardiac muscle. *Archivos del Instituto de Cardiologia de Mexico*. 1946;16:205-265
46. Wang J, Feng J, Nattel S. Class iii antiarrhythmic drug action in experimental atrial fibrillation. Differences in reverse use dependence and effectiveness between d-sotalol and the new antiarrhythmic drug ambasilide. *Circulation*. 1994;90:2032-2040
47. Wang J, Bourne GW, Wang Z, Villemaire C, Talajic M, Nattel S. Comparative mechanisms of antiarrhythmic drug action in experimental atrial fibrillation. Importance of use-dependent effects on refractoriness. *Circulation*. 1993;88:1030-1044
48. O'Hara G, Villemaire C, Talajic M, Nattel S. Effects of flecainide on the rate dependence of atrial refractoriness, atrial repolarization and atrioventricular node conduction in anesthetized dogs. *Journal of the American College of Cardiology*. 1992;19:1335-1342
49. Cox JL, Schuessler RB, D'Agostino HJ, Jr., Stone CM, Chang BC, Cain ME, Corr PB, Boineau JP. The surgical treatment of atrial fibrillation. Iii. Development of a definitive surgical procedure. *The Journal of thoracic and cardiovascular surgery*. 1991;101:569-583
50. Haissaguerre M, Jais P, Shah DC, Gencel L, Pradeau V, Garrigues S, Chouairi S, Hocini M, Le Metayer P, Roudaut R, Clementy J. Right and left atrial radiofrequency catheter therapy of paroxysmal atrial fibrillation. *Journal of cardiovascular electrophysiology*. 1996;7:1132-1144
51. Knecht S, O'Neill MD, Matsuo S, Lim KT, Arantes L, Derval N, Klein GJ, Hocini M, Jais P, Clementy J, Haissaguerre M. Focal arrhythmia confined within the coronary sinus and

maintaining atrial fibrillation. *Journal of cardiovascular electrophysiology*. 2007;18:1140-1146

52. Rostock T, Rotter M, Sanders P, Jais P, Hocini M, Takahashi Y, Sacher F, Jonsson A, O'Neill MD, Hsu LF, Clementy J, Haissaguerre M. Fibrillating areas isolated within the left atrium after radiofrequency linear catheter ablation. *Journal of cardiovascular electrophysiology*. 2006;17:807-812
53. Rostock T, Lutomsky B, Steven D, Willems S. The coronary sinus as a focal source of paroxysmal atrial fibrillation: More evidence for the 'fifth pulmonary vein'? *Pacing and clinical electrophysiology : PACE*. 2007;30:1027-1031
54. Natale A, Raviele A, Arentz T, Calkins H, Chen SA, Haissaguerre M, Hindricks G, Ho Y, Kuck KH, Marchlinski F, Napolitano C, Packer D, Pappone C, Prystowsky EN, Schilling R, Shah D, Themistoclakis S, Verma A. Venice chart international consensus document on atrial fibrillation ablation. *Journal of cardiovascular electrophysiology*. 2007;18:560-580
55. Hsu LF, Jais P, Sanders P, Garrigue S, Hocini M, Sacher F, Takahashi Y, Rotter M, Pasquie JL, Scavee C, Bordachar P, Clementy J, Haissaguerre M. Catheter ablation for atrial fibrillation in congestive heart failure. *N Engl J Med*. 2004;351:2373-2383
56. Nademanee K, Schwab MC, Kosar EM, Karwecki M, Moran MD, Visessook N, Michael AD, Ngarmukos T. Clinical outcomes of catheter substrate ablation for high-risk patients with atrial fibrillation. *Journal of the American College of Cardiology*. 2008;51:843-849
57. Mainigi SK, Sauer WH, Cooper JM, Dixit S, Gerstenfeld EP, Callans DJ, Russo AM, Verdino RJ, Lin D, Zado ES, Marchlinski FE. Incidence and predictors of very late recurrence of atrial fibrillation after ablation. *Journal of cardiovascular electrophysiology*. 2007;18:69-74
58. Hocini M, Sanders P, Jais P, Hsu LF, Takahashi Y, Rotter M, Clementy J, Haissaguerre M. Techniques for curative treatment of atrial fibrillation. *Journal of cardiovascular electrophysiology*. 2004;15:1467-1471
59. Pratola C, Baldo E, Notarstefano P, Toselli T, Ferrari R. Radiofrequency ablation of atrial fibrillation: Is the persistence of all intraprocedural targets necessary for long-term maintenance of sinus rhythm? *Circulation*. 2008;117:136-143
60. Shah D, Haissaguerre M, Jais P, Hocini M. Nonpulmonary vein foci: Do they exist? *Pacing and clinical electrophysiology : PACE*. 2003;26:1631-1635
61. Ouyang F, Antz M, Ernst S, Hachiya H, Mavrakis H, Deger FT, Schaumann A, Chun J, Falk P, Hennig D, Liu X, Bansch D, Kuck KH. Recovered pulmonary vein conduction as a dominant factor for recurrent atrial tachyarrhythmias after complete circular isolation of the pulmonary veins: Lessons from double lasso technique. *Circulation*. 2005;111:127-135
62. Hocini M, Jais P, Sanders P, Takahashi Y, Rotter M, Rostock T, Hsu LF, Sacher F, Reuter S, Clementy J, Haissaguerre M. Techniques, evaluation, and consequences of linear block at the left atrial roof in paroxysmal atrial fibrillation: A prospective randomized study. *Circulation*. 2005;112:3688-3696
63. Rotter M, Jais P, Garrigue S, Sanders P, Hocini M, Hsu LF, Takahashi Y, Rostock T, Sacher F, Clementy J, Haissaguerre M. Clinical predictors of noninducibility of sustained atrial fibrillation after pulmonary vein isolation. *Journal of cardiovascular electrophysiology*. 2005;16:1298-1303
64. Stevenson WG, Epstein LM. Endpoints for ablation of atrial fibrillation. *Heart rhythm : the official journal of the Heart Rhythm Society*. 2006;3:146-147
65. Jais P, Hocini M, Sanders P, Hsu LF, Takahashi Y, Rotter M, Rostock T, Sacher F, Clementy J, Haissaguerre M. Long-term evaluation of atrial fibrillation ablation guided by noninducibility. *Heart rhythm : the official journal of the Heart Rhythm Society*. 2006;3:140-145
66. Oral H, Crawford T, Frederick M, Gadeela N, Wimmer A, Dey S, Sarrazin JF, Kuhne M, Chalfoun N, Wells D, Good E, Jongnarangsin K, Chugh A, Bogun F, Pelosi F, Jr., Morady F. Inducibility of paroxysmal atrial fibrillation by isoproterenol and its relation to the mode of onset of atrial fibrillation. *Journal of cardiovascular electrophysiology*. 2008;19:466-470

67. Pappone C, Oreto G, Rosanio S, Vicedomini G, Tocchi M, Gugliotta F, Salvati A, Dicandia C, Calabro MP, Mazzone P, Ficarra E, Di Gioia C, Gulletta S, Nardi S, Santinelli V, Benussi S, Alfieri O. Atrial electroanatomic remodeling after circumferential radiofrequency pulmonary vein ablation: Efficacy of an anatomic approach in a large cohort of patients with atrial fibrillation. *Circulation*. 2001;104:2539-2544
68. Oral H, Knight BP, Tada H, Ozaydin M, Chugh A, Hassan S, Scharf C, Lai SW, Greenstein R, Pelosi F, Jr., Strickberger SA, Morady F. Pulmonary vein isolation for paroxysmal and persistent atrial fibrillation. *Circulation*. 2002;105:1077-1081
69. Arentz T, von Rosenthal J, Blum T, Stockinger J, Burkle G, Weber R, Jander N, Neumann FJ, Kalusche D. Feasibility and safety of pulmonary vein isolation using a new mapping and navigation system in patients with refractory atrial fibrillation. *Circulation*. 2003;108:2484-2490
70. Willems S, Klemm H, Rostock T, Brandstrup B, Ventura R, Steven D, Risius T, Lutomsky B, Meinertz T. Substrate modification combined with pulmonary vein isolation improves outcome of catheter ablation in patients with persistent atrial fibrillation: A prospective randomized comparison. *European heart journal*. 2006;27:2871-2878
71. Oral H, Chugh A, Lemola K, Cheung P, Hall B, Good E, Han J, Tamirisa K, Bogun F, Pelosi F, Jr., Morady F. Noninducibility of atrial fibrillation as an end point of left atrial circumferential ablation for paroxysmal atrial fibrillation: A randomized study. *Circulation*. 2004;110:2797-2801
72. Pappone C, Santinelli V, Manguso F, Vicedomini G, Gugliotta F, Augello G, Mazzone P, Tortoriello V, Landoni G, Zangrillo A, Lang C, Tomita T, Mesas C, Mastella E, Alfieri O. Pulmonary vein denervation enhances long-term benefit after circumferential ablation for paroxysmal atrial fibrillation. *Circulation*. 2004;109:327-334
73. Haissaguerre M, Sanders P, Hocini M, Takahashi Y, Rotter M, Sacher F, Rostock T, Hsu LF, Bordachar P, Reuter S, Roudaut R, Clementy J, Jais P. Catheter ablation of long-lasting persistent atrial fibrillation: Critical structures for termination. *Journal of cardiovascular electrophysiology*. 2005;16:1125-1137
74. Mesas CE, Pappone C, Lang CC, Gugliotta F, Tomita T, Vicedomini G, Sala S, Paglino G, Gulletta S, Ferro A, Santinelli V. Left atrial tachycardia after circumferential pulmonary vein ablation for atrial fibrillation: Electroanatomic characterization and treatment. *Journal of the American College of Cardiology*. 2004;44:1071-1079
75. Pappone C, Manguso F, Vicedomini G, Gugliotta F, Santinelli O, Ferro A, Gulletta S, Sala S, Sora N, Paglino G, Augello G, Agricola E, Zangrillo A, Alfieri O, Santinelli V. Prevention of iatrogenic atrial tachycardia after ablation of atrial fibrillation: A prospective randomized study comparing circumferential pulmonary vein ablation with a modified approach. *Circulation*. 2004;110:3036-3042
76. Gerstenfeld EP, Callans DJ, Dixit S, Russo AM, Nayak H, Lin D, Pulliam W, Siddique S, Marchlinski FE. Mechanisms of organized left atrial tachycardias occurring after pulmonary vein isolation. *Circulation*. 2004;110:1351-1357
77. Wright M, Haissaguerre M, Knecht S, Matsuo S, O'Neill MD, Nault I, Lellouche N, Hocini M, Sacher F, Jais P. State of the art: Catheter ablation of atrial fibrillation. *Journal of cardiovascular electrophysiology*. 2008;19:583-592
78. Kim RJ, Wu E, Rafael A, Chen EL, Parker MA, Simonetti O, Klocke FJ, Bonow RO, Judd RM. The use of contrast-enhanced magnetic resonance imaging to identify reversible myocardial dysfunction. *N Engl J Med*. 2000;343:1445-1453
79. De Cobelli F, Pieroni M, Esposito A, Chimenti C, Belloni E, Mellone R, Canu T, Perseghin G, Gaudio C, Maseri A, Frustaci A, Del Maschio A. Delayed gadolinium-enhanced cardiac magnetic resonance in patients with chronic myocarditis presenting with heart failure or recurrent arrhythmias. *Journal of the American College of Cardiology*. 2006;47:1649-1654

80. Rochitte CE, Tassi EM, Shiozaki AA. The emerging role of mri in the diagnosis and management of cardiomyopathies. *Current cardiology reports*. 2006;8:44-52
81. Laissy JP, Hyafil F, Feldman LJ, Juliard JM, Schouman-Claeys E, Steg PG, Faraggi M. Differentiating acute myocardial infarction from myocarditis: Diagnostic value of early- and delayed-perfusion cardiac mr imaging. *Radiology*. 2005;237:75-82
82. Higgins CB, Herfkens R, Lipton MJ, Sievers R, Sheldon P, Kaufman L, Crooks LE. Nuclear magnetic resonance imaging of acute myocardial infarction in dogs: Alterations in magnetic relaxation times. *The American journal of cardiology*. 1983;52:184-188
83. Karolle BL, Carlson RE, Aisen AM, Buda AJ. Transmural distribution of myocardial edema by nmr relaxometry following myocardial ischemia and reperfusion. *American heart journal*. 1991;122:655-664
84. Scholz TD, Martins JB, Skorton DJ. Nmr relaxation times in acute myocardial infarction: Relative influence of changes in tissue water and fat content. *Magnetic resonance in medicine : official journal of the Society of Magnetic Resonance in Medicine / Society of Magnetic Resonance in Medicine*. 1992;23:89-95
85. Garcia-Dorado D, Oliveras J. Myocardial oedema: A preventable cause of reperfusion injury? *Cardiovascular research*. 1993;27:1555-1563
86. Garcia-Dorado D, Oliveras J, Gili J, Sanz E, Perez-Villa F, Barrabes J, Carreras MJ, Solares J, Soler-Soler J. Analysis of myocardial oedema by magnetic resonance imaging early after coronary artery occlusion with or without reperfusion. *Cardiovascular research*. 1993;27:1462-1469
87. Nattel S, Shiroshita-Takeshita A, Brundel BJ, Rivard L. Mechanisms of atrial fibrillation: Lessons from animal models. *Progress in cardiovascular diseases*. 2005;48:9-28
88. Burstein B, Qi XY, Yeh YH, Calderone A, Nattel S. Atrial cardiomyocyte tachycardia alters cardiac fibroblast function: A novel consideration in atrial remodeling. *Cardiovascular research*. 2007;76:442-452
89. Anne W, Willems R, Roskams T, Sergeant P, Herijgers P, Holemans P, Ector H, Heidbuchel H. Matrix metalloproteinases and atrial remodeling in patients with mitral valve disease and atrial fibrillation. *Cardiovascular research*. 2005;67:655-666
90. Oakes RS, Badger TJ, Kholmovski EG, Akoum N, Burgon NS, Fish EN, Blauer JJ, Rao SN, DiBella EV, Segerson NM, Daccarett M, Windfelder J, McGann CJ, Parker D, MacLeod RS, Marrouche NF. Detection and quantification of left atrial structural remodeling with delayed-enhancement magnetic resonance imaging in patients with atrial fibrillation. *Circulation*. 2009;119:1758-1767
91. Wittkampf FH, Vonken EJ, Derksen R, Loh P, Velthuis B, Wever EF, Boersma LV, Rensing BJ, Cramer MJ. Pulmonary vein ostium geometry: Analysis by magnetic resonance angiography. *Circulation*. 2003;107:21-23
92. Hauser TH, Yeon SB, McClennen S, Katsimaglis G, Kissinger KV, Josephson ME, Rofsky NM, Manning WJ. A method for the determination of proximal pulmonary vein size using contrast-enhanced magnetic resonance angiography. *Journal of cardiovascular magnetic resonance : official journal of the Society for Cardiovascular Magnetic Resonance*. 2004;6:927-936
93. Peters DC, Wylie JV, Hauser TH, Nezafat R, Han Y, Woo JJ, Taclas J, Kissinger KV, Goddu B, Josephson ME, Manning WJ. Recurrence of atrial fibrillation correlates with the extent of post-procedural late gadolinium enhancement: A pilot study. *JACC: Cardiovascular Imaging*. 2009;2:308-316
94. Rajappan K, Kistler PM, Earley MJ, Thomas G, Izquierdo M, Sporton SC, Schilling RJ. Acute and chronic pulmonary vein reconnection after atrial fibrillation ablation: A prospective characterization of anatomical sites. *Pacing and Clinical Electrophysiology*. 2008;31:1598-1605

95. Cappato R, Negroni S, Pecora D, Bentivegna S, Lupo PP, Carolei A, Esposito C, Furlanello F, De Ambroggi L. Prospective assessment of late conduction recurrence across radiofrequency lesions producing electrical disconnection at the pulmonary vein ostium in patients with atrial fibrillation. *Circulation*. 2003;108:1599-1604
96. Nanthakumar K, Plumb VJ, Epstein AE, Veenhuyzen GD, Link D, Kay GN. Resumption of electrical conduction in previously isolated pulmonary veins: Rationale for a different strategy? *Circulation*. 2004;109:1226-1229
97. Klemm HU, Steven D, Johnsen C, Ventura R, Rostock T, Lutomsky B, Risius T, Meinertz T, Willems S. Catheter motion during atrial ablation due to the beating heart and respiration: Impact on accuracy and spatial referencing in three-dimensional mapping. *Heart rhythm : the official journal of the Heart Rhythm Society*. 2007;4:587-592
98. Badger TJ, Daccarett M, Akoum NW, Adjei-Poku YA, Burgon NS, Haslam TS, Kalvaitis S, Kuppahally S, Vergara G, McMullen L, Anderson PA, Kholmovski E, MacLeod RS, Marrouche NF. Evaluation of left atrial lesions after initial and repeat atrial fibrillation ablation: Lessons learned from delayed-enhancement mri in repeat ablation procedures. *Circ Arrhythm Electrophysiol*. 2010;3:249-259
99. Reddy VY, Schmidt EJ, Holmvang G, Fung M. Arrhythmia recurrence after atrial fibrillation ablation: Can magnetic resonance imaging identify gaps in atrial ablation lines? *Journal of cardiovascular electrophysiology*. 2008;19:434-437
100. Gepstein L, Hayam G, SA B-H. A novel method for non-fluoroscopic catheter based electroanatomic mapping of the heart. *Circulation*. 1993:12
101. Dong J, Dickfeld T, Dalal D, Cheema A, Vasamreddy CR, Henrikson CA, Marine JE, Halperin HR, Berger RD, Lima JA, Bluemke DA, Calkins H. Initial experience in the use of integrated electroanatomic mapping with three-dimensional mr/ct images to guide catheter ablation of atrial fibrillation. *Journal of cardiovascular electrophysiology*. 2006;17:459-466
102. Wittkampf FH, Nakagawa H. Rf catheter ablation: Lessons on lesions. *Pacing and clinical electrophysiology : PACE*. 2006;29:1285-1297
103. Zhong H, Lacomis JM, Schwartzman D. On the accuracy of cartomerge for guiding posterior left atrial ablation in man. *Heart rhythm : the official journal of the Heart Rhythm Society*. 2007;4:595-602
104. Taclas JE, Nezafat R, Wylie JV, Josephson ME, Hsing J, Manning WJ, Peters DC. Relationship between intended sites of rf ablation and post-procedural scar in af patients, using late gadolinium enhancement cardiovascular magnetic resonance. *Heart rhythm : the official journal of the Heart Rhythm Society*. 2010;7:489-496
105. Patel P, Dokainish H, Tsai P, Lakkis N. Update on the association of inflammation and atrial fibrillation. *Journal of cardiovascular electrophysiology*. 2010;21:1064-1070
106. Ridker PM, Hennekens CH, Buring JE, Rifai N. C-reactive protein and other markers of inflammation in the prediction of cardiovascular disease in women. *N Engl J Med*. 2000;342:836-843
107. Ridker PM, Rifai N, Stampfer MJ, Hennekens CH. Plasma concentration of interleukin-6 and the risk of future myocardial infarction among apparently healthy men. *Circulation*. 2000;101:1767-1772
108. Di Biase L, Elayi CS, Fahmy TS, Martin DO, Ching CK, Barrett C, Bai R, Patel D, Khaykin Y, Hongo R, Hao S, Beheiry S, Pelargonio G, Russo AD, Casella M, Santarelli P, Potenza D, Fanelli R, Massaro R, Wang P, Al-Ahmad A, Arruda M, Themistoclakis S, Bonso A, Rossillo A, Raviele A, Schweikert RA, Burkhardt DJ, Natale A. Atrial fibrillation ablation strategies for paroxysmal patients / clinical perspective. *Circulation: Arrhythmia and Electrophysiology*. 2009;2:113-119
109. Oral H, Chugh A, Good E, Sankaran S, Reich SS, Igic P, Elmouchi D, Tschopp D, Crawford T, Dey S, Wimmer A, Lemola K, Jongnarangsin K, Bogun F, Pelosi F, Jr., Morady F. A tailored

approach to catheter ablation of paroxysmal atrial fibrillation. *Circulation*. 2006;113:1824-1831

110. Weerasooriya R, Khairy P, Litalien J, Macle L, Hocini M, Sacher F, Lellouche N, Knecht S, Wright M, Nault I, Miyazaki S, Scavee C, Clementy J, Haissaguerre M, Jais P. Catheter ablation for atrial fibrillation: Are results maintained at 5 years of follow-up? *Journal of the American College of Cardiology*. 2011;57:160-166
111. Saeed M, Wendland MF, Takehara Y, Higgins CB. Reversible and irreversible injury in the reperfused myocardium: Differentiation with contrast material-enhanced mr imaging. *Radiology*. 1990;175:633-637
112. Peters DC, Wylie JV, Hauser TH, Kissinger KV, Botnar R, Essebag V, Josephson ME, Manning WJ. Detection of pulmonary vein and left atrial scar after catheter ablation with three dimensional navigator-gated delayed enhancement mr imaging: Initial experience. *Radiology*. 2007;243:690-695
113. Ibrahim T, Hackl T, Nekolla SG, Breuer M, Feldmair M, Schomig A, Schwaiger M. Acute myocardial infarction: Serial cardiac mr imaging shows a decrease in delayed enhancement of the myocardium during the 1st week after reperfusion. *Radiology*. 2010;254:88-97
114. Friedrich MG. Myocardial edema--a new clinical entity? *Nat Rev Cardiol*. 2010;7:292-296
115. Knowles BR, Caulfield D, Cooklin M, Rinaldi CA, Gill J, Bostock J, Razavi R, Schaeffter T, Rhode KS. 3-d visualization of acute rf ablation lesions using mri for the simultaneous determination of the patterns of necrosis and edema. *Biomedical Engineering, IEEE Transactions on*. 2010;57:1467-1475
116. Rogers W. Regression standard errors in clustered samples. *Stata Technical Bulletin.* 1994;3:7
117. Kellman P, Aletras AH, Mancini C, McVeigh ER, Arai AE. T2-prepared ssfp improves diagnostic confidence in edema imaging in acute myocardial infarction compared to turbo spin echo. *Magnetic resonance in medicine : official journal of the Society of Magnetic Resonance in Medicine / Society of Magnetic Resonance in Medicine*. 2007;57:891-897
118. McGann CJ, Kholmovski EG, Oakes RS, Blauer JJE, Daccarett M, Segerson N, Airey KJ, Akoum N, Fish E, Badger TJ, DiBella EVR, Parker D, MacLeod RS, Marrouche NF. New magnetic resonance imaging-based method for defining the extent of left atrial wall injury after the ablation of atrial fibrillation. *Journal of the American College of Cardiology*. 2008;52:1263-1271
119. Badger TJ, Oakes RS, Daccarett M, Burgon NS, Akoum N, Fish EN, Blauer JJE, Rao SN, Adjei-Poku Y, Kholmovski EG, Vijayakumar S, Di Bella EVR, MacLeod RS, Marrouche NF. Temporal left atrial lesion formation after ablation of atrial fibrillation. *Heart rhythm : the official journal of the Heart Rhythm Society*. 2009;6:161-168
120. Knowles BR, Caulfield D, Cooklin M, Rinaldi CA, Gill J, Bostock J, Razavi R, Schaeffter T, Rhode KS. 3-d visualization of acute rf ablation lesions using mri for the simultaneous determination of the patterns of necrosis and edema. *IEEE Trans Biomed Eng*. 2010;57:1467-1475
121. McGann C, Kholmovski E, Blauer J, Vijayakumar S, Haslam T, Cates J, DiBella E, Burgon N, Wilson B, Alexander A, Prastawa M, Daccarett M, Vergara G, Akoum N, Parker D, MacLeod R, Marrouche N. Dark regions of no-reflow on late gadolinium enhancement magnetic resonance imaging result in scar formation after atrial fibrillation ablation. *Journal of the American College of Cardiology*. 2011;58:177-185
122. Schwartzman D, Ren J, Devine W, Callans D. Cardiac swelling associated with linear radiofrequency ablation in the atrium. *Journal of Interventional Cardiac Electrophysiology*. 2001;5:159-166
123. Saeed M, Wendland MF, Masui T, Higgins CB. Reperfused myocardial infaarctions on t1- and susceptibility-enhanced mri: Evidence for loss of compartmentalization of contrast media. *Magnetic Resonance in Medicine*. 1994;31:31-39

124. Vergara GR, Marrouche NF. Tailored management of atrial fibrillation using a lge-mri based model: From the clinic to the electrophysiology laboratory. *Journal of cardiovascular electrophysiology*. 2011;22:481-487
125. Brueckmann M, Wolpert C, Bertsch T, Sueselbeck T, Liebetrau C, Kaden JJ, Huhle G, Neumaier M, Borggrefe M, Haase KK. Markers of myocardial damage, tissue healing, and inflammation after radiofrequency catheter ablation of atrial tachyarrhythmias. *Journal of cardiovascular electrophysiology*. 2004;15:686-691
126. Segerson NM, Daccarett M, Badger TJ, Shabaan A, Akoum N, Fish EN, Rao S, Burgon NS, Adjei-Poku Y, Kholmovski E, Vijayakumar S, Dibella EVR, Macleod RS, Marrouche NF. Magnetic resonance imaging-confirmed ablative debulking of the left atrial posterior wall and septum for treatment of persistent atrial fibrillation: Rationale and initial experience. *Journal of cardiovascular electrophysiology*. 2010;21:126-132
127. Ouyang F, Tilz R, Chun J, Schmidt B, Wissner E, Zerm T, Neven K, Kokturk B, Konstantinidou M, Metzner A, Fuernkranz A, Kuck K-H. Long-term results of catheter ablation in paroxysmal atrial fibrillation: Lessons from a 5-year follow-up. *Circulation*. 2010;122:2368-2377
128. Abdel-Aty H, Zagrosek A, Schulz-Menger J, Taylor AJ, Messroghli D, Kumar A, Gross M, Dietz R, Friedrich MG. Delayed enhancement and t2-weighted cardiovascular magnetic resonance imaging differentiate acute from chronic myocardial infarction. *Circulation*. 2004;109:2411-2416
129. Okumura Y, Johnson SB, Bunch TJ, Henz BD, O'Brien CJ, Packer DL. A systematical analysis of in vivo contact forces on virtual catheter tip/tissue surface contact during cardiac mapping and intervention. *Journal of cardiovascular electrophysiology*. 2008;19:632-640
130. Koa-Wing M, Kojodjojo P, Malcolme-Lawes LC, Salukhe TV, Linton NW, Grogan AP, Bergman D, Lim PB, Whinnett ZI, McCarthy K, Ho SY, O'Neill MD, Peters NS, Davies DW, Kanagaratnam P. Robotically assisted ablation produces more rapid and greater signal attenuation than manual ablation. *Journal of cardiovascular electrophysiology*. 2009;20:1398-1404
131. Di Biase L, Natale A, Barrett C, Tan C, Elayi CS, Ching CK, Wang P, Al-Ahmad A, Arruda M, Burkhardt JD, Wisnoskey BJ, Chowdhury P, De Marco S, Armaganijan L, Litwak KN, Schweikert RA, Cummings JE. Relationship between catheter forces, lesion characteristics, "popping," and char formation: Experience with robotic navigation system. *Journal of cardiovascular electrophysiology*. 2009;20:436-440
132. Di Biase L, Wang Y, Horton R, Gallinghouse GJ, Mohanty P, Sanchez J, Patel D, Dare M, Canby R, Price LD, Zagrodzky JD, Bailey S, Burkhardt JD, Natale A. Ablation of atrial fibrillation utilizing robotic catheter navigation in comparison to manual navigation and ablation: Single-center experience. *Journal of cardiovascular electrophysiology*. 2009;20:1328-1335
133. Hlivak P, Mlcochova H, Peichl P, Cihak R, Wichterle D, Kautzner J. Robotic navigation in catheter ablation for paroxysmal atrial fibrillation: Midterm efficacy and predictors of postablation arrhythmia recurrences. *Journal of cardiovascular electrophysiology*. 2011;22:534-540
134. Geschwind JF, Wendland MF, Saeed M, Lauerma K, Derugin N, Higgins CB. Aur memorial award. Identification of myocardial cell death in reperfused myocardial injury using dual mechanisms of contrast-enhanced magnetic resonance imaging. *Academic radiology*. 1994;1:319-325
135. Lardo AC, McVeigh ER, Jumrussirikul P, Berger RD, Calkins H, Lima J, Halperin HR. Visualization and temporal/spatial characterization of cardiac radiofrequency ablation lesions using magnetic resonance imaging. *Circulation*. 2000;102:698-705
136. Dickfeld T, Kato R, Zviman M, Nazarian S, Dong J, Ashikaga H, Lardo AC, Berger RD, Calkins H, Halperin H. Characterization of acute and subacute radiofrequency ablation lesions with nonenhanced magnetic resonance imaging. *Heart rhythm : the official journal of the Heart Rhythm Society*. 2007;4:208-214

137. Okada T, Yamada T, Murakami Y, Yoshida N, Ninomiya Y, Shimizu T, Toyama J, Yoshida Y, Ito T, Tsuboi N, Kondo T, Inden Y, Hirai M, Murohara T. Prevalence and severity of left atrial edema detected by electron beam tomography early after pulmonary vein ablation. *Journal of the American College of Cardiology*. 2007;49:1436-1442
138. Arujuna A, Caulfield D, Rashed K, Knowles BR, Rinaldi CA, Cooklin M, ONeill M, Rhode KS, Gili J, Razavi R. Acute pulmonary vein isolation lesions consist of interstitial oedema and tissue necrosis: Possible mechanism of pulmonary vein reconnection. *Journal of Cardiovascular Magnetic Resonance*. 2011;13:1
139. Peel SA, Morton G, Nagel E, Botnar RM. Non-selective double inversion recovery pre-pulse for flow-independent black blood myocardial scar imaging: Optimization of the t1 suppression range. *Proceedings of ISMRM 2011 Montreal*. 2011
140. Eick OJ. Factors influencing lesion formation during radiofrequency catheter ablation. *Indian Pacing Electrophysiology Journal*. 2003;3:12
141. Kuck KH, Reddy VY, Schmidt B, Natale A, Neuzil P, Saoudi N, Kautzner J, Herrera C, Hindricks G, Jais P, Nakagawa H, Lambert H, Shah DC. A novel radiofrequency ablation catheter using contact force sensing: Toccata study. *Heart rhythm : the official journal of the Heart Rhythm Society*. 2012;9:18-23
142. Kim RJ, Fieno DS, Parrish TB, Harris K, Chen EL, Simonetti O, Bundy J, Finn JP, Klocke FJ, Judd RM. Relationship of mri delayed contrast enhancement to irreversible injury, infarct age, and contractile function. *Circulation*. 1999;100:1992-2002
143. Schmidt A, Azevedo CF, Cheng A, Gupta SN, Bluemke DA, Foo TK, Gerstenblith G, Weiss RG, Marban E, Tomaselli GF, Lima JA, Wu KC. Infarct tissue heterogeneity by magnetic resonance imaging identifies enhanced cardiac arrhythmia susceptibility in patients with left ventricular dysfunction. *Circulation*. 2007;115:2006-2014
144. Amado LC, Gerber BL, Gupta SN, Rettmann DW, Szarf G, Schock R, Nasir K, Kraitchman DL, Lima JA. Accurate and objective infarct sizing by contrast-enhanced magnetic resonance imaging in a canine myocardial infarction model. *Journal of the American College of Cardiology*. 2004;44:2383-2389
145. Beek AM, Bondarenko O, Afsharzada F, van Rossum AC. Quantification of late gadolinium enhanced cmr in viability assessment in chronic ischemic heart disease: A comparison to functional outcome. *Journal of cardiovascular magnetic resonance : official journal of the Society for Cardiovascular Magnetic Resonance*. 2009;11:6
146. Wylie JV, Jr., Peters DC, Essebag V, Manning WJ, Josephson ME, Hauser TH. Left atrial function and scar after catheter ablation of atrial fibrillation. *Heart rhythm : the official journal of the Heart Rhythm Society*. 2008;5:656-662
147. Y. Boykov, O. Veksler, Zabih R. Fast approximate energy minimization via graph cuts. *IEEE Transactions on pattern analysis and machine intelligence*. 2011:18
148. Boykov Y, Funka-Lea G. Graph cuts and efficient and image segmentation. *International Journal of Computer Vision*. 2006;70:30
149. van der Lijn F, den Heijer T, Breteler MM, Niessen WJ. Hippocampus segmentation in mr images using atlas registration, voxel classification, and graph cuts. *NeuroImage*. 2008;43:708-720
150. Song Z, Tustison N, Avants B, Gee JC. Integrated graph cuts for brain mri segmentation. *Medical image computing and computer-assisted intervention : MICCAI ... International Conference on Medical Image Computing and Computer-Assisted Intervention*. 2006;9:831-838
151. Linte CA, Moore J, Peters TM. How accurate is accurate enough? A brief overview on accuracy considerations in image-guided cardiac interventions. *Conference proceedings : ... Annual International Conference of the IEEE Engineering in Medicine and Biology Society. IEEE Engineering in Medicine and Biology Society. Conference*. 2010;2010:2313-2316

152. Linte CA, Lang P, Rettmann ME, Cho DS, Holmes DR, 3rd, Robb RA, Peters TM. Accuracy considerations in image-guided cardiac interventions: Experience and lessons learned. *International journal of computer assisted radiology and surgery*. 2011

Table of Figures and Tables

APPENDIX I

Publications and submitted manuscripts pending review during this period of research.

Gao G, Penney G, Ma Y, Gogin N, Cathier P, **Arujuna A**, Morton G, Caulfield D, Gill J, Aldo Rinaldi C, Hancock J, Redwood S, Thomas M, Razavi R, Gijsbers G, Rhode K. Registration of 3D trans-esophageal echocardiography to X-ray fluoroscopy using image- based probe tracking.Med Image Anal. 2011 May 12. [Epub ahead of print] PMID: 21624845.

Arujuna A, Karim R, Caulfield D, Knowles B, Rhode K, Schaeffter T, Kato B, , Rinaldi CA, Cooklin M, Razavi R, O'Neill M ,Gill J. Acute Pulmonary Vein Isolation is Achieved by a Combination of Reversible and Irreversible Atrial Injury following Catheter Ablation:Evidence from Magnetic Resonance Imaging. Accepted for publication Circulation Arrhythmia and Electrophysiology Jan 19th 2012.

Arujuna A, Karim R, Rhode K, Schaeffter T, Kato B, ,Wright M, Rinaldi CA, Cooklin M, Razavi R, O'Neill M ,Gill J. Remote Robotic Navigation versus Standard Catheter Ablation: A Cardiac MR Comparison with Clinical Outcomes. Pending review from Circulation Arrhythmia and Electrophysiology.

Arujuna A, Peel S, Harrison J, Karim R, Rhode K, Rinaldi CA, Cooklin M, Oneill M, Gill J, Razavi R, Schaeffter T, Botnar R. Double Inversion Recovery: An improved technique for Left Atrial Scar Visualisation. Pending review from JCMR-

Arujuna A, Housden J, Ma YL , Gao G,Nijhof N, Cathier P, Gijsbers G, Rajani R, Kapetanakis S, Hancock J, Rinaldi CA, Cooklin M, Gill J, Razavi R, O'Neill M, Rhode K. Novel System for Real-Time Integration of 3D Echo and Fluoroscopy for Image Guidance: Experimental Validation and Clinical Feasibility. Pending review from Circulation Imaging.

Arujuna A, Murphy C, Hayat A, Seffens H, Gill J. A Linear Ablating System In The Left And Right Atrium. Accepted for publication by Indian Journal of Pacing and Electrophysiology November 21st 2011

Karim R, **Arujuna A**, Brazier A, Matharu K, Gill J, Rinaldi CA, O'Neill M, Razavi R, Rueckert D, Schaeffter T and Rhode K. A Fast and Automatic Segmentation of Left Atrial Fibrosis from Delayed-Enhancement MR Images following Radiofrequency Catheter Ablation.Pending review of revised manuscript from IEEE Transactions on Biomedical Engineering.

Krueger M, Seemann G, Keller DUJ, **Arujuna A**, Rhode K ,Razavi R, D¨ossel O. Personalized Atrial Models for the Evaluation and Planing of Radio-Frequency-Ablation of AtrialFibrillation. Submitted to IEEE Transactions of Medical Imaging.

Abstracts and presentations at national and international scientific conferences.

Arujuna A, Karim R, Caulfield D, Knowles B, Rhode K, Schaeffter T, Kato B, , Rinaldi CA, Cooklin M, Razavi R, O'Neill M ,Gill J. Acute Pulmonary Vein Isolation Lesions Consist of Interstitial Oedema and Tissue Necrosis: Possible Mechanism of Pulmonary Vein Reconnection. SCMR 2011 Nice – 2011 SCMR/ EuroCMR Joint Scientific Sessions 3-6 FEB 2011 / / Nice Acropolis Convention Centre. Oral moderated poster presentation. Shortlisted for Young Investigator's Prize.

Karim R, **Arujuna A**, O'Neil M, Gill J, Razavi R, Rueckert D, Schaeffter T, Rhode K. An automatic segmentation algorithm for improved visualization of atrial ablation lesions using magnetic resonance imaging. SCMR 2011 Nice – 2011 SCMR/ EuroCMR Joint Scientific Sessions 3-6 FEB 2011 / / Nice Acropolis Convention Centre.

Arujuna A, Karim R,, Rhode K, Schaeffter T, Kato B, , Rinaldi CA, Cooklin M, Razavi R, O'Neill M ,Gill. Are Robotic Assisted Catheter Ablation Lesions on Cardiac MR Different from Standard Catheter Ablation in Paroxysmal AF patients ? : Novel FindingsECAS 2011 Paris – poster presentation10-12 April 2011 European Cardiac Arrhythmia Society , Paris, France16-126 Abstract 15-52.

Karim R, Gao G, Harrison J, **Arujuna A**, Gill J,Razavi R, Schaeffter T, Rhode K, O'Neill M. A novel technique to display tissue contact force in the left atrium following catheter ablation for paroxysmal atrial fibrillation using a force sensing ablation catheter. Abstract only. Accepted as oral presentation at ECAS 2011 Paris.

Arujuna A, Karim R,, Rhode K, Schaeffter T, Kato B, , Rinaldi CA, Cooklin M, Razavi R, O'Neill M ,Gill.Assessment of left atrial injury by cardiac MR: a randomised prospective comparison of robotic versus manual AF ablation.HRS 2011 San Francisco Oral Abstract Presenter for Heart Rhythm 2011, the Heart Rhythm Society's 32nd Annual Scientific Sessions, to be held in San Francisco, California, May 4-7, 2011.– oral presentation (Abstract # 6622)AB36 5/6/2011 2:00:00 PM - 5/6/2011 2:15:00 PM (Abstract Plus Session Innovations in Ablation and Mapping of Atrial Arrhythmias).

Arujuna A, Karim R, Rhode K, Schaeffter T, Kato B, , Rinaldi CA, Cooklin M, Razavi R, O'Neill M ,Gill J.
Interstitial Oedema, Delayed Enhancement and Recurrences following Catheter Ablation in Paroxysmal AF: How are they related?HRS 2011 San Francisco Oral Abstract Presenter for Heart Rhythm 2011, the Heart Rhythm Society's 32nd Annual Scientific Sessions, to be held in San Francisco, California, May 4-7, 2011- oral presentation(Abstract # 6727).

Arujuna A, Ma YL , Gao G,Nijhof N, Cathier P, Gijsbers G, Rajani R, Kapetanakis S, Hancock J, Rinaldi CA, Cooklin M, Gill J, Razavi R, O'Neill M, Rhode K Novel Hybrid 3D Echo-Fluoroscopy Imaging: A Clinical Feasibility Study HRS 2011 SanFrancisco Oral Abstract Presenter for Heart Rhythm 2011, the Heart Rhythm Society's 32nd Annual Scientific Sessions, to be held in San Francisco, California, May 4-7, 2011 (Abstract 8) Clinical Innovations 5/6/2011 9:30 -1700**.**

Karim R, **Arujuna A**, Brazier A, O'Neil M, Gill J, Razavi R, Rueckert D, Schaeffter T, Rhode K.Evaluation of a Rapid Quantification Algorithm for Delayed Enhancement MRI following Left Atrial Ablation.Accepted as oral presentation in Heart Rhythm 2011.

Karim R, Gao G, Harrison J, **Arujuna A**, Lambert H, Leo G, Gill J, Razavi R, Schaeffter T, Rhode K. Magnetic Resonance Imaging Analysis of Tissue-contact Force Following Catheter Ablation for Paroxysmal Atrial Fibrillation. Accepted as oral presentation in Heart Rhythm 2011.

Arujuna A, Karim R, Rhode K, Schaeffter T, Rinaldi CA, Cooklin M, Razavi R, O'Neill M ,Gill J.
Novel pilot data - Cardiac MR Imaging Post Catheter Ablation: Does T2 and DE ratios matter in predicting clinical outcomeISMRM 2011 Montreal - poster presentation session: Myocardial Imaging & Spectroscopy Day/Date: Tuesday, May 10th ; Session Start Time: 13:30 (Abstract 4447).
Arujuna A, Karim R, Schaeffter T, Rinaldi CA, Cooklin M, Razavi R, O'Neill M ,Gill J, Rhode K. Are Robotic-Assisted Catheter Ablation Lesions Different from Standard CatheterAblation in Paroxysmal AF Patients? : Novel CMRI Findings Made Possible with Semi-automatic 3-DVisualisation. FIMH 2011 New York International Conference on Functional Imaging and Modeling of the Heart May 25-27, 2011 New York, USA (Abstract ID: 48).

Karim R, **Arujuna A**, Brazier A, O'Neil M, Gill J, Razavi R, Rueckert D, Schaeffter T, Rhode K.Automatic Segmentation of Left Atrial Scar from Delayed-Enhancement Magnetic Resonance Imaging. To appear in Functional Imaging and Modeling of the Heart (FIMH) 2011.

Karim R, Gao G, Harrison J,**Arujuna A**, Lambert H, Leo G, Gill J, Razavi R, Schaeffter T, Rhode K.Mapping Contact Force during Catheter Ablation for the Treatment of Atrial Fibrillation: New Insights into Ablation Therapy. As a clinical abstract in Functional Imaging and Modeling of the Heart (FIMH) 2011.

Arujuna A, Karim R, Rhode K, Schaeffter T, Rinaldi CA, Cooklin M, Razavi R, O'Neill M ,Gill J.
A Cardiac MR Comparison of Wide Area Circumferential Ablation Lesions created using Robotic Navigation assistance versus Standard Catheter Ablation in Paroxysmal AF Patients. EHRA 2011 Madrid – EHRA EUROPACE 2011 June28th 2011, 8:30-12:30pm (Abstract ID 947)

Arujuna A, Karim R, Rhode K, Schaeffter T, Wright M, Rinaldi CA, Cooklin M, Razavi R, O'Neill M ,Gill J. Increased Catheter Stability with Robotic Assisted Navigation during Pulmonary Vein Isolation, Does it Matter ? Novel Cardiac MR findings. World Cardiac Coongress - WCC12-ABS-2120 Oral presentation Thursday, April 17th 2012 8:30am.
Peel S, **Arujuna A**, Rhode K, Razavi R, Gill J, ONeill M SchaeffterT,BotnarR.Inversion recovery

Arujuna A, Karim R, Rhode K, Schaeffter T, Wright M, Rinaldi CA, Cooklin M, O'Neill M ,Gill J, Razavi R.Cardiac MR Imaging and Technology Assessment: A randomized prospective comparison of Robotic Assisted versus Standard Catheter AF ablation. ISMRM 2012 Melbourne – electronic poster presentation Wednesday, May 9th:

Session 1430.

Arujuna A, Peel S, Karim R, Rhode K, Schaeffter T, Wright M, Rinaldi CA, Cooklin M, Razavi R, O'Neill M,Botnar R,Gil J**.** Novel Dual Inversion Recovery Pre-pulse Imaging Technique Improves Post Ablation Cardiac MR Scar Visualization. Heart Rhythm Society 2012 poster presentation (Abstract ID #8422).

Arujuna A, Karim R, Rhode K, Schaeffter T, Wright M, Rinaldi CA, Cooklin M, Razavi R, O'Neill M ,Gill J. Remote Robotic Assisted Catheter Ablation Confers Greater Long Term Scar on Cardiac MR Evaluation Compared to Standard Catheter Ablation. Heart Rhythm Society 2012 poster presentation (Abstract ID #6898

Acknowledgements

I would like to thank my supervisors Dr Jaswinder Gill and Professor Reza Razavi for their time, advice and support during this period. I am grateful to Dr C. Aldo Rinaldi for his support, advice and encouragement during this period. I would like to thank my colleagues at Guy's and St Thomas' Hospitals for their help in performing some of the procedures involved in the clinical study within this thesis. This work would not have been possible without an educational grant from St Jude Medical UK.

The help of the following is also gratefully acknowledged:

Dr Mark O'Neill for his time, advice and help in writing some of the submitted manuscripts.

From the Imaging Sciences team, I am grateful to Dr Kawal Rhode and his group - Dr RashedKarim, Dr Ying-Liang Ma and Dr James Housdenfor their time and input into the image analysis.

Stephen Sinclair, Annette Dahl and Lorna Smith for their help in the acquisition of the cardiac MR scans.

Dr StamKapetanakis and Dr RonakRajani for their help in acquiring the TOE images.

Dr Bernet Kato for his help and advice on statistical analysis.

Javed Osman, Kami Lecamwasam and Bobby Willis from Hansen Medical UK for their attentive support throughout all the remote robotic ablation cases.

The many patients who kindly attended all the required follow-ups including the 3 CMR scans despite rain, sleet or snow.

Most of all I would like to thank my family and close ones for their incredible patience and support enabling me to complete this work within the 2 and half year period.